AD-A189 175 PROPELLER DESIGN FOR NAVAL AUXILIARY AO-177 JUMBO(U) 1/1
DAVID W TAYLOR NAVAL SHIP RESEARCH AND DEVELOPMENT
CENTER BETHESDA MD SHIP H YDROMECHANICS DEPT K KIM
UNCLASSIFIED SEP 87 DTNSRDC/SHD-1227-01 F/G 13/10 NL

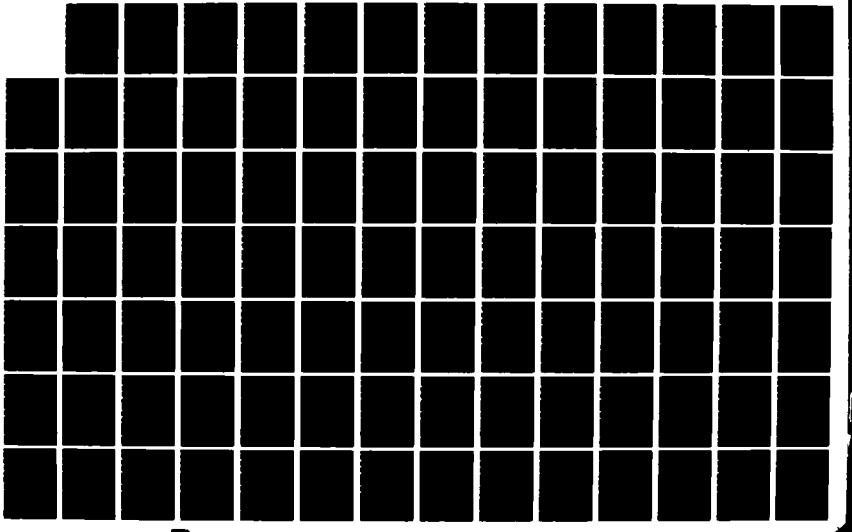

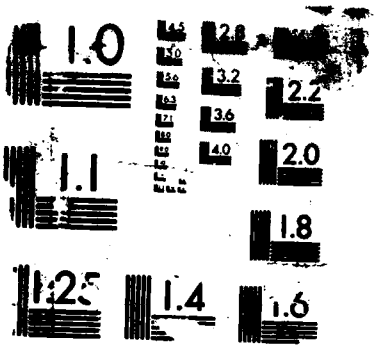

MICROCOPY RESOLUTION TEST CHART

David W. Taylor Naval Ship Research and Development Center

Bethesda, MD 20084-5000

DTNSRDC/SHD-1227-01 September 1987

SHIP HYDROMECHANICS DEPARTMENT

DEPARTMENTAL REPORT

PROPELLER DESIGN FOR NAVAL AUXILIARY AO-177 JUMBO

by

Ki-Han Kim

DTNSRDC/SHD-1227-01 PROPELLER DESIGN FOR NAVAL AUXILIARY AO-177 JUMBO

UNCLASSIFIED
SECURITY CLASSIFICATION OF THIS PAGE

REPORT DOCUMENTATION PAGE

1a REPORT SECURITY CLASSIFICATION UNCLASSIFIED	1b RESTRICTIVE MARKINGS
2a SECURITY CLASSIFICATION AUTHORITY	3 DISTRIBUTION / AVAILABILITY OF REPORT Approved for public release; distribution is unlimited.
2b DECLASSIFICATION / DOWNGRADING SCHEDULE	
4 PERFORMING ORGANIZATION REPORT NUMBER(S) DTNSRDC/SHD-1227-01	5 MONITORING ORGANIZATION REPORT NUMBER(S)
6a NAME OF PERFORMING ORGANIZATION David W. Taylor Naval Ship Research & Development Center 6b OFFICE SYMBOL (If applicable) CODE 1544	7a NAME OF MONITORING ORGANIZATION
6c ADDRESS (City, State, and ZIP Code) Bethesda, MD 20084-5000	7b ADDRESS (City, State, and ZIP Code)
8a NAME OF FUNDING SPONSORING ORGANIZATION Naval Sea Systems Command 8b OFFICE SYMBOL (If applicable) SEA 55W3	9 PROCUREMENT INSTRUMENT IDENTIFICATION NUMBER
8c ADDRESS (City, State, and ZIP Code) Crystal City Washington, D.C. 20362	10 SOURCE OF FUNDING NUMBERS PROGRAM ELEMENT NO: 64567N PROJECT NO: WR10462 TASK NO: S1803527 WORK UNIT ACCESSION NO: DN506088

11 TITLE (Include Security Classification)

Propeller Design for Naval Auxiliary AO-177 Jumbo

12 PERSONAL AUTHOR(S)
Kim, Ki-Han

13a TYPE OF REPORT	13b TIME COVERED	14 DATE OF REPORT (Year, Month, Day)	15 PAGE COUNT
Final	FROM 7/86 TO 4/87	1987 September	86

16 SUPPLEMENTARY NOTATION

17 COSATI CODES			18 SUBJECT TERMS (Continue on reverse if necessary and identify by block number)
FIELD	GROUP	SUB-GROUP	Propeller Design, Lifting-Surface, Lifting-Line, Blade Surface Cavitation

19 ABSTRACT (Continue on reverse if necessary and identify by block number)

The design of a fixed-pitch propeller for the U.S. Navy's auxiliary oiler, AO-177 JUMBO is presented. The jumboized AO-177 represents the AO-177 class with a 108 foot parallel-midbody section inserted. The design process is discussed in detail including considerations of cavitation and propeller-excited vibratory forces. The objective was to design a propeller which provides an increased thrust and improved cavitation performance compared to the existing propeller. The speed at full power (24,000 shp) was predicted to be 20.81 knots. The sustained speed was predicted to be met at 5 percent less than design sustained power. The thrust breakdown criteria of 10 percent speed margin on back bubble cavitation at full power was calculated to be met. Calculations predicted that, at full-power design condition. the final 5-bladed propeller with diameter of 21.0 feet will produce unsteady thrust and torque of 2.5 and 1.8 percent of the design thrust and torque, respectively. At full-power design conditions, stresses throughout the blades are calculated to be well below the allowable limit of 12,500 psi.

20 DISTRIBUTION / AVAILABILITY OF ABSTRACT	21 ABSTRACT SECURITY CLASSIFICATION	
☒ UNCLASSIFIED/UNLIMITED ☐ SAME AS RPT ☐ DTIC USERS	UNCLASSIFIED	
22a NAME OF RESPONSIBLE INDIVIDUAL Ki-Han Kim	22b TELEPHONE (Include Area Code) (202) 227-1450	22c OFFICE SYMBOL Code 1544

DD FORM 1473, 84 MAR — 83 APR edition may be used until exhausted. All other editions are obsolete.

SECURITY CLASSIFICATION OF THIS PAGE
UNCLASSIFIED

CONTENTS

	Page
NOMENCLATURE	vii
ABSTRACT	1
ADMINISTRATIVE INFORMATION	1
INTRODUCTION	1
PROPELLER DESIGN REQUIREMENTS	3
WAKE SURVEY AND MODEL PROPULSION EXPERIMENTS	3
PROPELLER DESIGN	5
REVIEW OF PREVIOUS DESIGNS	5
DESIGN CONDITIONS AND PROCEDURE	6
DESIGN WAKE	9
LIFTING-LINE DESIGN	11
Circulation Distribution	12
Chord Length and Thickness Distribution	14
LIFTING-SURFACE DESIGN	15
Unsteady Forces and Skew Distribution	16
Final Pitch and Camber Distribution	17
PERFORMANCE PREDICTION	18
BLADE SURFACE CAVITATION	18
OPEN-WATER PERFORMANCE	21
PREDICTION OF DELIVERED POWER AND RPM	21
FINAL DESIGN GEOMETRY	22
OPEN-WATER AND POWERING EXPERIMENTS USING DESIGN PROPELLER	23
DISCUSSION	25
ACKNOWLEDGEMENTS	26

CONTENTS (Continued)

Page

APPENDIX A - PROPELLER DESIGN REQUIREMENTS FOR AO-177 JUMBO..... 75

B - STRESS ANALYSIS OF AO-177 JUMBO PROPELLER BY USING FINITE ELEMENT METHOD..... 77

REFERENCES..... 82

FIGURES

1 - Body Plan of AO-177 JUMBO..... 27

2 - Illustration of flow-accelerating Fin Configuration Designed by SSPA..... 28

3 - Circumferential Variation in the Axial, Tangential and Radial Velocity Components..... 29

4 - Radial Distribution of Circumferential Average of Axial and Tangential Velocity Components..... 34

5 - Radial Distribution of Circumferential Average and Variation of Angle of Advance..... 35

6 - Comparison of Circumferential Mean Axial Velocity Between Original and Jumboized AO-177..... 36

7 - Harmonic Content of Axial Wake Velocity..... 37

8 - Design Procedure for AO-177 JUMBO Propeller..... 38

9 - Circulation Distributions Investigated During Design and Corresponding Hydrodynamic Pitch Distributions..... 39

10- Hydrodynamic Pitch Angle and Lifting-Line Pitch Distribution..... 40

11- Radial Distribution of Chord Length..... 41

12- Radial Distribution of Thickness..... 42

13- Skew Distributions Investigated During Design..... 43

14- Effect of Skew on the Calculated Pitch Using Lifting-Surface Code, PBD-10..... 44

15- Final Pitch Distribution (P/D) Predicted by Lifting-Surface Code, PBD-10..... 45

FIGURES (Continued)

Page

16- Final Camber Distribution (f_M/c) Predicted by Lifting-Surface Code, PBD-10..... 46

17- Cavitation Bucket for Different Thickness Distributions at Full-Power Design Condition for AO-177 JUMBO..... 47

18- Inception Speed of Various Cavitations for Different Thickness Distributions..... 48

19- Open-Water Performance Predicted by Lifting-Surface Code, PSF-2..... 49

20- Predicted Full-Scale Power and RPM of AO-177 JUMBO at Full Load Condition..... 50

21- Predicted Full-Scale Power and RPM of AO-177 JUMBO at Ballast Condition..... 51

22- Final Geometry of AO-177 JUMBO Propeller (DTNSRDC Propeller 5027A)..... 52

23- Comparison of Open-Water Performance Between Experiments and Predictions for AO-177 JUMBO Propeller (DTNSRDC Propeller 5027A).... 53

24- Predicted Full-Scale Power and RPM of AO-177 JUMBO at Full Load Condition Based on Design Propeller Experiments..... 54

25- Predicted Full-Scale Power and RPM of AO-177 JUMBO at Ballast Condition Based on Design Propeller Experiments..... 55

B-1 - Finite Element Model of AO-177 JUMBO Propeller..... 78

B-2 - Von Mises Stress Contours on Pressure Side at Full Load, Full Power Ahead Condition..... 79

B-3 - Von Mises Stress Contours on Suction Side at Full Load, Full Power Ahead Condition..... 80

B-4 - Blade Displacement at Full Load, Full Power Ahead Condition..... 81

TABLES

Page

1 - Circumferential Average of Wake Velocity, Mean and Variation of Angle of Advance..... 57

2 - Harmonic Contents of Axial and Tangential Velocity Components..... 58

3 - Powering Predictions at Full-Load Condition Based on Model Propulsion Test with Stock Propeller (Model 4677)..... 60

4 - Estimated Powering Performance at Ballast Condition..... 61

5 - Model Nominal and Effective Wake..... 62

6 - Effect of Radial Circulation Distribution on Propeller Performance at Full Power..... 63

7 - Computer Output from Lifting-Line Code, EPPD..... 64

8 - Effect of Skew on Blade-Frequency Thrust and Torque..... 66

9 - Pitch Distribution (P/D) from Lifting-Surface Computation Using Computer Code PBD-10..... 67

10- Camber Distribution (f_M/c) from Lifting-Surface Computation Using Computer Code PBD-10..... 68

11- Geometric Characteristics of Design Propeller of AO-177 JUMBO..... 69

12- Predicted Ship Speed and RPM of AO-177 JUMBO at Full Load and Ballast Condition..... 70

13- Offsets of AO-177 JUMBO Design Propeller..... 71

14- Comparison of Full-Scale Powering Predictions Based on Model Powering Experiments Using Stock and Design Propellers..... 73

15- Comparison of EHP and Propeller/Hull Interaction Coefficients Between Stock and Design Propellers..... 74

NOMENCLATURE

A_E	Expanded blade area: $Z\int_{r_h}^{R} c\,dr = \frac{ZD^2}{2}\int_{x_h}^{1}\left(\frac{c}{D}\right)dx$
A_e	Aspect ratio
A_E/A_O	Expanded area ratio (EAR): $\left(\frac{2Z}{\pi}\right)\int_{x_h}^{1}\left(\frac{c}{D}\right)dx$
A_O	Propeller disc area: $\frac{\pi D^2}{4}$
c	Blade chord length
C_A	Correlation allowance
C_D	Blade section drag coefficient, per unit span: $C_D = \frac{\text{Drag}}{\frac{1}{2}\rho V_r^2 c}$
C_F	Frictional drag coefficient
C_L	Blade section lift coefficient, per unit span: $C_L = \frac{\text{Lift}}{\frac{1}{2}\rho V_r^2 c}$
C_P	Power loading coefficient based on ship speed: $\frac{2\pi nQ}{\frac{1}{2}\rho\pi R^2 V^3}$
C_{TS}	Thrust loading coefficient based on ship speed: $\frac{T}{\frac{1}{2}\rho\pi R^2 V^2}$
D	Propeller diameter
D_h	Hub diameter
f_M	Maximum camber
g	Acceleration due to gravity
G	Nondimensional circulation: $\frac{\Gamma}{\pi DV}$
H	Depth of immersion at propeller shaft centerline, not including atmospheric head
i_T	Total rake; axial distance of midchord line from a plane containing blade reference line
J_A	Advance coefficient based on advance speed, V_A: $J_A = \frac{V_A}{nD} = \frac{V(1-w_T)}{nD}$

J	Advance coefficient based on ship speed: $\frac{V}{nD}$
K_Q	Torque coefficient: $\frac{Q}{\rho n^2 D^5}$
K_T	Thrust coefficient: $\frac{T}{\rho n^2 D^4}$
n	Propeller rotational speed (revolution per unit time)
P	Propeller pitch
P_A	Atmospheric pressure
P_D	Delivered power at propeller: $2\pi nQ$
P_E	Effective power: RV
P_S	Shaft power
P_v	Vapor pressure
Q	Torque absorbed by propeller
R	Propeller tip radius or ship resistance
R_n	Reynolds number
r	Local propeller radius
r_h	Propeller hub radius
T	Thrust produced by propeller
t	Thrust deduction fraction: $t = \frac{T-R}{T}$ or blade maximum thickness
u_a	Axial induced velocity at lifting line
u_t	Tangential induced velocity at lifting line
V	Ship speed
V_A	Propeller speed of advance: $V(1-w_T)$
V_r	Resultant inflow speed to lifting line: $\sqrt{(V_X+u_a)^2 + (2\pi nr-u_t)^2}$
V_R	Radial velocity component: positive inward according to DTNSRDC definition, positive outward according to MIT definition
V_T	Tangential velocity component, positive counterclockwise when looking upstream
V_X	Local axial speed, circumferential mean

w_T Propeller effective wake fraction as determined from thrust identity from self-propulsion experiment, also called Taylor wake fraction

w_v Volume mean wake fraction: $1 - w_v = \dfrac{2\int_{x_h}^{1} \left(\dfrac{V_x}{V}\right) \cdot x \cdot dx}{1 - x_h^2}$

x Nondimensional radius: r/R

x_h Nondimensional hub radius: $r_h/R = D_h/D$

Z Number of blades

α Angle of attack

α_i Ideal angle of attack

β Advance angle at local radius r: $\beta = \tan^{-1} \dfrac{V_x}{2\pi nr}$

β_i Hydrodynamic flow angle at lifting line at local radius r: $\beta_i = \tan^{-1}\left[\dfrac{V_x + u_a}{2\pi nr - u_t}\right]$

$\bar{\beta}$ Circumferential mean advance angle

$+\Delta\beta$ Variation of the maximum advance angle from the mean

$-\Delta\beta$ Variation of the minimum advance angle from the mean

Γ Circulation about lifting line

ε Local section drag-lift ratio: C_D/C_L

η_D Propulsive efficiency: P_E/P_D

η_H Hull efficiency: $\dfrac{1-t}{1-w_T}$

θ_S Blade skew angle in degrees

ϱ Fluid density: ϱ = 1.9905 lb·sec^2/ft^4 for salt water at 59°F (15°C)
1.9384 lb·sec^2/ft^4 for fresh water at 59°F (15°C)

ϱ_p Density of propeller material

σ Section cavitation number: $\dfrac{P_A + \varrho g(H - r) - P_v}{\frac{1}{2}\varrho V_r^2}$

ϕ Pitch angle at local radius r: $\phi = \tan^{-1}\left[\dfrac{P}{2\pi r}\right]$

ABSTRACT

The design of a fixed-pitch propeller for the U.S. Navy's auxiliary oiler AO-177 JUMBO is presented. The jumboized AO-177 represents the AO-177 class with a 108 foot parallel-midbody section inserted. The design process is discussed in detail including considerations of cavitation and propeller-excited vibratory forces. The objective was to design a propeller which provides an increased thrust and improved cavitation performance compared to the existing propeller. The speed at full power (24,000 shp) was predicted to be 20.81 knots. The sustained speed was predicted to be met at 5 percent less than design sustained power. The thrust breakdown criteria of 10 percent speed margin on back bubble cavitation at full power was calculated to be met. Calculations predicted that, at full-power design condition, the final 5-bladed propeller with diameter of 21.0 feet will produce unsteady thrust and torque of 2.5 and 1.8 percent of the design thrust and torque, respectively. At full-power design conditions, stresses throughout the blades are calculated to be well below the allowable limit of 12,500 psi.

ADMINISTRATIVE INFORMATION

This project was carried out for the Naval Sea Systems Command (NAVSEA) under Work Request N00024-86-WR-10462. The work was performed at the David W. Taylor Naval Ship Research and Development Center under Work Unit Number 1-1544-405.

INTRODUCTION

The Naval Sea Systems Command (NAVSEA) requested the David W. Taylor Naval Ship Research Center (DTNSRDC) to design a propeller for the naval auxiliary oiler, AO-177 JUMBO. The AO-177 JUMBO represents the AO-177 class with a 108-foot (32.92 m) parallel-middle-body section inserted to the original configuration (see Figure 1). As a result, the full-load displacement has been increased from 27,380 to 37,575 long tons. The

existing 24,000 shp propulsion machinery plant is to be retained. A new propeller design is required to provide the increased thrust and cavitation performance comparable to or better than that of the existing AO-177. In addition, the propeller-induced unsteady shaft forces and moments must not exceed allowable limits as determined from machinery vibration analysis.

The AO-177, first of a new class of Naval Auxiliary Oilers, was the subject of extensive investigations several years ago in relation to the high levels of airborne noise, heavily localized vibration and initial-stage erosion damage on its highly-skewed, seven-bladed propeller during builder's trials [1]*. These undesirable effects were mainly due to the fine stern shape providing a large deficit in the axial velocity in the vicinity of the top of the propeller plane.

Among several options to improve the stern flow, different flow-improving stern fins were extensively studied [2,3]. Based on the improved performance of the blade-rate hull pressure, the flow-accelerating fin (see Figure 2), which was designed by the Maritime Research & Consulting (SSPA) in Sweden, was selected as the final design modification for installation on the ship. The flow-accelerating fin configuration proved to be effective in reducing blade-rate hull surface pressure excitation due to reduction in propeller cavitation through an improvement of the magnitude and steepness of the nominal wake. It also produced a significant reduction of airborne noise on the ship to levels within the specifications [1].

This report presents the design procedure and rationale which led to the final geometric configuration of a 5-bladed propeller with a 21-foot (6.4 m) diameter for the AO-177 JUMBO. The following sections describe the specified design conditions, the pertinent information used as input to the

*References are listed on page 82.

design problem, the design procedure, performance prediction, and a summary of the final design geometry.

PROPELLER DESIGN REQUIREMENTS

The design requirements for the AO-177 JUMBO propeller were provided by NAVSEA. The primary performance requirement is cavitation performance which is to be comparable to or better in terms of propeller-induced vibration/noise relative to the original AO-177 propeller. The sustained speed should be a minimum of 18.8 knots (9.67 m/sec) at 80 percent of the maximum shaft power of 24,000 SHP (17,897 kW). The propeller rotational speed is required to be 100 rpm at full power (24,000 SHP). From the geometry of the ship stern, the propeller diameter was specified as 21 feet (6.4 m). The depth of submergence of the shaft centerline in calm water is 22 feet (6.71 m) with even keel condition. The maximum acceptable blade-rate forces and moments are less than 2.5 percent of the mean loads. The vibration study showed little obvious preference between five and seven-bladed propellers [4]. Since the experiments at SSPA [5] indicated that five-bladed propeller produced less cavitation induced hull pressure, it was decided that the new propeller will have five blades. The details of the design requirements specified by NAVSEA are presented in Appendix A.

WAKE SURVEY AND MODEL PROPULSION EXPERIMENTS

Wake survey, resistance, and self-propulsion tests were conducted in the towing tank of Tracor Hydronautics, Inc., using a model representing the AO-177 JUMBO with a scale ratio of 25.682. The wake was measured at model conditions corresponding to design draft, zero trim and model speed equivalent to 19 knots full-scale. The model was equipped with the flow-accelerating fin designed by SSPA. The measured values of the circumferential

variations in the axial, tangential and radial velocity components at five nondimensional radii; 0.41, 0.55, 0.65, 1.04 and 1.14 are shown in Figure 3.

From these data, similar results were obtained for other radii by interpolation. The sign conventions for the velocity components are as follows: the axial velocity is positive downstream, the radial velocity is positive inward and the tangential velocity is positive clockwise when looking downstream. The circumferential average of the axial and tangential velocity components* and the mean and variation of the angle of advance are summarized in Table 1, and the same data are presented graphically in Figures 4 and 5. Figure 6 shows the comparison of the circumferential mean axial velocity for the original and jumboized AO-177. The volume mean wake for AO-177 JUMBO was reduced from 0.761 to 0.703. The reduction occurred more or less uniformly from the hub to the tip.

Subsequently, the harmonic content of the circumferential variations were computed by Fourier analysis. The results of Fourier analysis up to the 8th harmonic are presented in Table 2. More detailed wake survey results will be presented in a separate report. The resistance and self-propulsion tests were carried out with the seven-bladed propeller (DTNSRDC Propeller 4677) designed for the original AO-177. The powering data for both full-load and ballast conditions necessary for propeller design were provided by NAVSEA and are presented in Tables 3 and 4, respectively. The effective power in the tables includes still air drag but no power margin. The powering data for full-load condition were based on the model tests at Tracor Hydronautics, Inc. The data for ballast condition were estimated.

*The radial velocity component was not available during the design period, and thus not used in the present design.

PROPELLER DESIGN

REVIEW OF PREVIOUS DESIGNS

The original seven-bladed propeller for AO-177 was designed by Valentine and Chase [6]. This propeller has relatively short chord lengths, especially near the tip, which might have contributed to the observed adverse cavitation behavior. Although this propeller has 45 deg of projected skew angle at the tip, the narrow chord lengths near the tip appear to reduce the tendency of skew to reduce cavitation [7, 8] by reducing the sweepback angle of the leading edge. The full-scale cavitation observed on the AO-177 propeller showed a two-dimensional character indicative of the narrow blades.

As a possible solution in the event the flow-accelerating fin did not solve the excessive propeller induced airborne noise and propeller erosion problems, Jessup [9] designed a five-bladed propeller for the ship fitted with the flow-accelerating fin. Jessup incorporated some basic modifications to the original design in an attempt to improve performance related to blade cavitation. He increased the chord lengths and incorporated large skew variation near the tip. From the standpoint of unsteady thrust and torque, a five-bladed propeller is not the best choice. As shown in Figure 7, the magnitude of the 5th harmonic of the axial wake velocity is the largest. This large 5th harmonic component of the axial wake will induce large blade-frequency thrust and torque. However, after careful consideration of other aspects such as a possible hull resonance problem and acceptable geometry, a five-bladed design was selected as the best compromise between the primary design objective and the various constraints. Jessup's redesign, however, was not subjected to experimental evaluation since the

flow-accelerating fin was accepted as the final design modification to the existing hull.

The basic philosophy of the current design for the jumboized ship follows closely that of Jessup, except for more extensive efforts in the present design to consider the different design requirements.

DESIGN CONDITIONS AND PROCEDURE

The propeller was designed for the full-power condition of 24,000 shaft horsepower at 100 rpm. The design input was based on the full-scale extrapolation of model-scale results from a wake survey and resistance and propulsion experiments. The model-scale results were obtained at full-load condition using a stock propeller. The extrapolation was performed for the ship with clean hull in calm seas with a correlation allowance of 0.0005; still air drag was included but the powering margin was not included (see Table 3).

Figure 8 presents a schematic representation of the design procedure adopted in the current design. The propeller was designed in six phases, namely:

(a) Preliminary Design: In this phase estimates are made of number of blades, diameter, blade area ratio and blade outline. These estimates are made so that at the design conditions the propeller is compatible with the ship and the propulsion machinery from the standpoint of efficiency and vibration. In the current design, the number of blades and propeller diameter were specified as part of the design requirements. Due to reduced clearance with the fin and other constraints, the diameter had to remain at 21 feet (6.4 m) which is the same as the original AO-177 propeller diameter.

(b) Lifting-Line Design: In this phase the radial load distribution and the radial hydrodynamic pitch distribution are computed using Lerbs induction factor method [10]. These radial distributions of load and pitch will be input to lifting-surface calculations. Lifting-line calculations are made based on the initial geometry selected in phase (a).

(c) Propeller Global Geometry: In this phase the initial EAR, blade chord length and thickness distributions are refined by considering various hydrodynamic as well as structural aspects such as cavitation, thrust breakdown, erosion, and blade strength. Lifting-line calculations are repeated for different geometries as the refinement procedure goes on.

(d) Lifting-Surface Design: In this phase the final geometric pitch and camber distributions are determined using the lifting-surface design procedure of Greeley and Kerwin [11].

(e) Design Check: In this phase the unsteady forces and moments are calculated and compared with the design requirements. If the predicted values do not meet the design requirement, the skew distribution is modified. In general, larger skew will induce smaller vibratory forces and moments while producing larger blade stress. Therefore, the skew distribution must be optimized considering both the vibratory forces and the blade stresses. Since the skew distribution will affect the resulting pitch and camber distribution, the lifting-surface design procedure must be repeated for each new skew distribution. In this phase the design propeller is also reviewed to check the off-design performance and to summarize the final design predictions in terms of required speed margins and other specified constraints.

(f) Final Design Geometry: In this phase, the final propeller offsets are determined including the leading and trailing edge details, additional thickness to be added to the trailing edge where required, and

detailed tip geometry. These offsets will be the basis for manufacturing the model and full-scale propellers.

To reduce blade cavitation, propeller-induced hull forces and propeller erosion problems, a variety of geometry changes were incorporated in the current design. These changes are summarized as follows:

1. Reduced loading near blade tip [12]: In general, reduced loading near the blade tips will reduce the amount of cavitation at the price of reduced propulsive efficiency. This is routine practice in use at DTNSRDC to improve the cavitation performance. Propeller-induced hull forces may be reduced; however, the effect of tip unloading on cavitation erosion and cavity collapse is not fully understood. In some cases, tip unloading produces undesirable unstable cavity collapse.

2. Increased chord length [13]: A substantial change in this parameter could be achieved because of the abnormally short chord length at the outer radii on the existing propeller. Increasing chord lengths would reduce the loading per unit area on the blades, thus reducing the possibility and extent of cavitation. Increasing chord lengths will also decrease the propeller efficiency due to increased drag. Reducing the number of blades for the same expanded area ratio (EAR) would produce wider blades, possibly causing an increase in three-dimensional cavity structure, and reduced violence of collapse.

3. Large skew variation near the tip: A large variation (gradient) in projected skew angle near the blade tip will produce a highly swept tip. This type of blade outline, when heavily loaded in the wake peak, may induce turbulent separation along the leading edge extending to the blade tip [9]. If this occurs, then cavitation which forms along the leading edge will be convected into the tip vortex and off the blade. It is

believed that blade cavitation collapses gently off the blade when it merges with the tip vortex. This process has been observed by Jessup [9] and on the five-bladed stock propeller evaluated on the AO-177 model hull at SSPA [5]. This type of blade outline has been successfully adopted with controllable-pitch propellers for commercial ship applications and has produced significant reductions in propeller-induced hull vibration [14].

4. Increased thickness [15]: Increasing thickness will result in an increased margin against leading edge cavitation due to a wider cavitation bucket. However, this will be accomplished at the price of earlier onset of back bubble cavitation, and possibly thrust breakdown.

DESIGN WAKE

One of the essential pieces of information for propeller design is the ship's wake in which the propeller will be operating. The need for a complete knowledge of the ship's wake is not limited to the calculation of propulsive efficiency. The prediction of full-scale thrust, torque, delivered power, and shaft rotational speed, as well as cavitation and vibration performance, all depend upon the accuracy of the prediction of the full-scale wake field.

In general, the inflow to the propeller is measured in the towing tank or wind tunnel behind a ship model without a propeller in place. This wake is called the nominal wake. Two aspects must be considered for proper propeller design; the effect of full-scale Reynolds number on the full-scale nominal wake and the effect of propeller action on the wake.

The effect of different Reynolds number, or scale effect, between the model and full-scale ship wake should be properly accounted for since the designed propeller will be operating behind a full-scale ship. Scale effects are more important for naval auxiliary-class ships where the pro-

peller operates in the boundary layer of the ship hull than for surface combatants where the propeller shafts are inclined so that the propellers operate primarily in the potential flow outside of the ship's boundary layer.

However, the correlation between the model and full-scale performance of the original AO-177 as fitted with the flow-accelerating fin indicated that there were negligible scale effects up to a ship speed of 21 knots [16]. In other words, the predicted shaft power and propeller rpm based on the standard DTNSRDC prediction method [17] showed good agreement with full-scale measurements. Based on this favorable correlation, it was agreed between DTNSRDC and NAVSEA that the propeller would be designed using the measured model nominal wake with an appropriate adjustment for the effective wake.

When a propeller operates behind a ship, the inflow to the propeller is changed due to the action of the propeller. The propeller accelerates the flow over the stern, this results in a decrease in the pressure, which in turn changes the boundary layer characteristics. This inflow is 'loosely' called effective wake. Although one can use the method of Huang, et al, [18] in an attempt to calculate the effective wake, a simple average-correction method was used in the present design. This method has proven reasonably successful in the past for obtaining the desired ship speed and shaft rpm at design power. The nominal wake was scaled up to the value of the effective wake, $1-w_T$, obtained from the propulsion experiment based on the thrust identity:

$$(V_x/V)_{\text{Corrected}} = (V_x/V)_{\text{Nominal}} \times \frac{(1 - w_T)}{(1 - w_V)} \qquad (1)$$

where V_x/V is the nondimensional circumferential mean axial velocity compo-

nent from the wake survey, and $1-w_v$ is the volumetric mean nominal wake.

The measured model nominal and corrected velocity distributions are presented in Table 5. For the final propeller design, the corrected model-scale wake distribution was used.

LIFTING-LINE DESIGN

Based on the geometry, ship wake and powering characteristics, a preliminary design was developed using a lifting-line model to calculate the ship speed, effective power, blade lift coefficients at design condition, and other information necessary for lifting-surface design. The lifting-line computer code used in this report was EPPD (Extended Propeller Preliminary Design) developed by Kim [19]. EPPD is equivalent to the combination of two of the existing lifting-line codes in use at DTNSRDC, LL106 [20] and CIRC [21]. The input to EPPD can be either hydrodynamic pitch angle or circulation.

When predicting the propeller performance, viscous effects are included in EPPD by specifying the sectional drag coefficient C_D. A C_D value of 0.0085 usually gives reasonable estimates of model propeller drag. For propellers having thicker blades, the following empirical equation [22, 23] will give a better estimate of the section drag coefficient:

$$C_D = C_F \left[1 + 1.25 \, (t/c) + 125 \, (t/c)^4 \right] \qquad (2)$$

where C_F is the skin friction coefficient of a smooth flat plate. The value of C_F varies from 0.004 for a Reynolds number of approximately 10^8 to 0.008 for Reynolds number of approximately 10^6. In the present design, a constant C_D value of 0.0085 was used for all radii.

A provision was made in EPPD to compute the maximum camber distribu-

tion f_M/c for NACA a=0.8 meanline shape. In linear theory, the maximum camber (f_M/c) is proportional to the local lift coefficient C_L assuming that the propeller operates at an ideal angle of attack. Abbott and Von Doenhoff [22] (page 402) shows that at design lift coefficient of 1.0, the maximum camber-to-chord ratio is 0.0679. Therefore, for an arbitrary lift coefficient, the maximum camber-to-chord ratio will be:

$$f_M/c = 0.0679\ C_L \tag{3}$$

where C_L is the local lift coefficient defined by:

$$C_L = \frac{\text{Lift}}{(1/2)\,\rho\, V_r^2\, c} = \frac{2\pi G}{(c/D)(V_r/V)} \tag{4}$$

Circulation Distribution

Four circulation distributions were investigated as shown in Figure 9. The corresponding hydrodynamic pitch angle ($\tan\beta_i$) and the pitch ($\pi x \tan\beta_i$) distributions are shown in Figure 10. The Lerbs optimum circulation distribution, designated G_o, and the three different circulation distributions were investigated to serve as a guide to select the degree of tip unloading. Lerbs optimum is an estimate of the circulation distribution which will produce the highest efficiency for a wake-adapted propeller. This would be a logical circulation distribution for an application in which there are no cavitation or vibration problems.

How much of the circulation should be unloaded near the tip depends on the design requirement. There is no objective guideline to determine the amount of tip unloading. In general, it is determined by designer's experience. In the present design, the degree of tip unloading was defined as the ratio of the unloaded circulation value to Lerbs optimum circulation

value at 0.95 radius. This definition will serve as a useful guide for future designs.

Two circulation distributions, G_1 and G_2, were obtained by unloading the tip and the circulation distribution, G_3, was obtained by adding more loads to the optimum values. The ratios (G_1/G_o), (G_2/G_o) and (G_3/G_o) at 0.95 radius are 0.79, 0.85 and 1.08, respectively. The greater the tip unloading, the greater the potential improvement in suction-side cavitation, vibration and strength, but the greater the reduction in ship speed at design power and the increased possibility of pressure-side cavitation.

Table 6 shows the comparison of speed and propulsive efficiency predicted by the lifting-line program at full power (24,000 SHP at 100 rpm) for the various load distributions for a propeller diameter of 21 feet. In this preliminary calculation, the thickness and chord length distributions were taken from Jessup's design.

An interesting result was obtained in that the propulsive efficiency for G_3 is higher than that of Lerbs optimum efficiency! Similar results were also found recently by Brockett and Korpus [24] and by Kerwin, et al [25]. The question of whether this is physically correct or not is beyond the scope of the present design effort. However, three independent calculations confirmed that the tip-loaded circulation distribution produced higher efficiency than Lerbs optimum value. Since the practical consequenses of the tip-loaded propeller is not clear (see Holden [26]), the increase in efficiency is only of academic interest. Load distribution G_2 was selected as the final circulation distribution which represents a calculated sacrifice in ship speed at full power of 0.11 knot as compared to the Lerbs' optimum case.

Chord Length and Thickness Distribution

Next, the detailed blade geometry is selected (phase c); that is, the radial distribution of chord length, expanded area ratio, and radial distibution of thickness. Each of these should be carefully selected to provide adequate blade strength and simultaneously minimize the tendency towards cavitation erosion. In addition, propeller efficiency must not be materially sacrificed.

Burrill's cavitation criteria [27] indicated that for maximum 2.5 percent back cavitation the minimum EAR should be 1.07, whereas Keller's criteria [28] showed 0.79. The procedure to compute the minimum EAR based on both Burrill's and Keller's criteria have been implemented in the lifting-line code EPPD. Greater blade width generally increases strength, reduces the probability of cavitation but reduces speed for the same power due to increased viscous drag.

Since the shape of the chord length distribution (c/D) of Jessup's design produced an EAR of 0.819, it was decided to use the same chord length distribution in the present design. Figure 11 shows the chord length distribution for the current design together with that of the original AO-177 propeller. The new chord length has been increased substantially compared to the original one.

The thickness was selected based on strength, cavitation considerations and restrictions on the blade weight. The cavitation predictions indicated that substantial leading-edge sheet cavitation would occur for both the original 7-bladed propeller and the 5-bladed propeller designed by Jessup. Although the leading-edge sheet cavitation appears to be unavoidable for this ship, it could be improved by changing the thickness distribution.

Several different thickness distributions were investigated in relation to cavitation and strength performances. Starting from Jessup's thickness, new thickness distributions were obtained by adding thickness gradually from 0.4 radius to the tip. For each thickness distribution, the lifting-line code LL106 was run to compute blade weight, which was then compared to the design requirement specified as maximum weight of 56,400 lbs from LL106 calculation. For each thickness, blade surface cavitation characteristics were also computed by using two-dimensional theory. The cavitation performance for different thickness distributions will be discussed later in this report.

Figure 12 shows the three thickness distributions evaluated. The thickness distribution, designated T_3, was selected as the final thickness. T_3 has the maximum thickness near the tip region which satisfies the blade weight requirement. The final thickness near the tip was thicker than Jessup's by 75 percent. The maximum stress predicted by using simple beam theory incorporated in LL106 was 6,371 psi, which is well below the allowable limit of 12,500 psi.

Table 7 shows the output from EPPD at the full power design condition. The output consists of circulation, induced velocities, section cavitation number, lift coefficients, ideal angle of attack, maximum camber and factors estimating local angle of attack and propeller performance. The predicted ship speed at the full power design condition is 20.62 knots at rpm of 100 at an advance coefficient J_A of 0.771.

LIFTING-SURFACE DESIGN

The final pitch and camber distributions corresponding to the selected load distribution, skew distribution, and other geometry from lifting-line computations were determined from lifting-surface computations using the

computer code PBD-10 developed by Greeley and Kerwin [11]. A description of the theory is given in Reference [11] and a detailed user's instruction for the code is presented by Kerwin [29].

The pitch and camber distributions were obtained by an iterative process starting with a coarse singularity grid arrangement on the blade, and progressing to a finer grid arrangement. For the first three iterations, an 8x9 element grid arrangement was used for the key blade, and 4x9 elements were used for other blades. For the final iterations, a finer grid arrangement of 16x35 elements was used on the key blade, while a 4x9 element grid was used on other blades. From sensitivity analysis, a grid arrangement with 16x35 elements on the key blade and 4x9 elements on other blades should be sufficient for a conventional open propeller design [11].

Unsteady Forces and Skew Distribution

The skew distribution was determined to satisfy the requirements of unsteady forces and the blade strength. Three skew distributions were tested for this purpose; zero skew, 36-degree tip skew varying linearly from zero at the hub, and 40-degree tip skew from Jessup's design (see Figure 13). For each skew distribution, lifting-surface calculations were performed using PBD-10 to determine the corresponding pitch and camber distributions.

The skew distribution has a direct influence on the pitch distribution calculated by lifting-surface procedures. Figure 14 shows a comparison of the pitch distributions calculated by PBD-10 for zero skew and 40-deg tip skew while keeping all other geometric parameters identical. The 40-deg tip skew reduces the pitch near the tip substantially. The pitch distribution for no skew is very similar to the lifting-line pitch distribution

(π x tanβ_i). This is not surprising because the lifting-line theory does not account for the skew effect. Skew also has an influence on camber but to a much lesser degree than on the pitch.

Once the pitch and camber distributions were determined, the fluctuating forces and moments were calculated for each design with different skew distribution by using the unsteady lifting-surface code PUF-2 developed by Kerwin and Lee [30]. In Table 8 the blade-frequency (5th harmonic) thrust and torque values are compared for different skew distributions. The blade-frequency thrust and torque values were reduced with an increasing skew. The predicted blade-frequency thrust and torque values were 5.80% and 5.38% of the design thrust (K_T=0.287) and torque (K_Q=0.0558) values, respectively, for a propeller with zero skew and were reduced to 2.49% and 1.81%, respectively, for a propeller with a 40-degree tip skew. The design requirements on unsteady shaft forces and moments are equivalent to allowing maximum unsteady forces and moments of about 2.5% of the mean values. Therefore, the 40-degree tip skew distribution shown in Figure 13 was selected as the final skew distribution.

Final Pitch and Camber Distribution

Tables 9 and 10 present the computed radial distribution of pitch and camber, respectively, at each iteration for the final tip skew of 40 degrees. Figures 15 and 16 show the final values of pitch and camber distribution after six iterations, together with the lifting-line values.

In general, the pitch and camber calculated by PBD-10 are not smooth, as shown in Figures 15 and 16. Thus, in practice the computed values are faired to give a smoother radial variation in pitch and camber distributions without affecting hydrodynamic performance. From these calculations, it is recommended that at least 2 iterations should be made using the finer

grid arrangement in order to obtain a reasonably converged solution.

Since the very low pitch near the tip might render the blade susceptable to pressure-side cavitation, the flow field near the tip was investigated by using the unsteady lifting-surface code PUF-2. The computed angle of attack near the leading edge at 0.92 radius showed somewhat large negative values when the blade passes the area where the axial inflow velocity is high; i.e., near 156 degrees and 270 degrees at the 0.92 radius. Based on this investigation, the pitch near the tip was increased to reduce the negative angle of attack by about 2 degrees based on the flow field computation. This increased pitch represented by the solid line in Figure 15 was selected as the final pitch distribution. The final geometry of AO-177 JUMBO propeller is summarized in Table 11 at 11 standard radial stations.

It is to be noted that the K_T and K_Q values computed by the lifting-surface code PBD-10 are higher than the lifting-line values by 4.5% and 2.2%, respectively, for the same radial distribution of circulation. The same tendency was reported by Greeley and Kerwin [11]. At present, it is not known what causes the discrepancy.

PERFORMANCE PREDICTION

BLADE SURFACE CAVITATION

In order to select a blade shape for best cavitation characteristics, use was made of theoretically predicted cavitation inception data for two-dimensional sections [15]. The cavitation inception characteristics are presented by plotting the angle of attack variation with cavitation number on the minimum pressure envelopes, commonly called "cavitation bucket", for

prescribed thickness and meanline distribution; the NACA 66 (NSRDC modified) thickness distribution and the NACA a=0.8 meanline in the present design. The procedure has been incorporated in the computer code VAFOIL (Platzer, 1981). The insides of the "buckets" are cavitation-free regions. The top and bottom of the buckets where the curve is roughly parallel to the horizontal axis (cavitation number) indicate leading-edge suction side (back) and pressure side (face) cavitation, respectively. In the region roughly parallel to the vertical axis (angle of attack), the minimum pressure occurs near the midchord which causes back bubble cavitation.

From the wake survey, the range of advance angle, $(\bar{\beta} + \Delta\beta_{max})$ to $(\bar{\beta} - \Delta\beta_{min})$, and cavitation number experienced by each blade section during one revolution can be calculated. If a propeller is designed to operate at an ideal angle of attack α_i the operating angle of attack α can be approximated by [31]:

$$\alpha = \alpha_i - F(x) \, [\, \beta - \bar{\beta}] \tag{9}$$

where β is the local advance angle and $\bar{\beta}$ is the circumferential mean advance angle, both at design condition. In Equation (9),

$$F(x) = \frac{1}{1 + 2/A_e} \tag{10}$$

where A_e is the effective aspect ratio at the design condition defined by:

$$A_e = \frac{C_L}{\pi \tan(\beta_i - \beta)} \tag{11}$$

A study of these curves will immediately reveal a tradeoff choice, namely, that by the selection of t/c it is often possible to achieve increased latitude against leading-edge sheet cavitation due to fluctuating

angle of attack at the price of earlier onset of back bubble cavitation at or near ideal angle of attack.

In the present design, the thickness distribution was selected by considering primarily the blade cavitation and the weight requirement. Figure 17 shows the cavitation buckets calculated by VAFOIL at design condition for the three different thickness distributions which were investigated (see Figure 12). The thickness distribution, T_1 is Jessup's thickness [9], and T_2 and T_3 are the variations of T_1 obtained by adding additional thickness near the tip region. The thickness to chordlength ratio (t/c) at the tip* for T_1, T_2 and T_3 are 0.026, 0.051 and 0.046, respectively.

Figure 17 clearly indicates that a thicker blade section has a wider bucket and is less susceptible to leading-edge sheet cavitation. Figure 18 shows the inception speeds for various types of cavitation; namely suction and pressure side sheet cavitation starting from the leading edge and back bubble cavitation as a function of radius. The inception speed of the leading-edge sheet cavitation increases with increasing blade thickness while sacrificing the inception speed for back bubble cavitation. By changing the thickness from T_1 to T_3 (final), an approximate gain in the inception speed margin of the leading-edge sheet cavitation is about 3 knots, with similar sacrifice in the back bubble cavitation inception speed. However, since the inception speed of back bubble cavitation is out of the range of the ship operating speeds, it is of less practical importance.

*Since the chordlength is zero at the tip, t/c becomes infinity at the very tip. However, by extending t/c value smoothly, say from 0.95 radius to the tip, it gives an indication of how thick the blade is near the tip region.

OPEN-WATER PERFORMANCE

The open-water performance of the design propeller was predicted by using lifting-surface computer code PSF-2 developed by Greeley and Kerwin [11] based on the discrete vortex/source element method. A constant section drag coefficient of 0.0085 was used in the computation. Figure 19 shows the computed K_T and K_Q values as a function of advance coefficient J. At lower advance coefficients where the loading is high, the convergence of the wake alignment process in the computation was very slow. At J=0.2, the wake alignment process failed to converge. Thus, the values for K_T and K_Q were extrapolated to J=0.2.

At the design advance coefficient J_A of 0.770, K_T and K_Q values were 0.303 and 0.0597, respectively. The thrust coefficient is almost identical to the design value from the lifting-surface code PBD-10 but the torque coefficient is about 4.7% higher than that from PBD-10. The discrepancy is presumably due to the increased pitch near the tip region.

PREDICTION OF DELIVERED POWER AND RPM

Once the propeller open-water performance and the ship powering characteristics are known, the propeller rotational speed and the delivered power can be estimated assuming that the propeller/hull interaction coefficients, $(1-t)$ and $(1-w_T)$, are same for both the stock and the design propellers.

For a given ship speed V, the advance coefficient J can be obtained from the intersection of K_T/J^2 curve and the propeller open-water curve (K_T versus J). From this J the propeller rotational speed can be computed as follows:

$$n = \frac{V\ (1-w_T)}{J\ D} \qquad (12)$$

The delivered power P_D can be obtained from the effective power P_E and the estimated propulsive efficiency η_D:

$$P_D = P_E/\eta_D \tag{13}$$

The propulsive efficiency is obtained from the propeller open-water efficiency η_O, relative-rotative efficiency η_R, and the hull efficiency η_H:

$$\eta_D = \eta_O \eta_R \eta_H \tag{14}$$

The estimated propeller RPM and the delivered power at both full-load and ballast conditions are summarized in Table 12 and are presented graphically in Figures 20 and 21. For each loading condition, two curves are shown; one for no EHP margin and the other for a 6% EHP margin. At full power design condition, the estimated ship speed is 20.81 knots and propeller RPM is 99.5. These values are close enough to the design speed of 20.62 knots and RPM of 100. At 80% full power with 6% EHP margin, the estimated ship speed is 19.13 knots, which meets the design requirement of 18.8 knots.

FINAL DESIGN GEOMETRY

The final geometric properties necessary for manufacture, including the details of the leading and trailing edges, were obtained by fairing the basic data at 11 standard radial stations (see Table 11) at each 2.5 percent of propeller radius from hub to 95 percent radius and at each 1 or less percent of propeller radius from the 0.95 radius to the tip.

It is a common practice to add extra thickness in the trailing-edge region in order to ensure adequate strength. The amount of the extra thickness is determined somewhat subjectively. In the present case, the extra thickness was added such that the trailing-edge thickness would be at

least 0.4 inches from the hub to the 0.85 radius. In the region from 0.85 radius to the tip, the trailing edge was thickened to about 10 % of the maximum thickness at a given radial section. In the region from the hub to the 0.6 radius, the basic thickness at the trailing edge was already thicker than 0.4 inches, thus no additional thickness was added. For a given radius, the additional thickness is added from the maximum thickness location to the trailing edge.

After thickening the trailing edge, the standard trailing edge details currently in use at DTNSRDC were incorporated. Near the hub ($0.2 \leq r/R \leq 0.3$), a round trailing edge is employed so that lifting slings can be used to move the propeller. In the round trailing-edge region, the trailing-edge radius was taken as the half thickness (including the additional thickness if any) of the blade at the trailing edge. Further out along the radius of the blade, hydrodynamic considerations are more important and an anti-singing trailing edge is specified. This region is called the 'knuckle region'. In this region the trailing-edge radius was taken as 1/64 inch or one tenth of the trailing-edge thickness, whichever is smaller.

The final offsets of the full-scale propeller are shown in Table 13. In this table, the trailing-edge details such as rounding and anti-singing knuckles are not included for simplicity. Figure 22 shows the manufacturing drawing of the model propeller based on the final offsets in Table 13.

OPEN-WATER AND POWERING EXPERIMENTS USING DESIGN PROPELLER

Based on the offsets shown in Table 13, an aluminum model propeller (DTNSRDC Propeller 5027) was manufactured at SSPA in Sweden. In Figure 23, experimental and predicted open-water performances are compared. The predicted K_T and K_Q values from the lifting-surface code PSF-2 are in good

agreement with the experimental values near the design advance coefficient of 0.77. For J values larger than 1.0, the predicted K_T and K_Q values are substantially higher than the experimental values.

The powering experiments were carried out at DTNSRDC using Model 5326-2 with design Propeller 5027. Preliminary predictions* of full-scale powering performance for AO-177 JUMBO, based on model tests with the design propeller, are presented in Figures 24 and 25 for full-load and ballast conditions, respectively. At each loading condition, predictions were made for two cases with and without power (P_E) margin.

It is disturbing that the preliminary effective power data at full-load condition measured at DTNSRDC (see Table 15) and at Tracor Hydronautics (see Table 3) are somewhat different; at the design speed of 20.8 knots, the DTNSRDC P_E value is about 4.5 % lower than that of Tracor Hydronautics. Although exact cause of the difference is not known, the difference in trim condition might be one source of the discrepancy; i.e., the experiments at Tracor Hydronautics were made at 1.5 feet trim by bow whereas at DTNSRDC the experiments were conducted with an even keel condition.

This difference in effective power will affect the speed and rpm. For example, at a ship speed of 21 knots, the DTNSRDC P_E requires the propeller to rotate about 1.5 rpms lower than the Tracor Hydronautics P_E. At full power, however, the ship speed and propeller rotational speed for the DTNSRDC P_E are higher by about 0.2 knot and 0.0 rpm.

Table 14 compares the performance predictions made before and after the design propeller was built and tested. The early-stage predictions are

*The predictions were made and provided by Code 1521, DTNSRDC via Memorandum dated 9 October 1986.

in excellent agreement with final predictions. The propellre shaft speed is off by 0.5 rpm from the design value of 100. This excellent agreement is mainly due to the fact that the propeller/hull interaction coefficients, 1-t and $1-w_T$, are in good agreement between the stock and the design propellers and that the open-water performance have been predicted reasonably well.

DISCUSSION

The results of the propulsion experiments proved that the AO-177 JUMBO propeller is a successful design, satisfying all the design requirements. The successful design may be mainly due to the fact that the propeller/hull interaction coefficients, 1-t and $1-w_T$, for stock and design propellers are very close, especially near design speed (see Table 15). Although not presented in this report, cavitation tests at SSPA, Sweden also proved that the design propeller showed substantially improved performance in cavitation and cavitation-induced hull pressure compared to the original AO-177 propeller.

Propeller design requires complex trade-offs to satisfy various design requirements. Several assumptions are required at various design stages. Perhaps the most important assumption regarding the powering performance is the wake. The effective wake used in the design is obtained from model tests with stock propellers in conjunction with whatever adjustment is deemed appropriate to account for the differences in scale between model and ship. In the present design, the model wake has been used in surface-ship design, assuming there are negligible scale effects. Therefore, the performance of the full-scale propeller at sea is very much dependent upon how well the full-scale wake was predicted, as well as the quality of the model-scale effective wake.

The method of estimating the effective wake based on the nominal wake is also worth mentioning. In the present design, the nominal wake has been increased by a constant factor throughout the radii (see Equation (1)) to obtain the effective wake. As a result, the amount of increase was larger at the outer radii than at the inner radii. The predicted effective wake for a body of revolution using a more rational approach [18] showed different behavior, i.e., the increase in the mean axial velocity is larger near the hub than near the tip. Some parametric studies would be useful in determining the differences in performance between designs using different effective wake distributions.

It is to be noted that the K_T and K_Q values computed by the lifting-surface code PBD-10 are higher than lifting-line values by 4.5% and 2.2%, respectively, for the same radial circulation distribution. A careful evaluation of PBD-10 is recommended to identify the source of the discrepancy.

ACKNOWLEDGEMENTS

The author is grateful to the Propulsor Design Review Committee of Code 1544, DTNSRDC; F. Peterson, A. Reed and S. Jessup, for their discussions and critique of the design. Careful readings by A. Reed and R. Cummings substantially improved the style of the report.

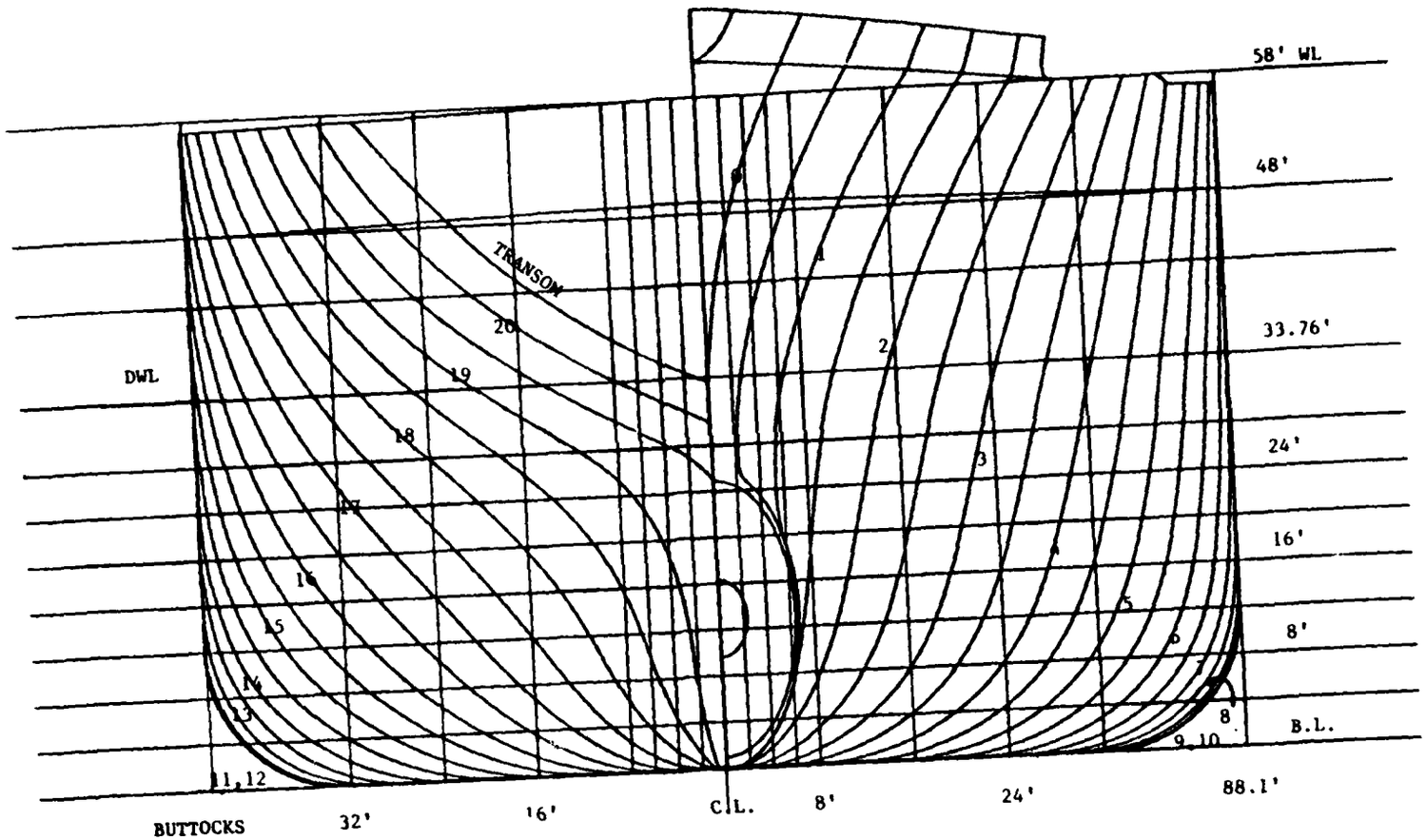

Fig. 1. Body plan of AO-177 JUMBO.

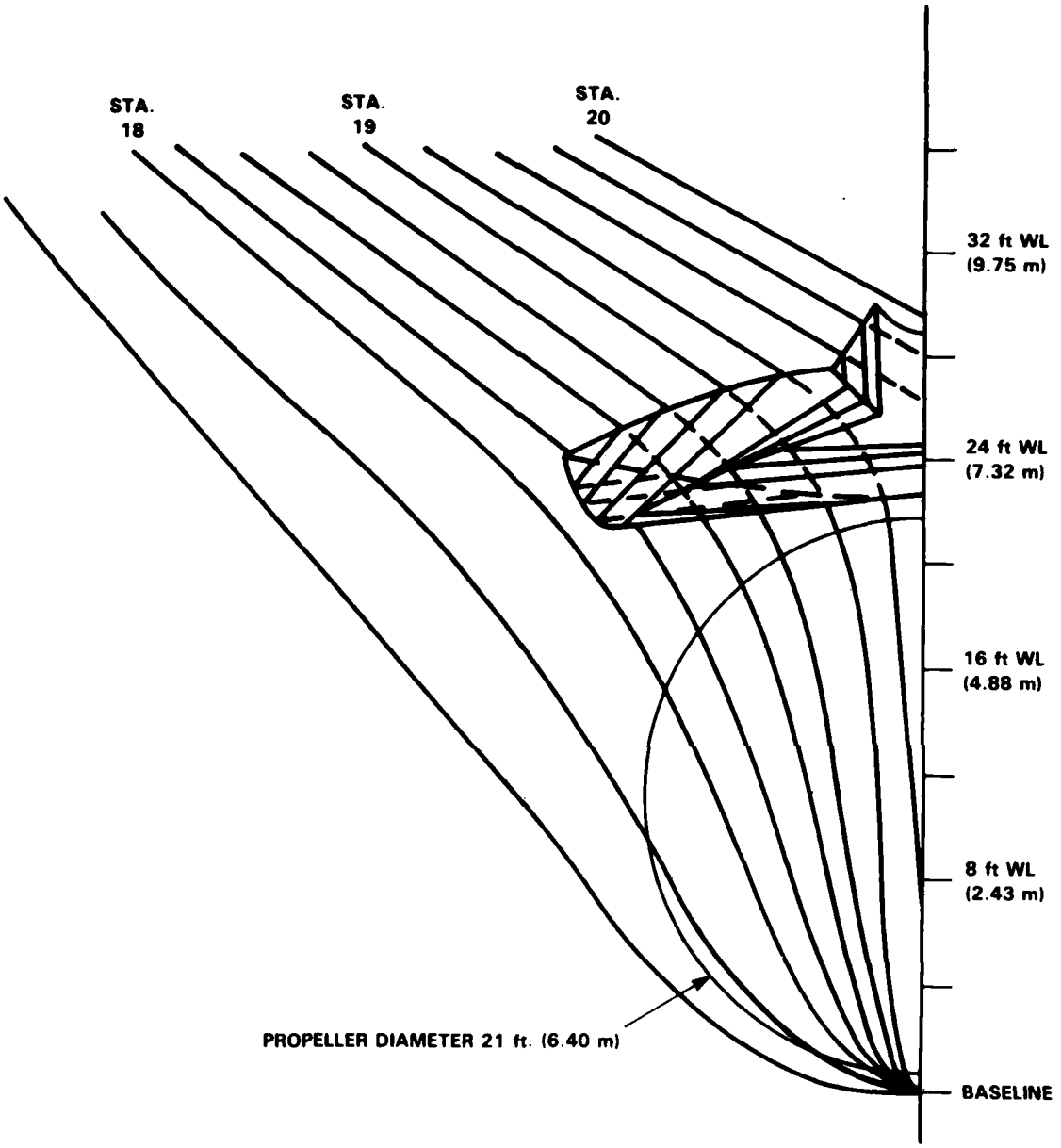

Fig. 2. Illustration of flow-accelerating fin configuration designed by SSPA.

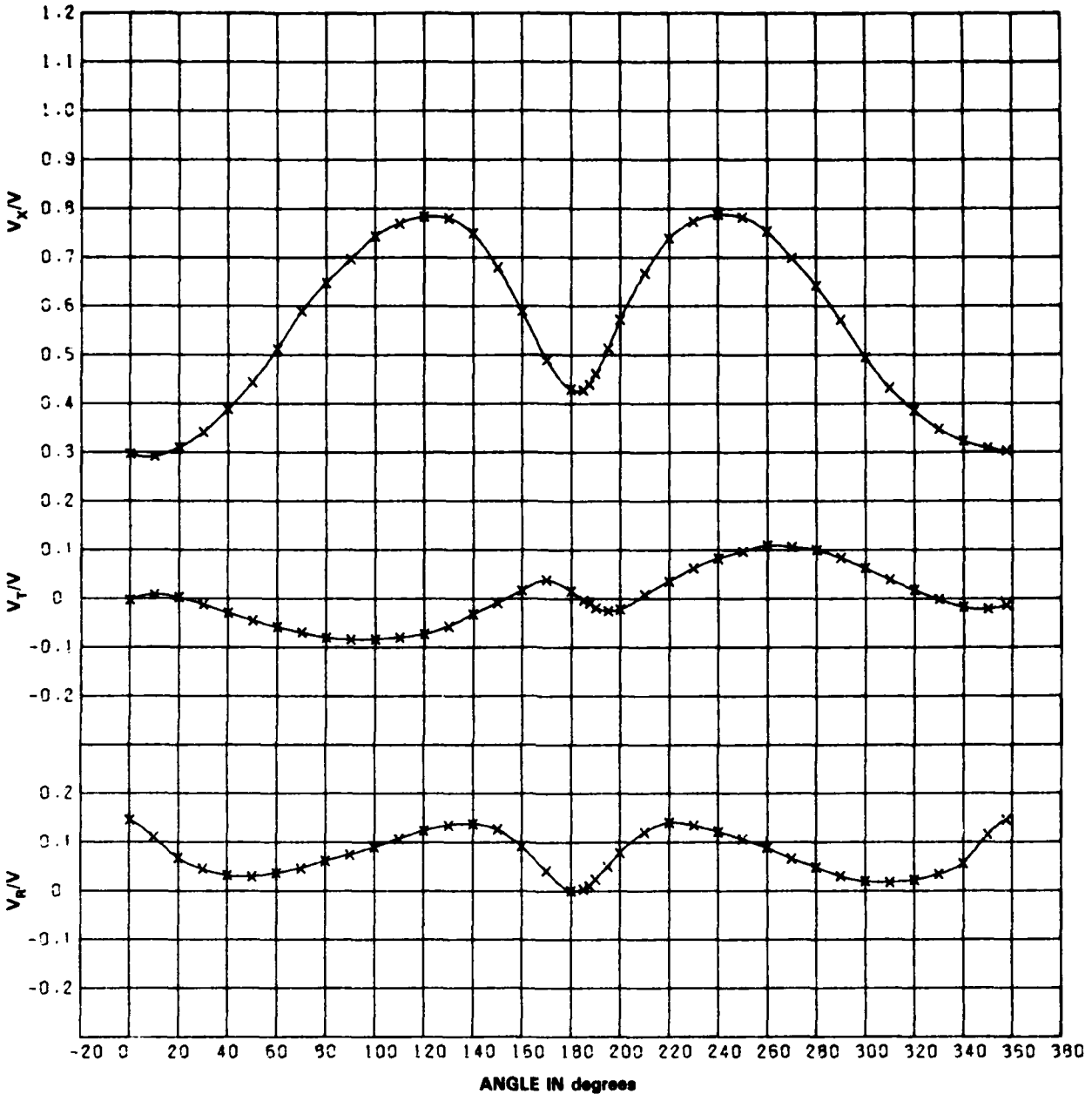

Fig. 3a. r/R = 0.41

Fig. 3. Circumferential variation in the axial, tangential and radial velocity components.

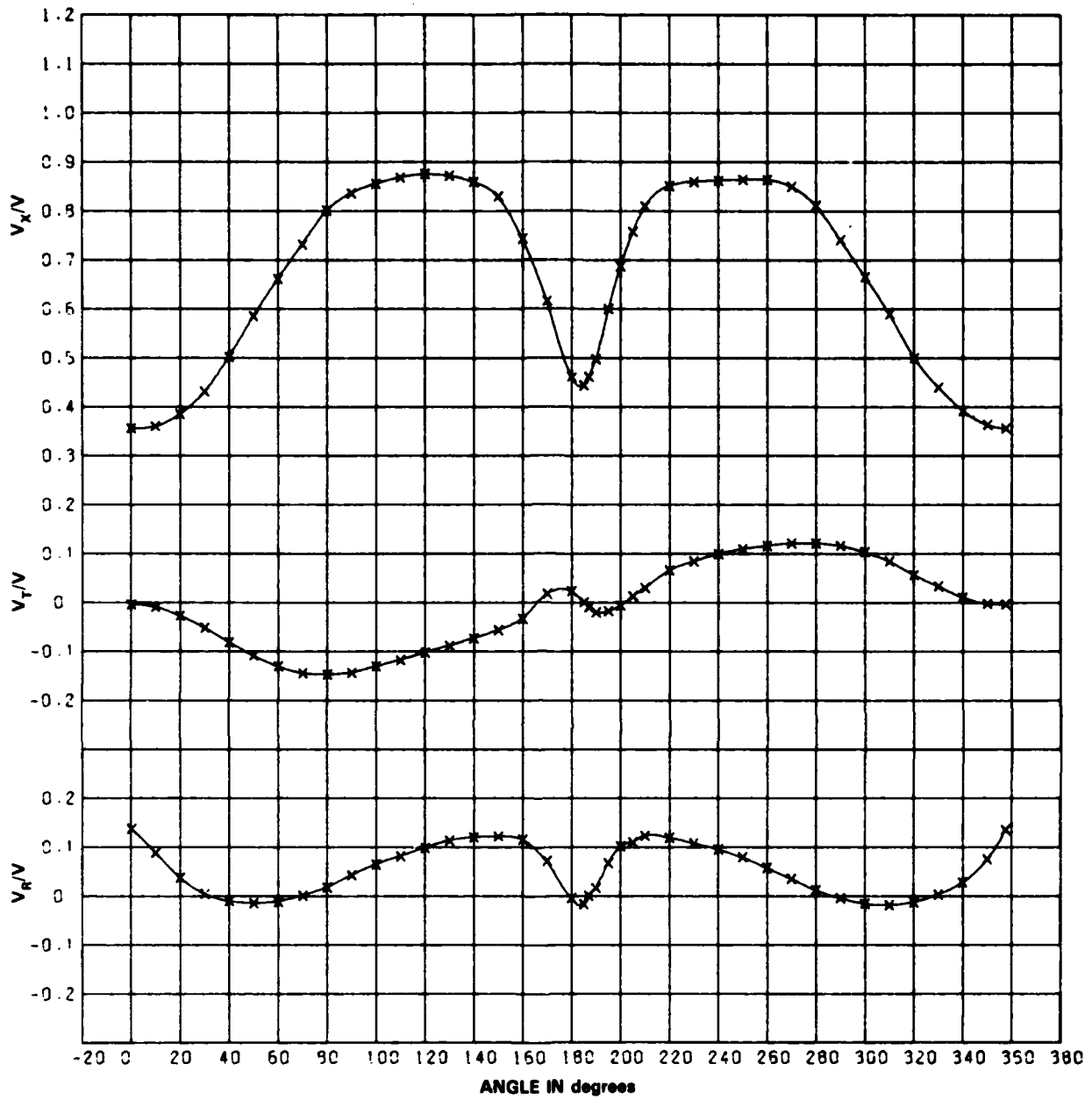

Fig. 3b. r/R = 0.55

Fig. 3. (Continued)

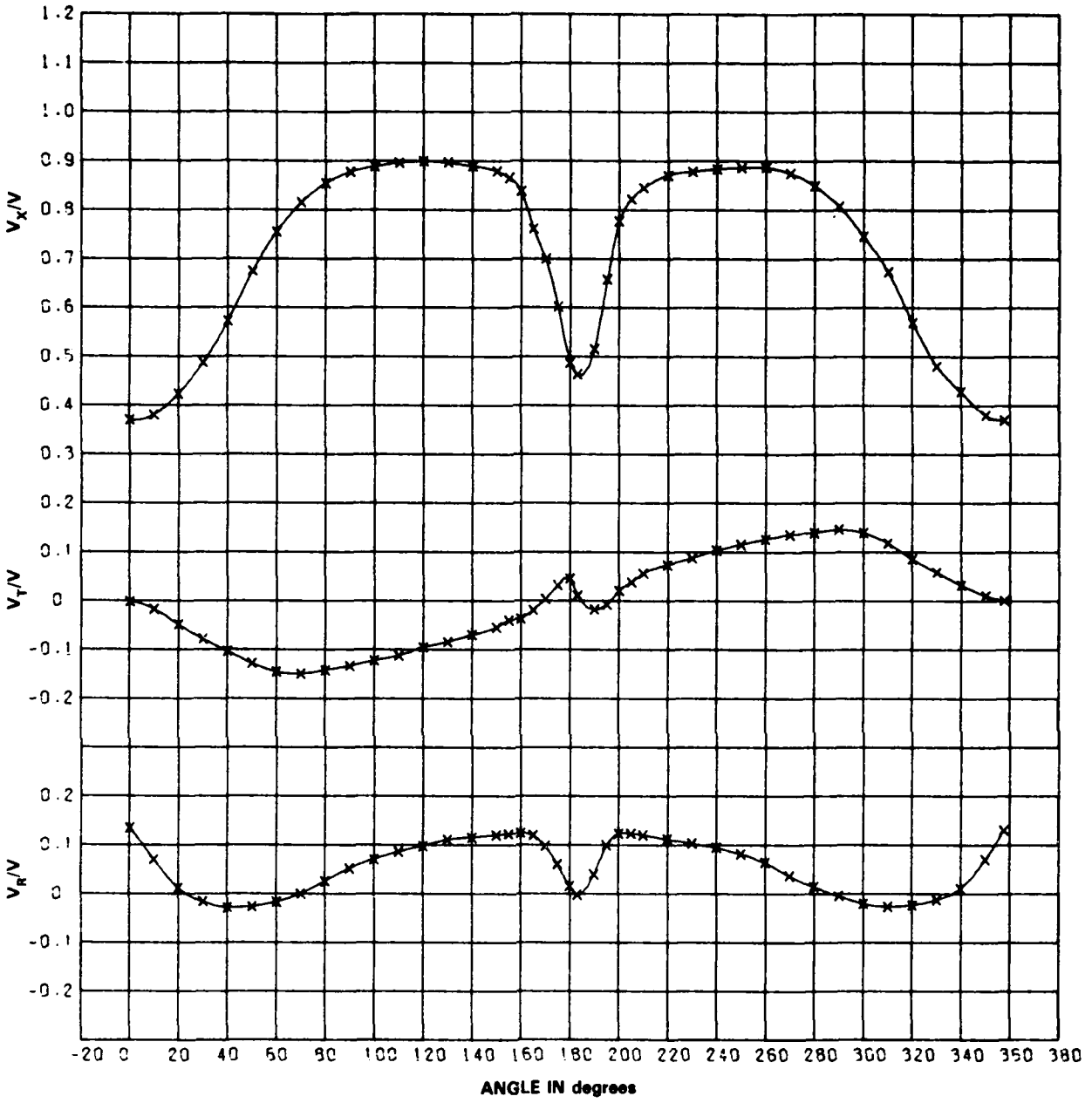

Fig. 3c. r/R = 0.65

Fig. 3. (Continued)

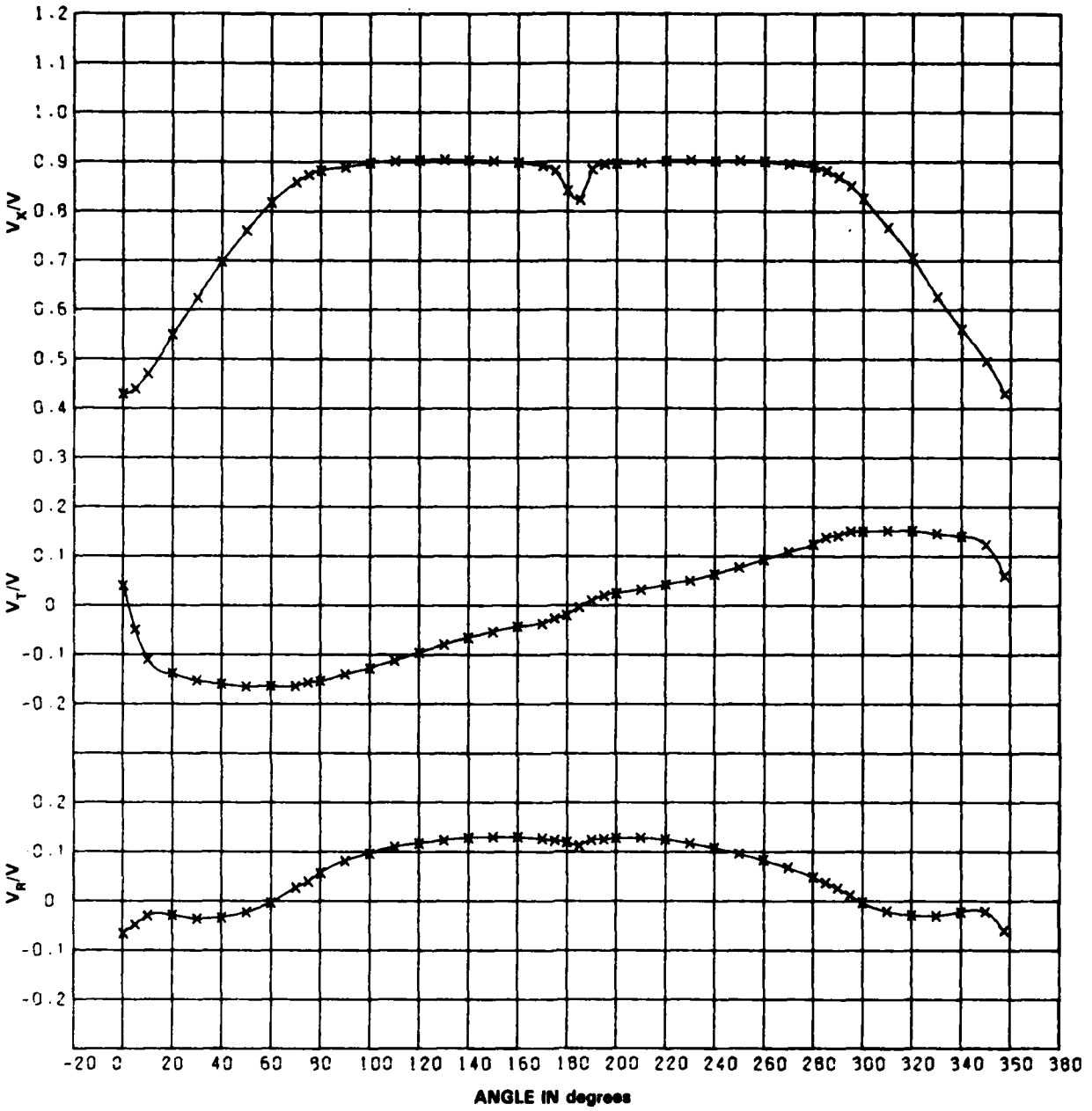

Fig. 3d. r/R = 1.04

Fig. 3. (Continued)

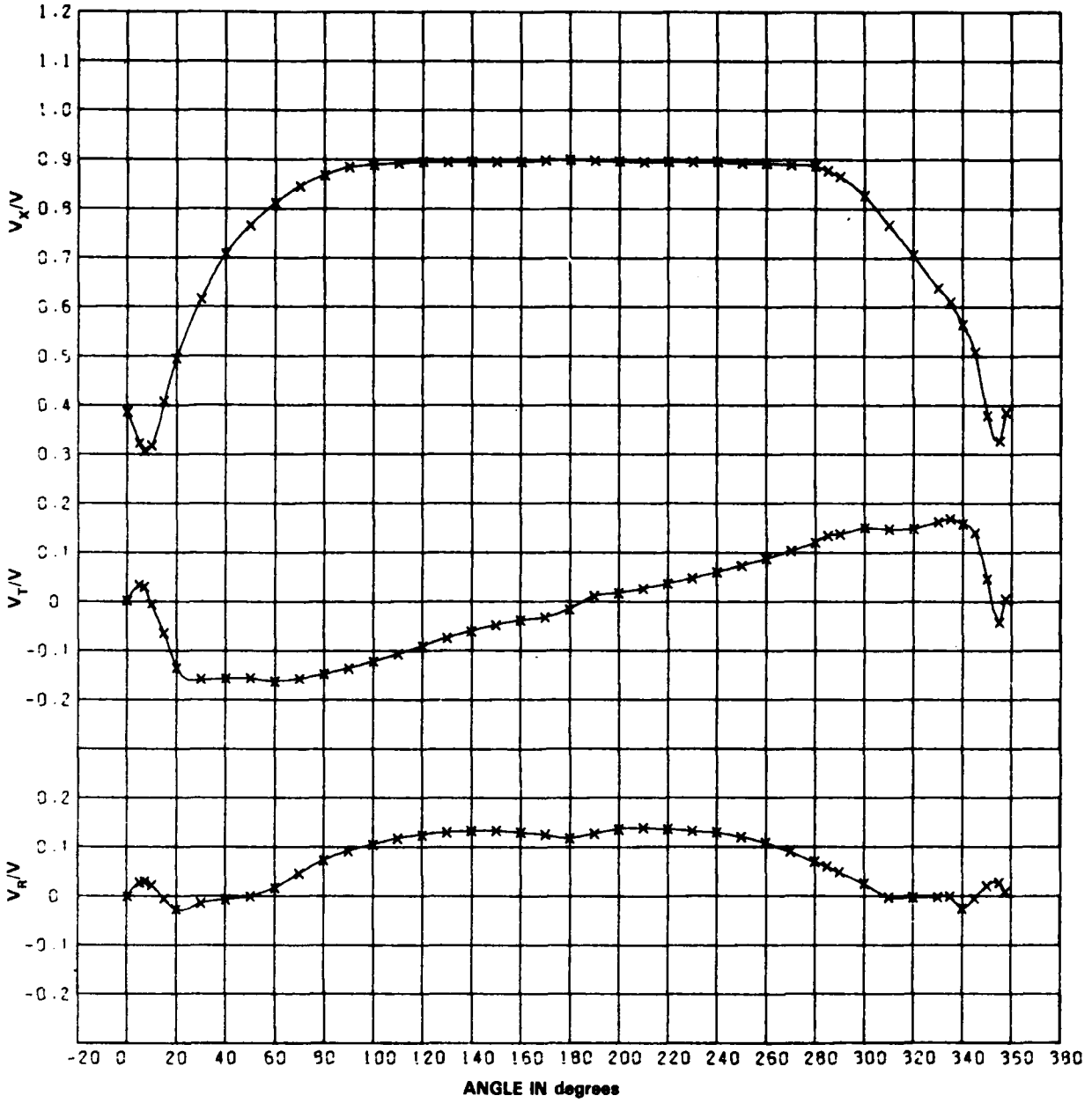

Fig. 3e. r/R = 1.14

Fig. 3. (Continued)

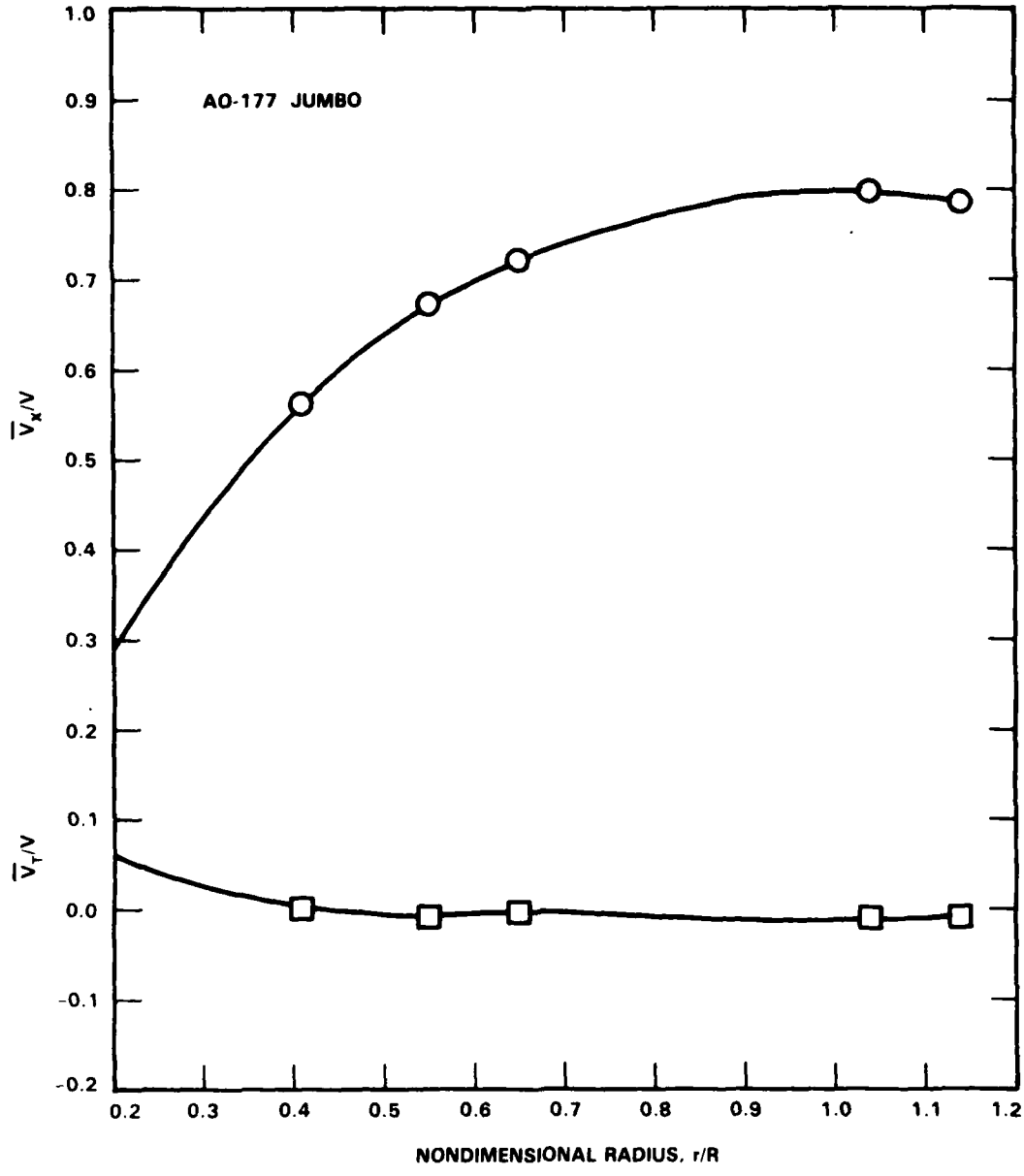

Fig. 4. Radial distribution of circumferential average of axial, and tangential velocity components.

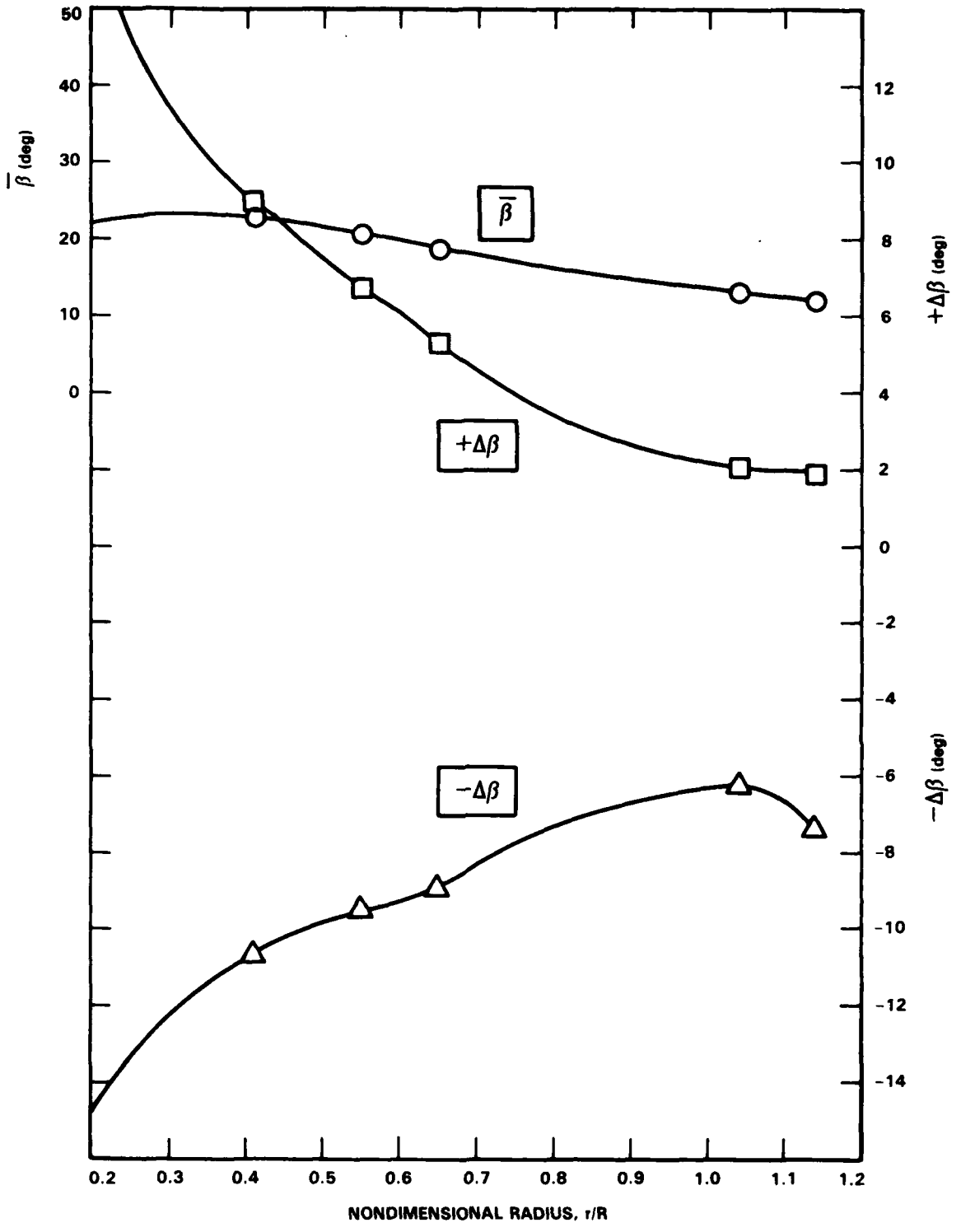

Fig. 5. Radial distribution of circumferential average and variation of angle of advance.

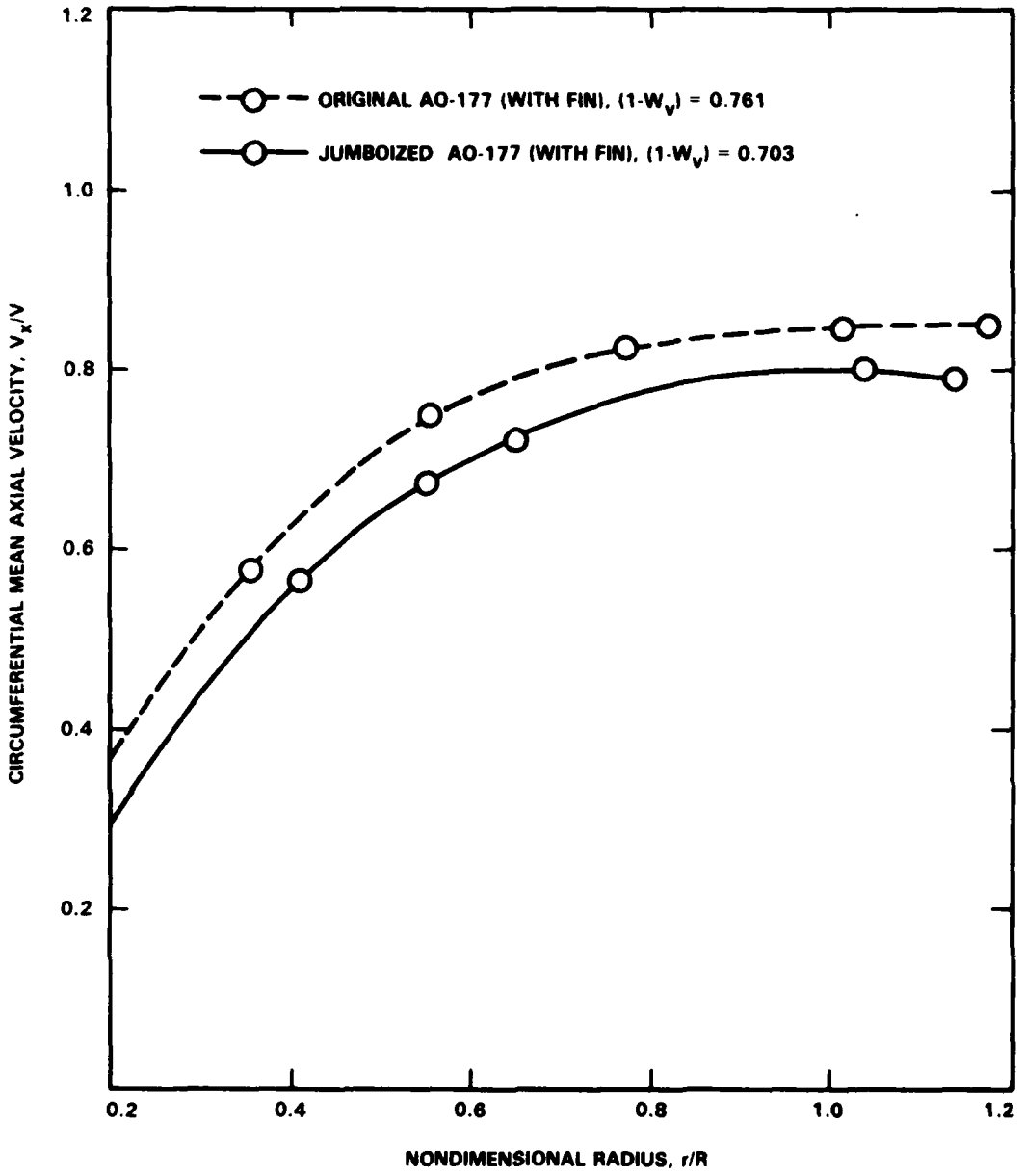

Fig. 6. Comparison of circumferential mean axial velocity between original and jumboized AO-177.

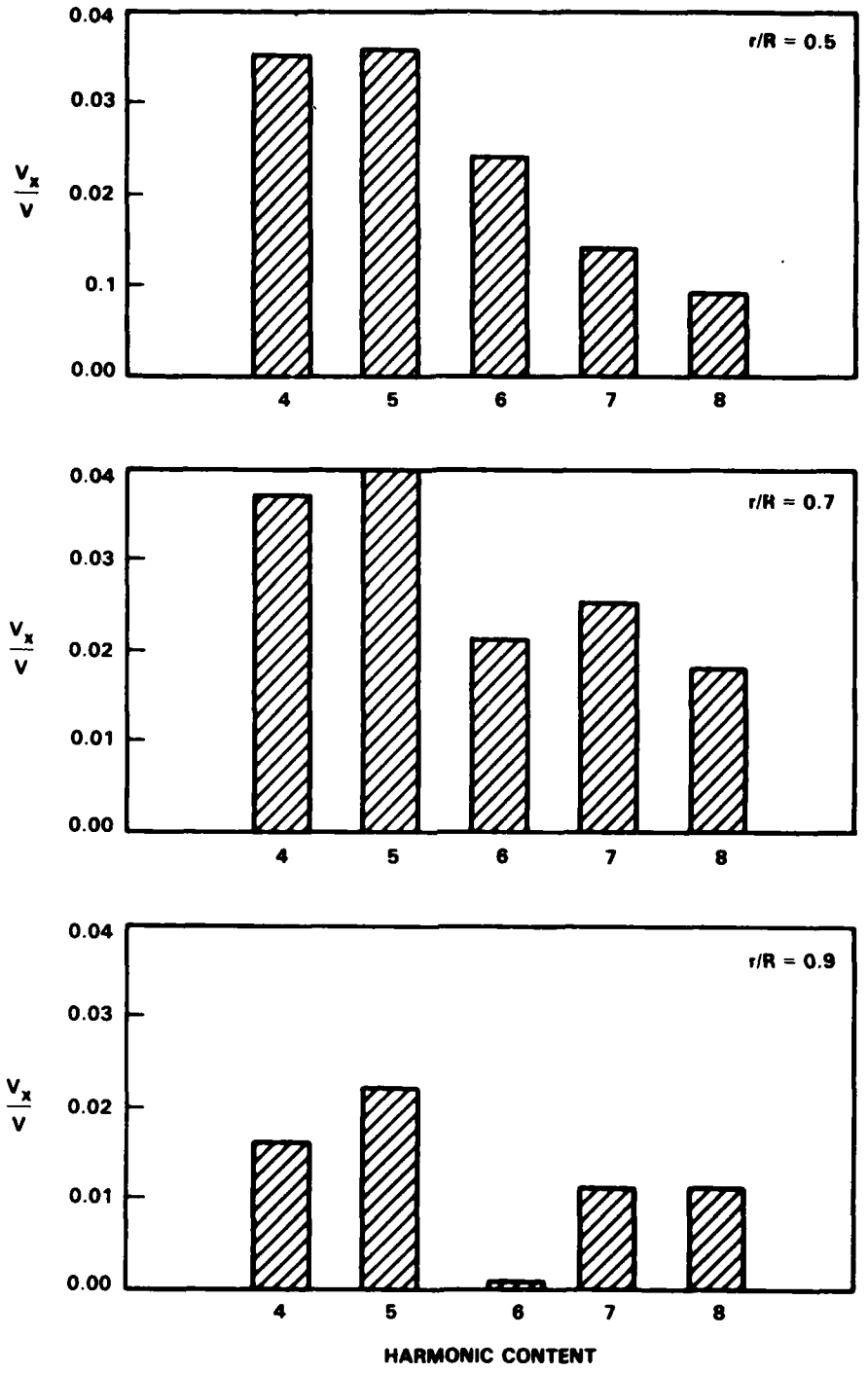

Fig. 7. Harmonic content of axial wake velocity.

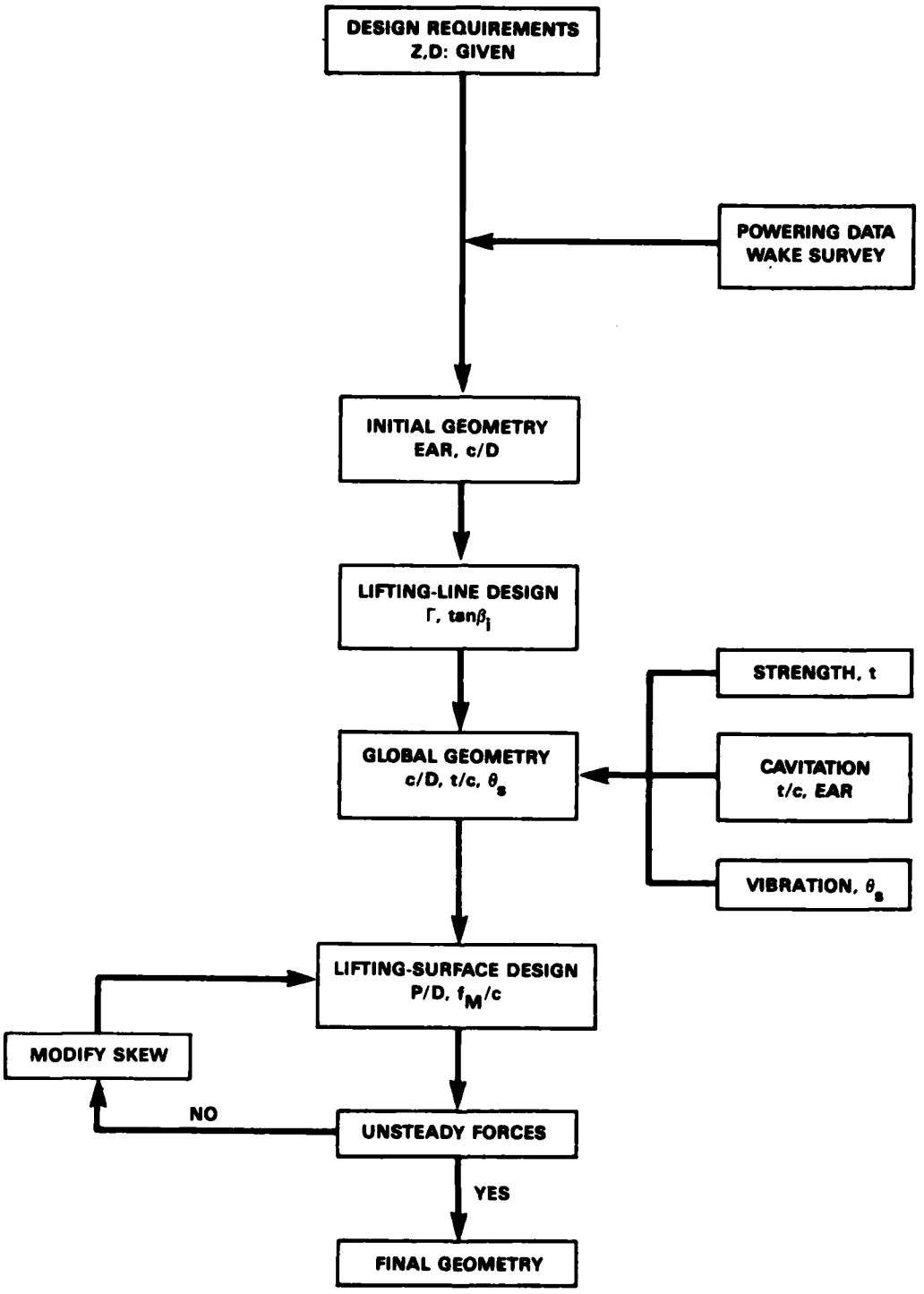

Fig. 8. Design procedure for AO-177 JUMBO propeller.

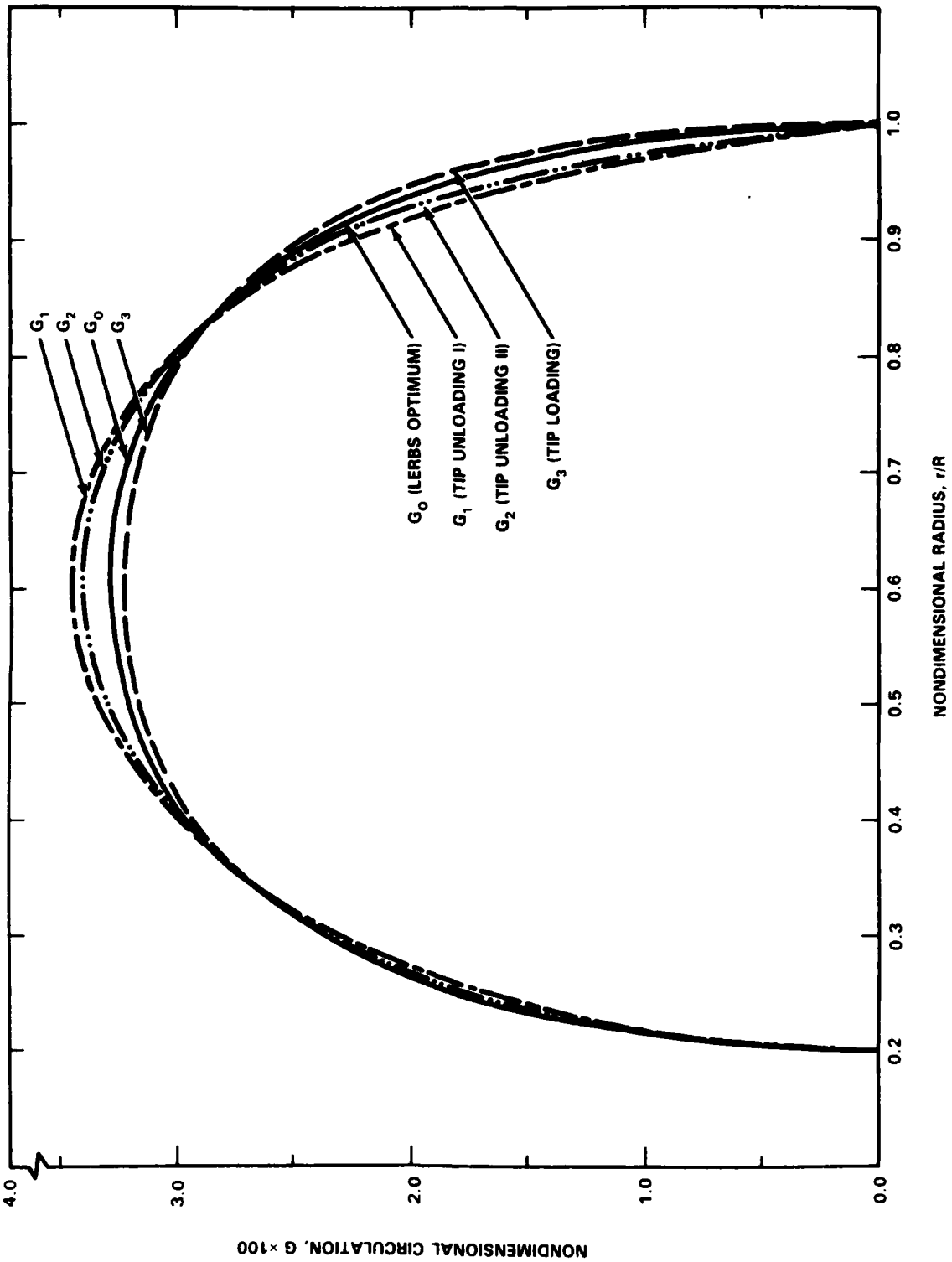

Fig. 9. Circulation distributions investigated during design

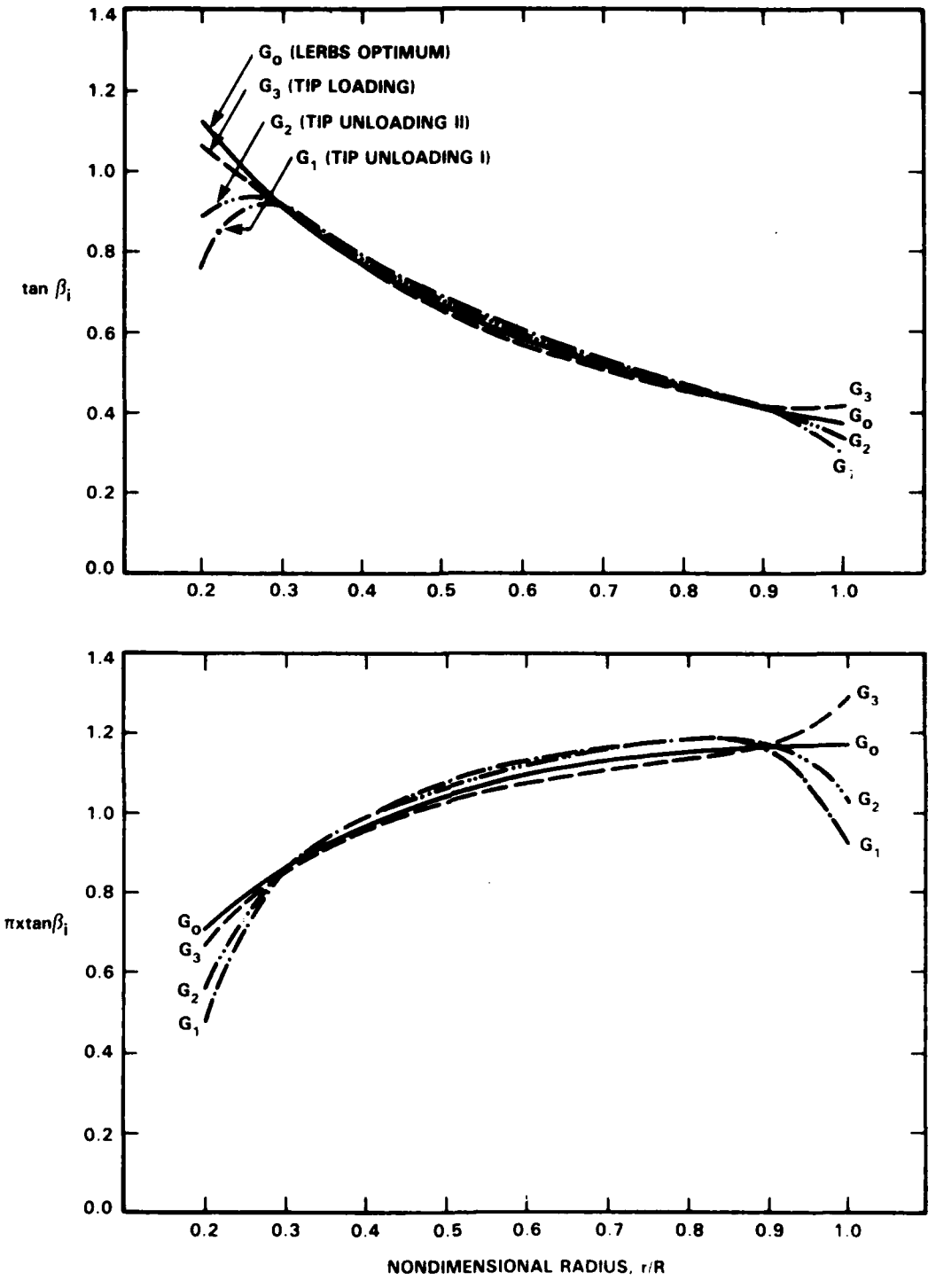

Fig. 10. Hydrodynamic pitch angle and lifting-line pitch distribution.

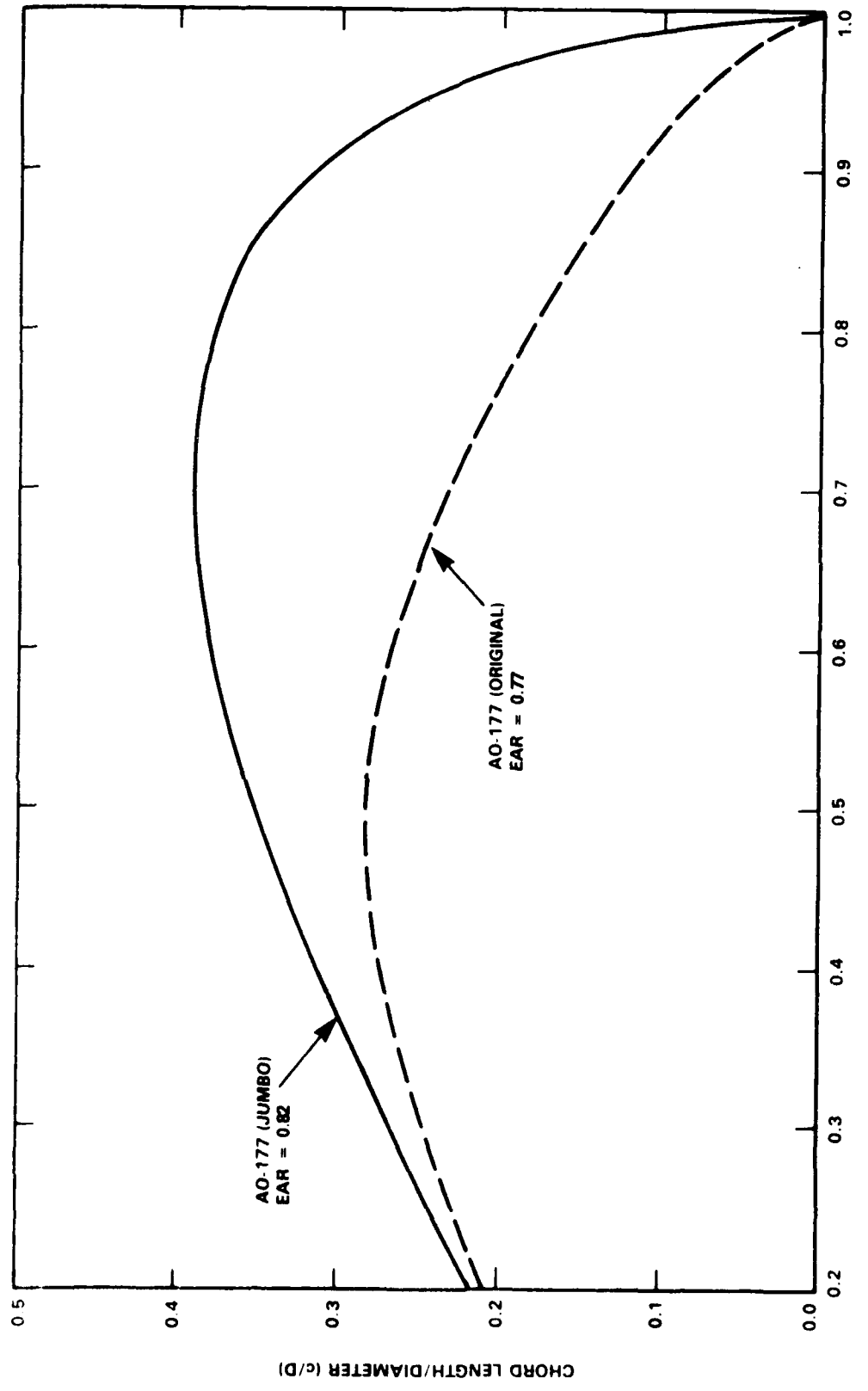

Fig. 11. Radial distribution of chord length.

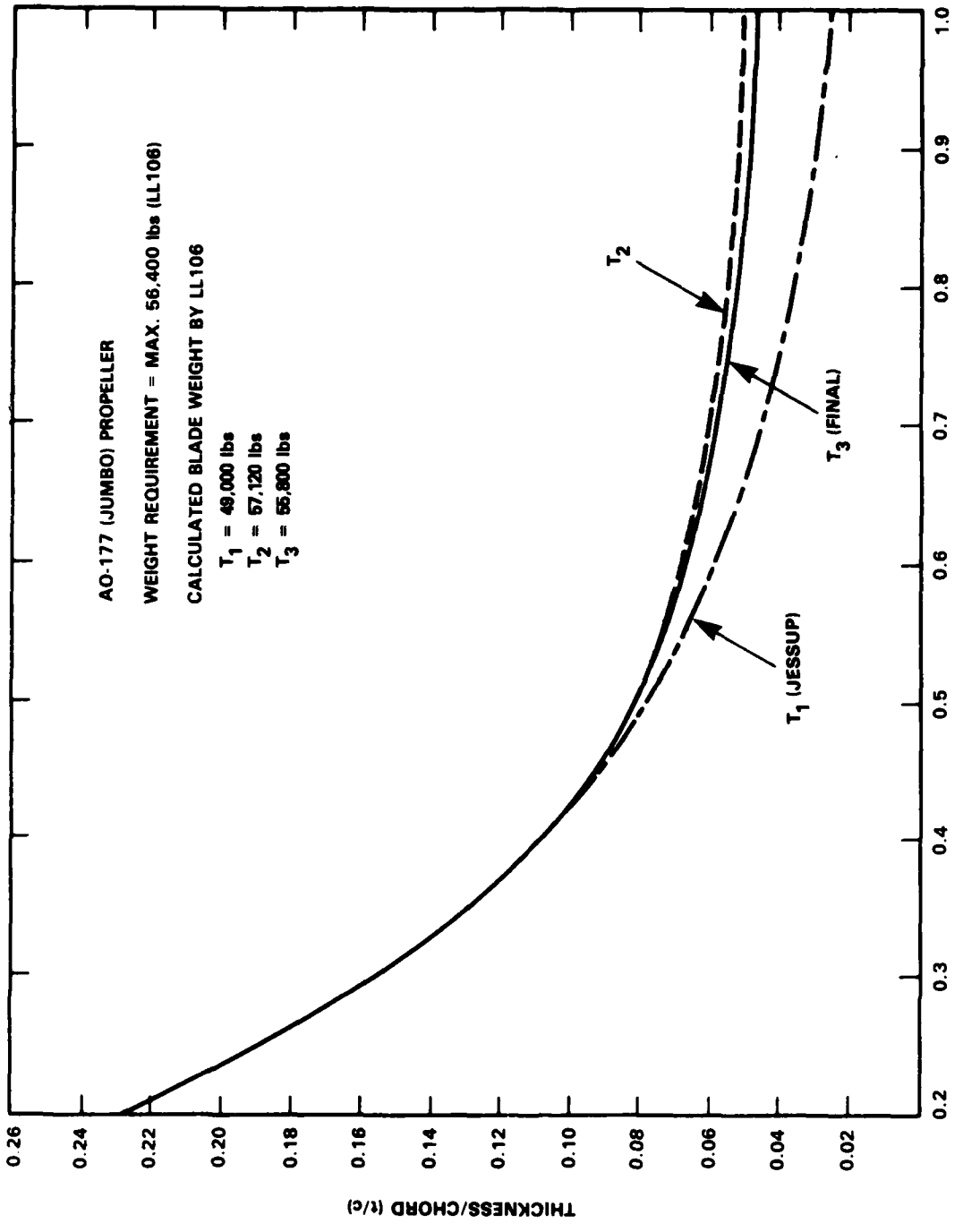

Fig. 12. Radial distribution of thickness.

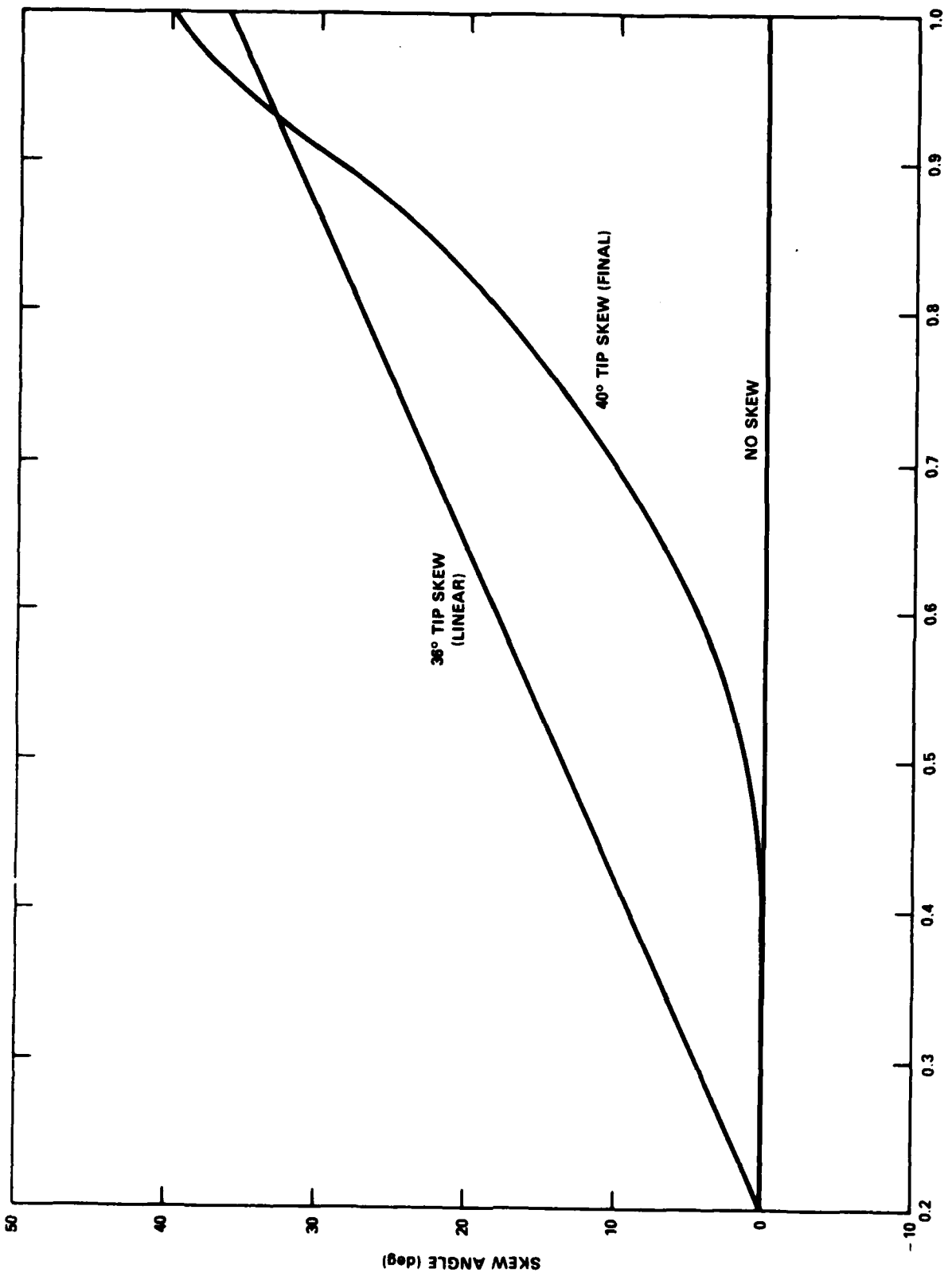

Fig. 13. Skew distribution investigated during design.

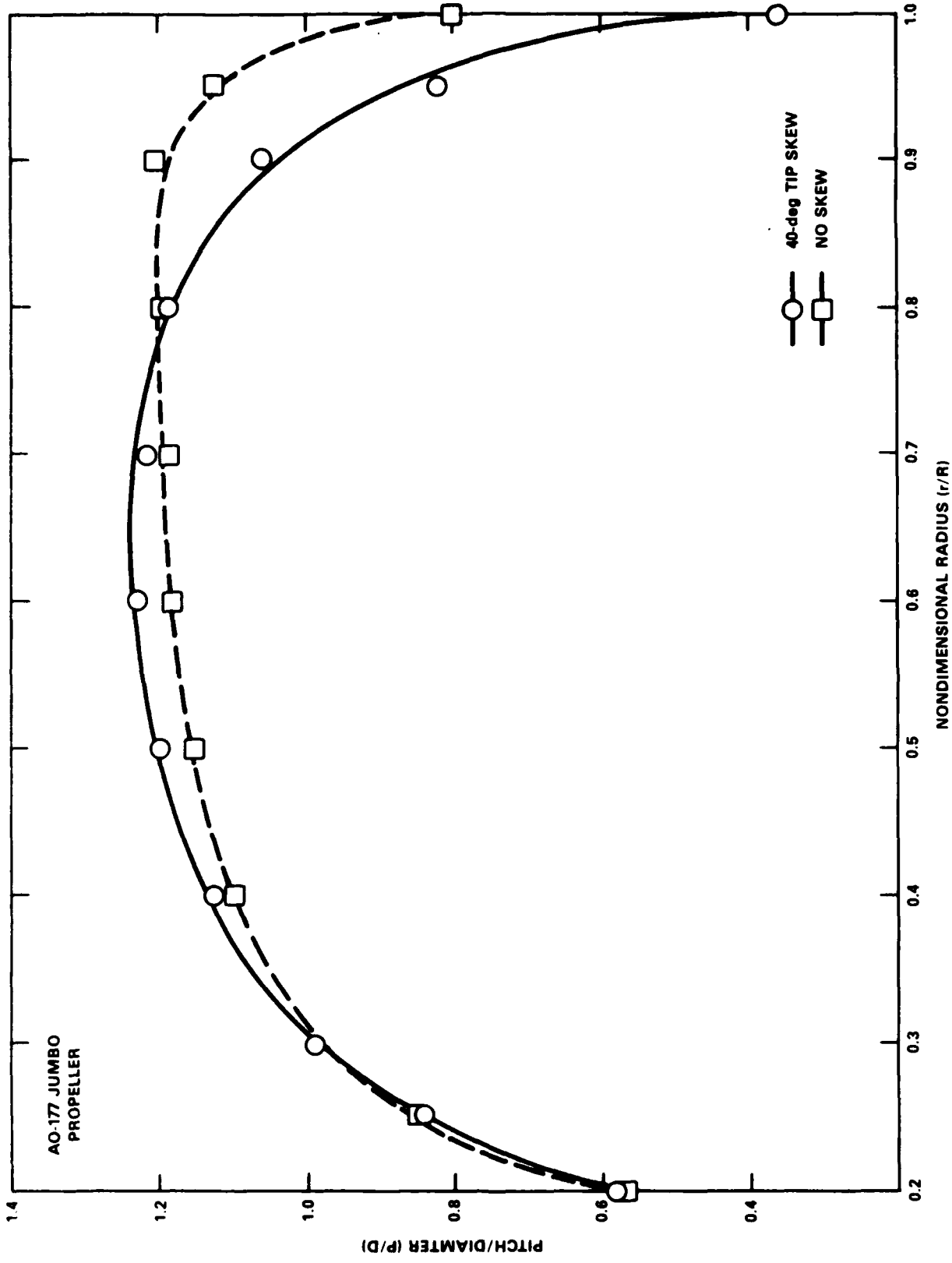

Fig. 14. Effect of skew on the calculated pitch using lifting-surface code, PBD-10.

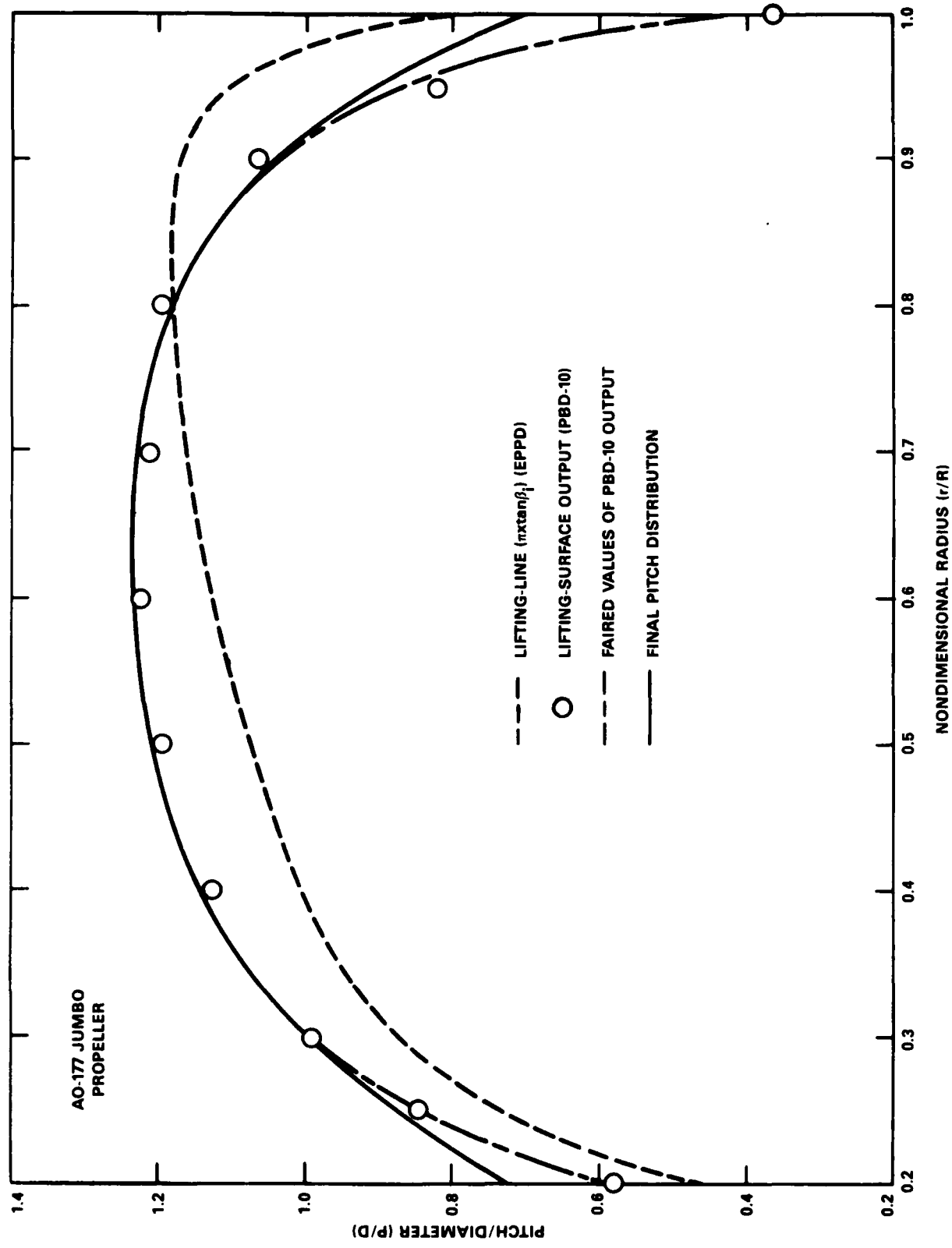

Fig. 15. Final pitch distribution (P/D) predicted by lifting-surface code, PBD-10.

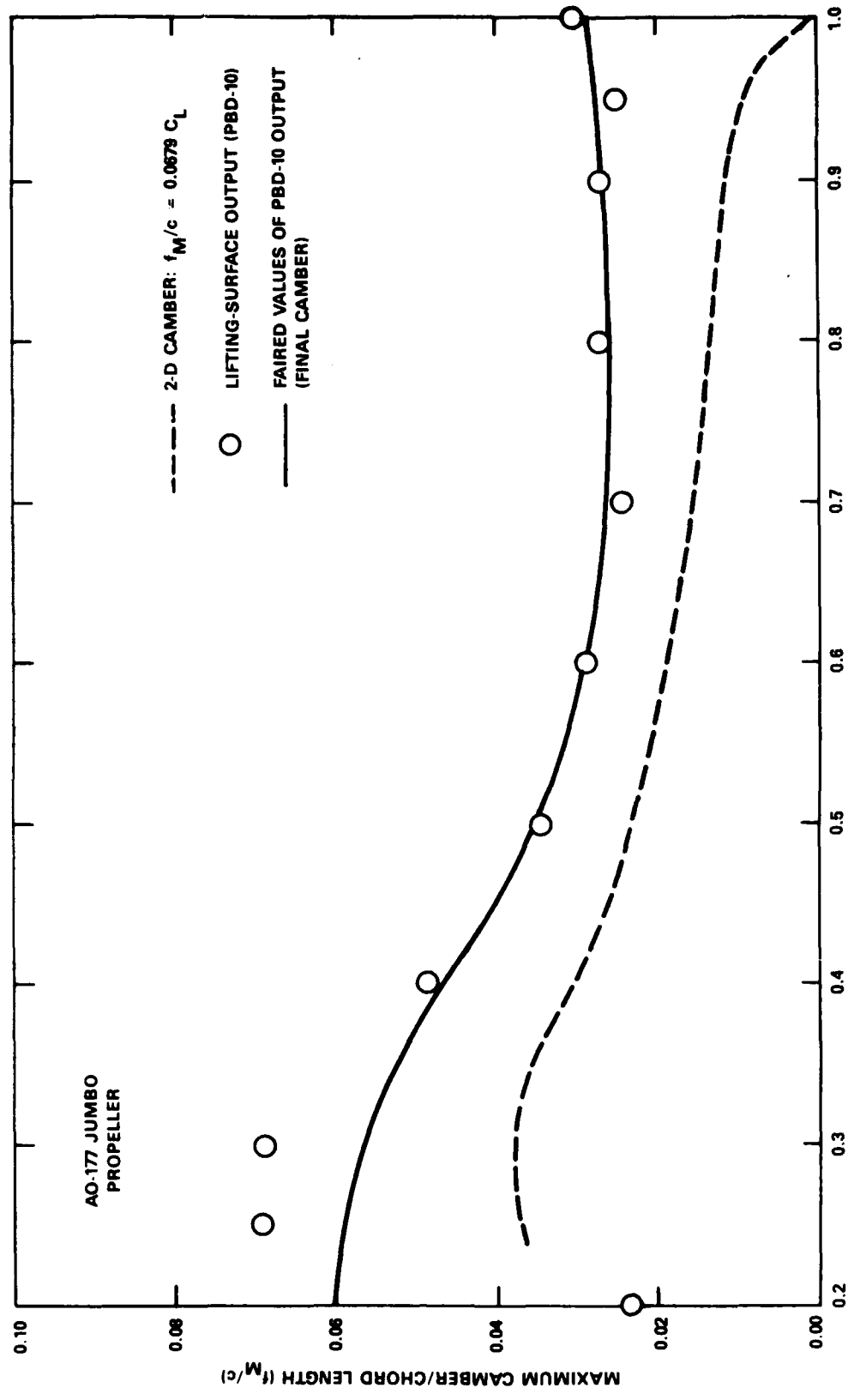

Fig. 16. Final camber distribution (f_M/c) predicted by lifting-surface code, PBD-10.

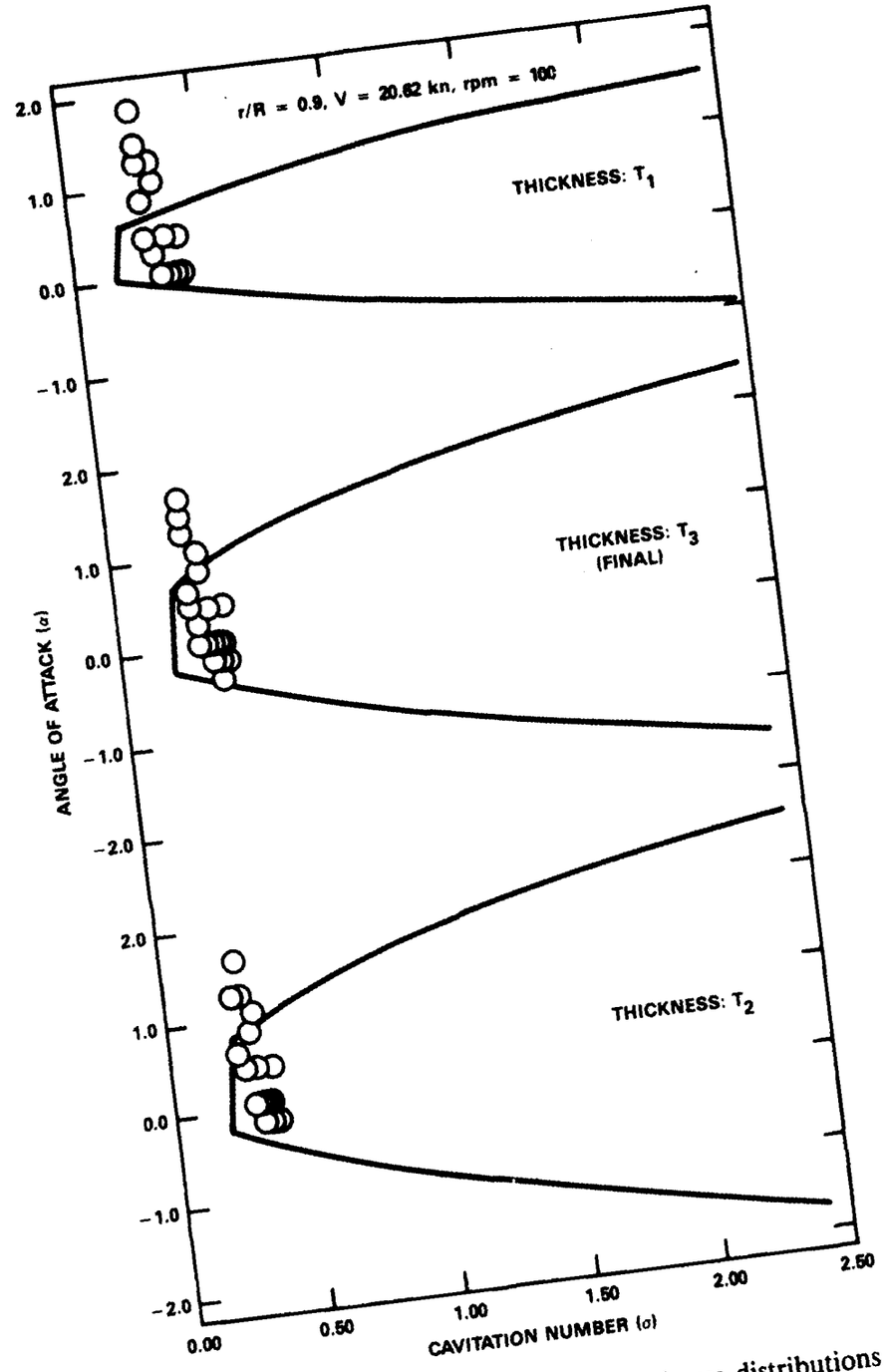

Fig. 17. Cavitation bucket for different thickness distributions at full-power design condition for AO-177 JUMBO.

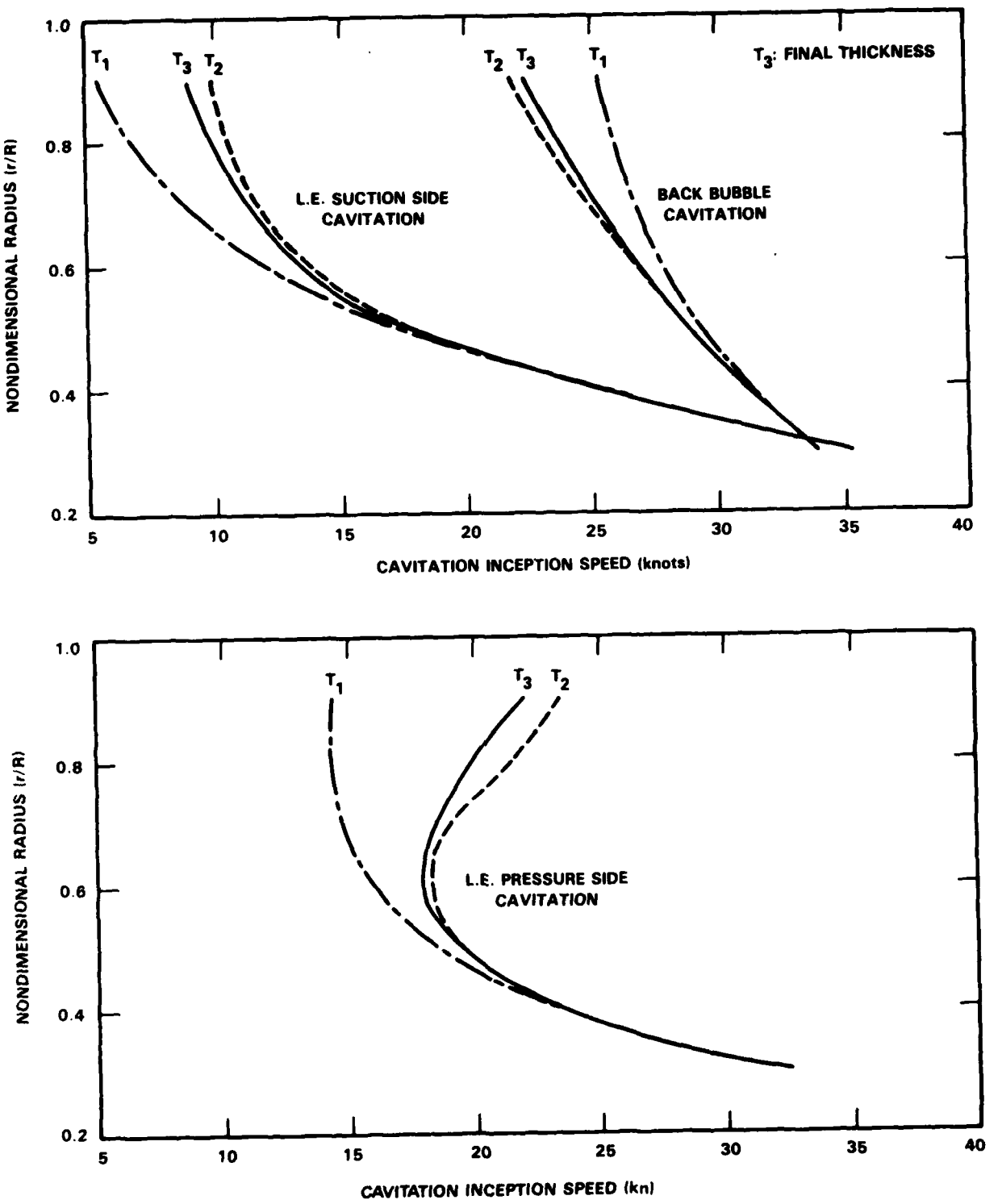

Fig. 18. Inception speed of various cavitations for different thickness distribution.

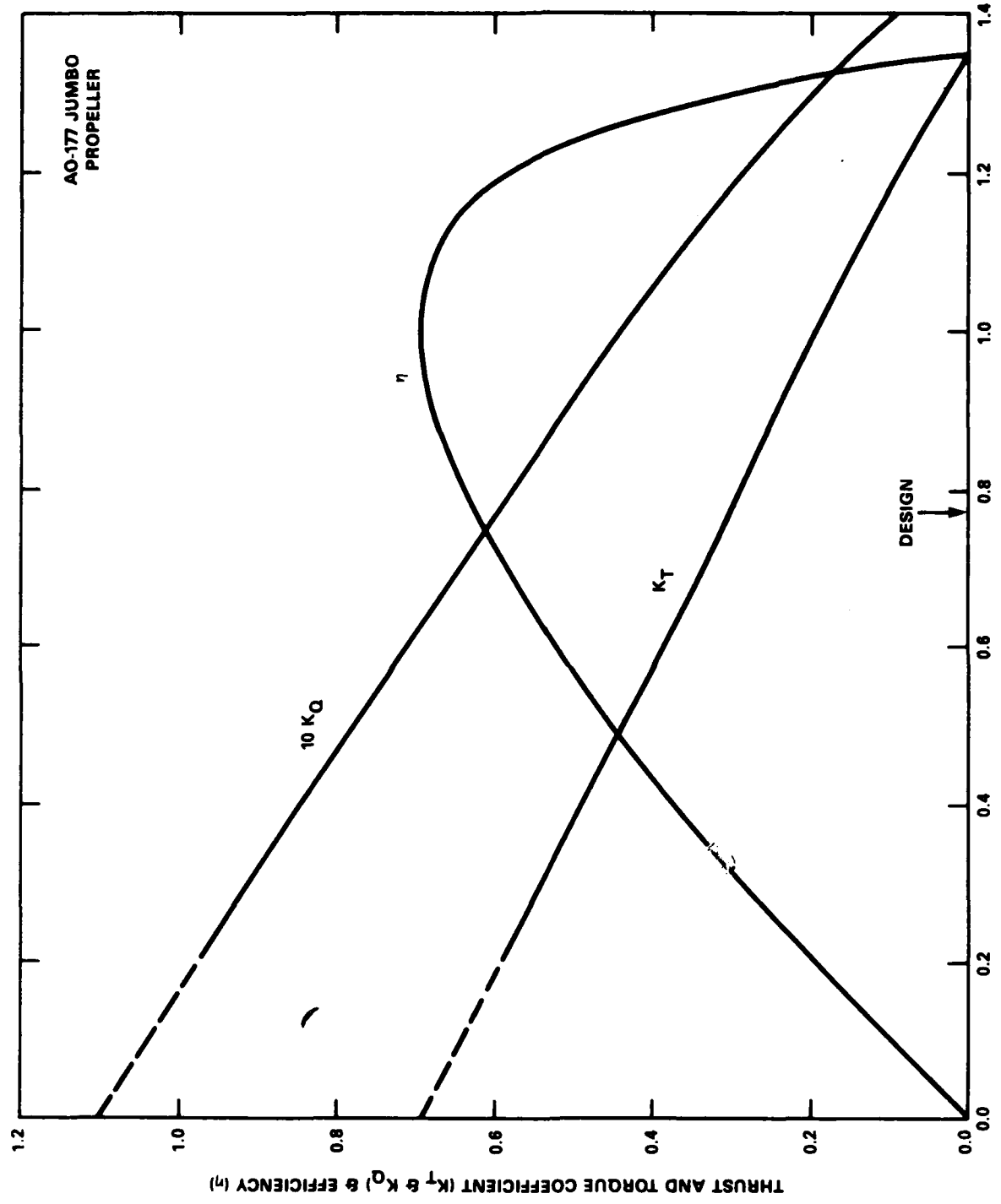

Fig. 19. Open-water performance predicted by lifting-surface code, PSF-2.

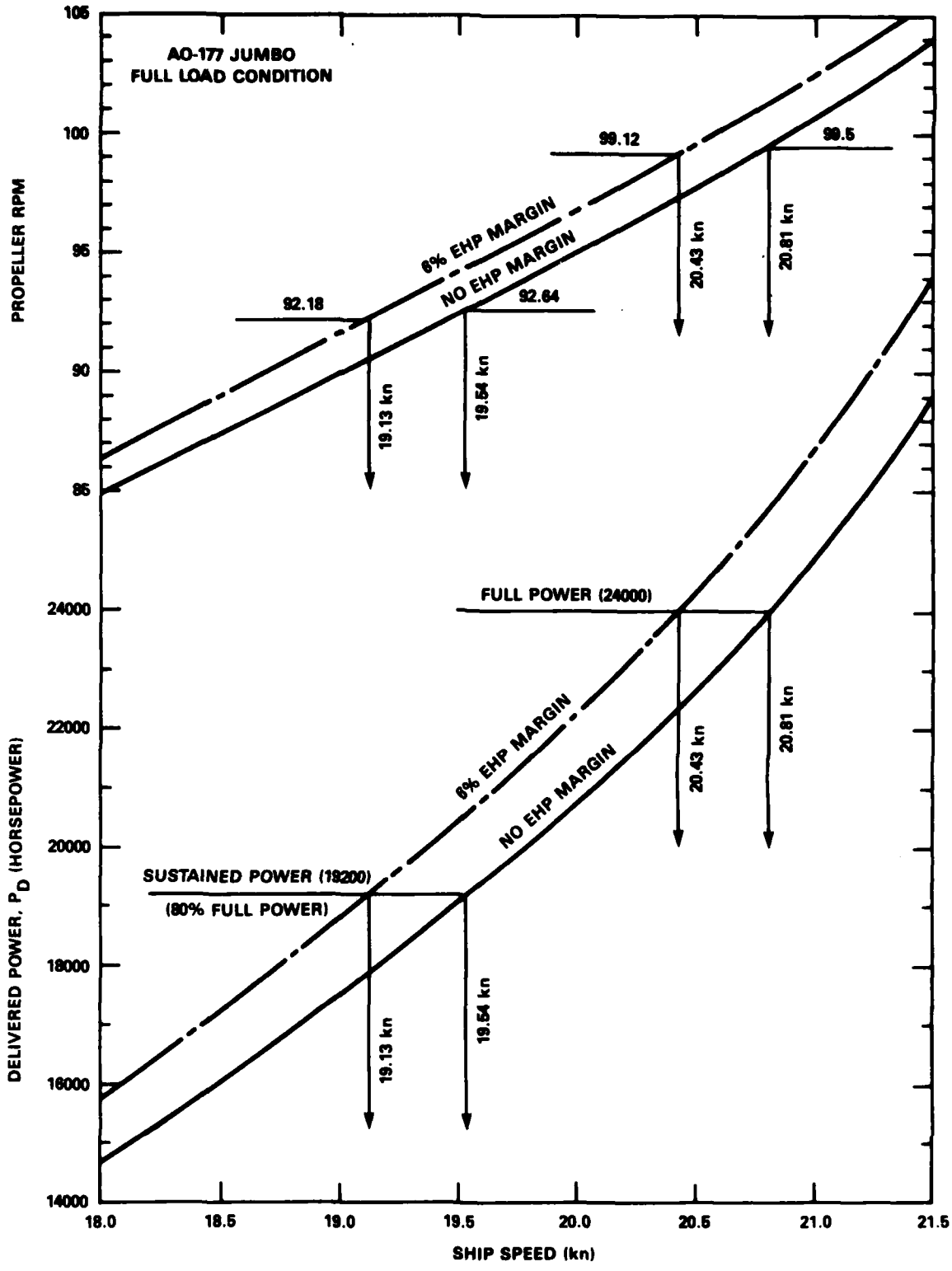

Fig. 20. Predicted full-scale power and rpm of AO-177 JUMBO at full load condition.

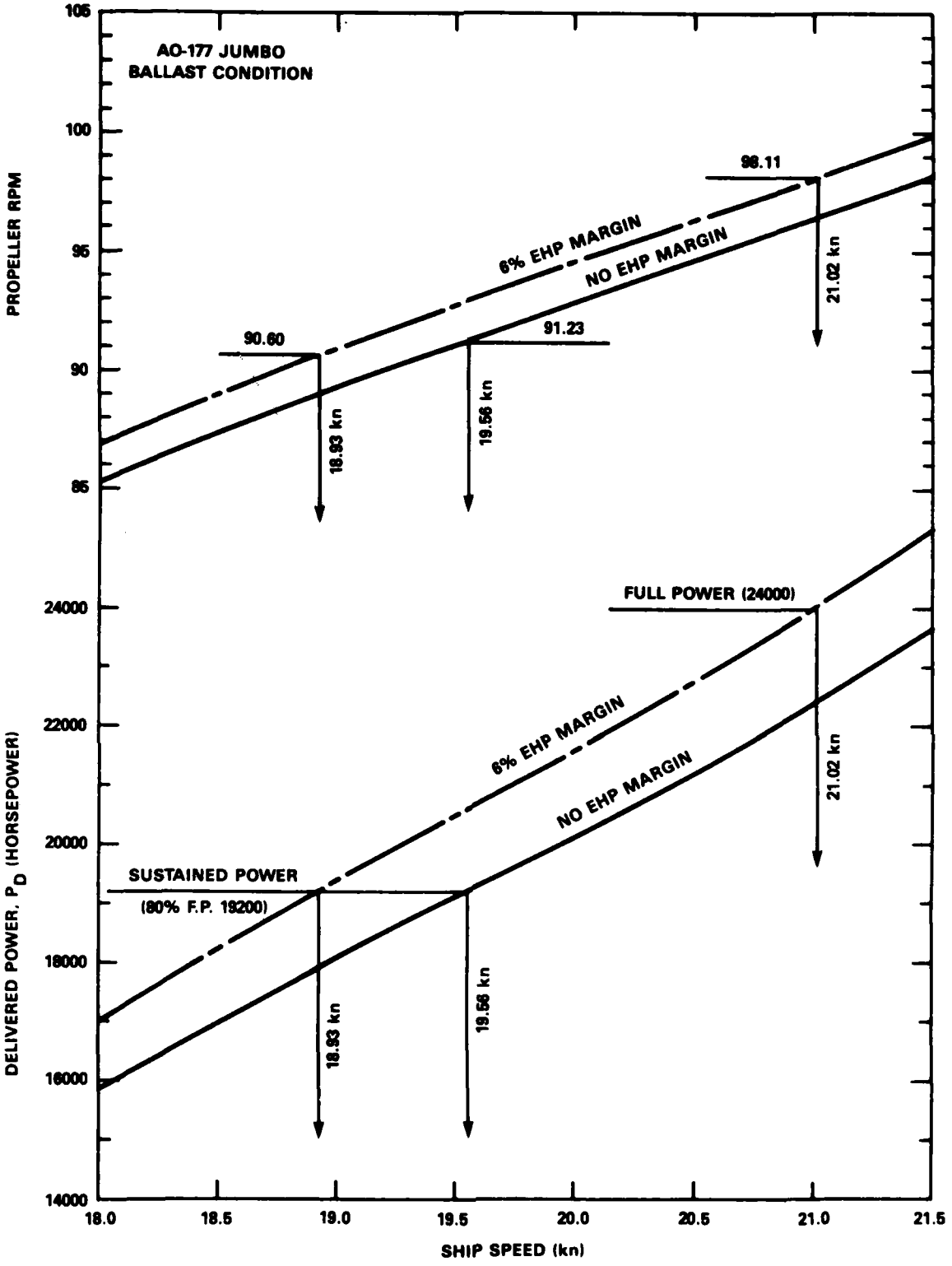

Fig. 21. Predicted full-scale power and rpm of AO-177 JUMBO at ballast condition.

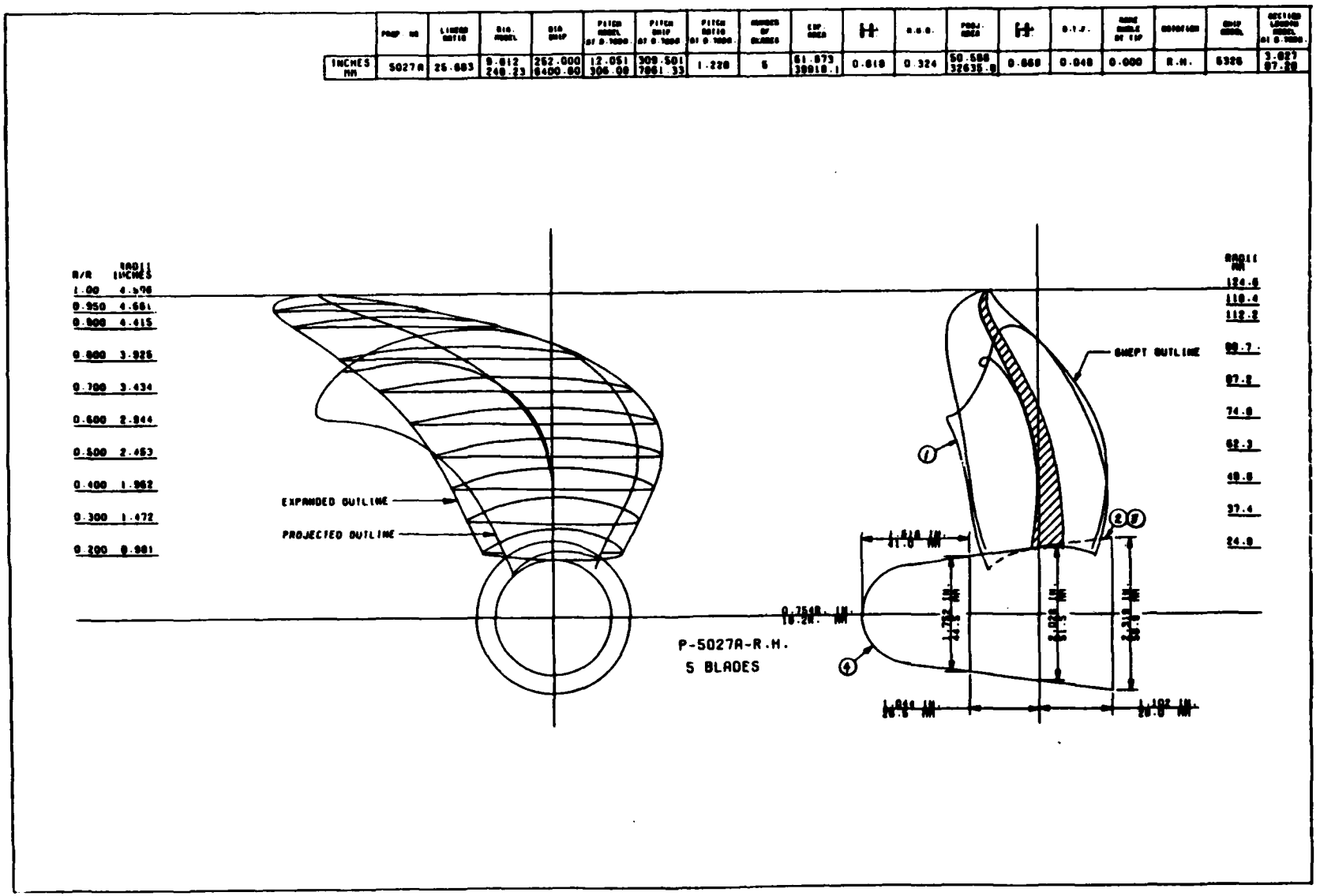

Fig. 22. Final geometry of AO-177 JUMBO propeller (DTNSRDC Propeller 5027A).

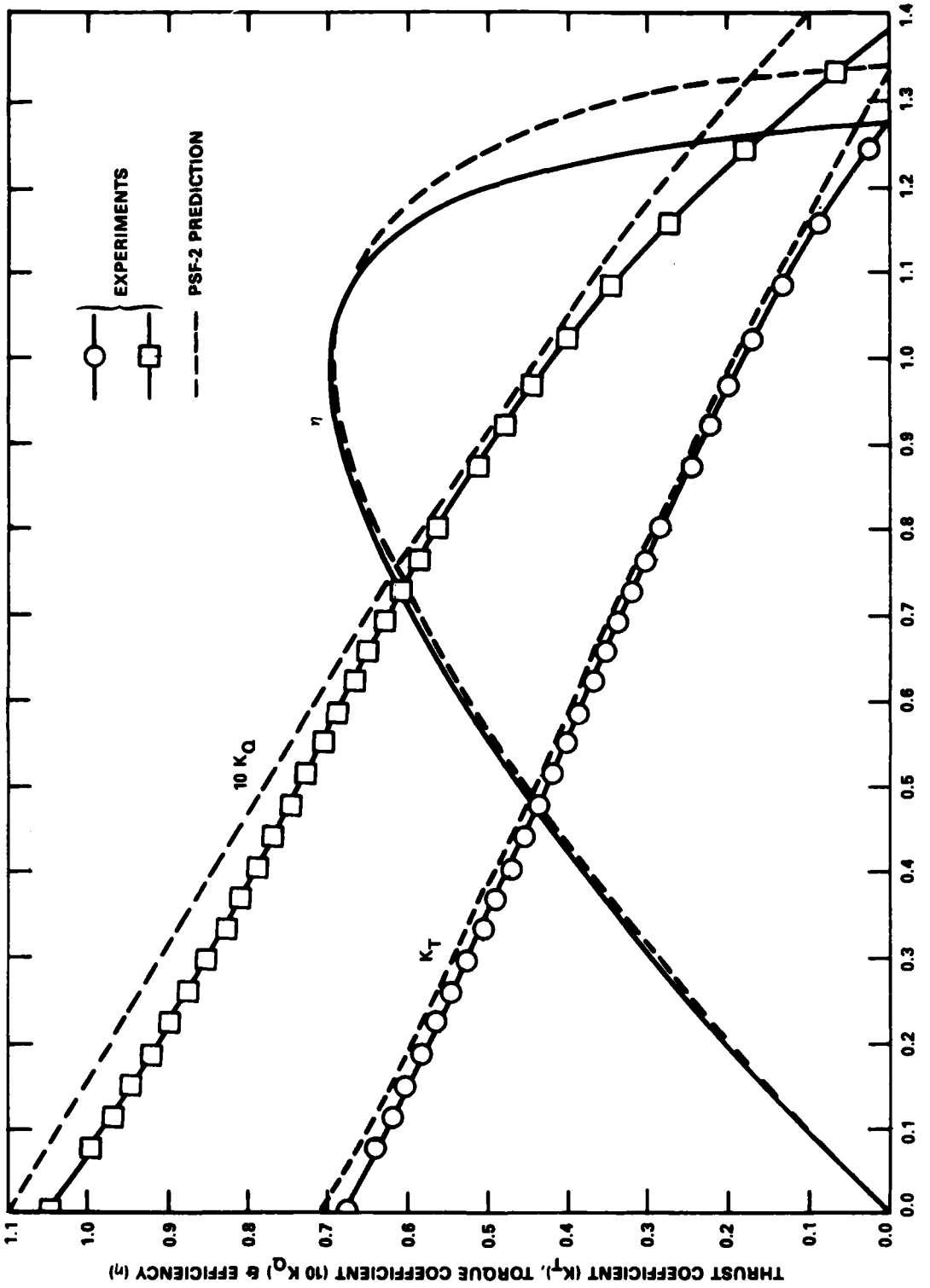

Fig. 23. Comparison of open-water performance between experiments and predictions for AO-177 JUMBO propeller (DTNSRDC Propeller 5027A).

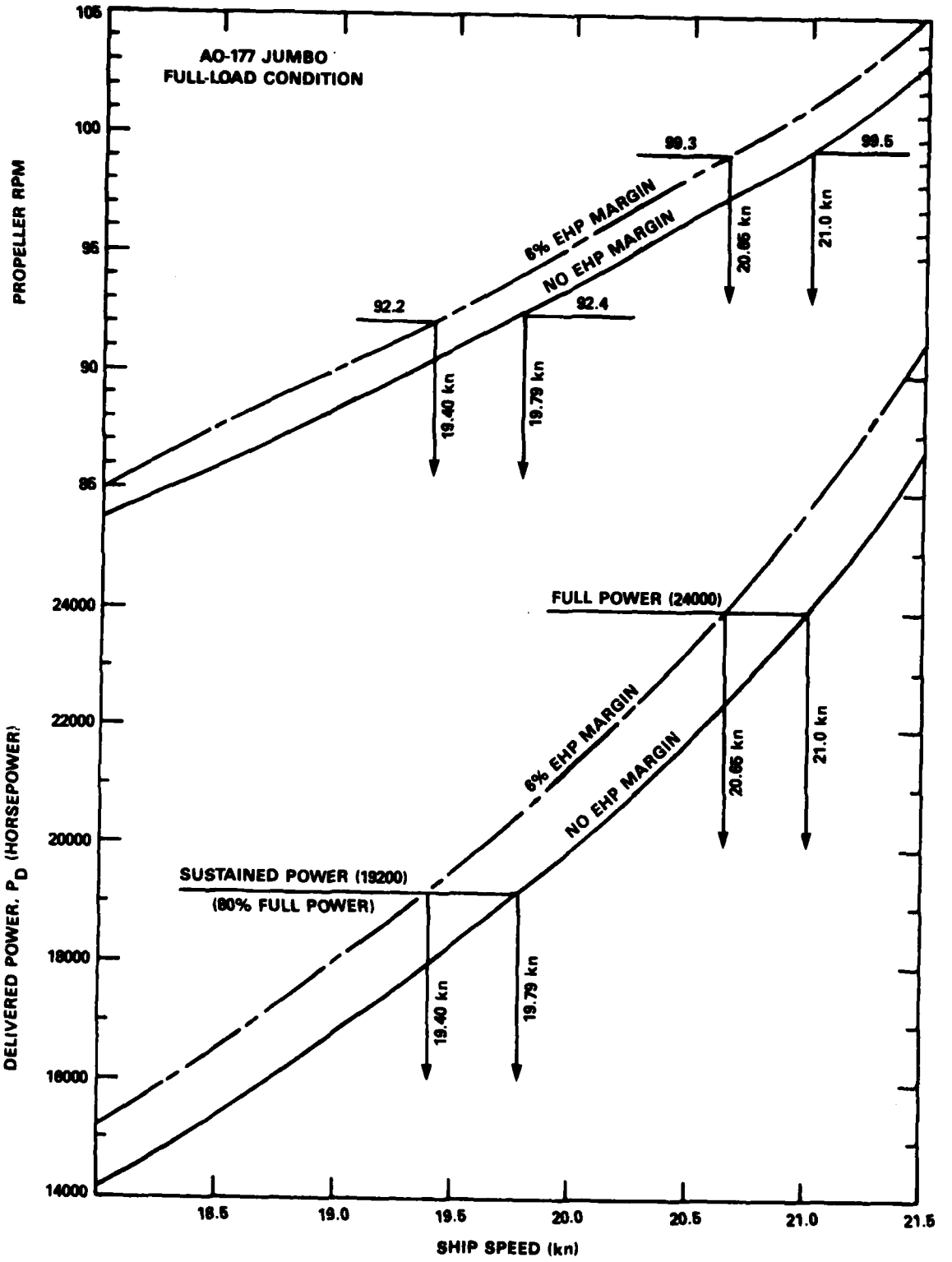

Fig. 24. Predicted full-scale power and rpm of AO-177 JUMBO at full load condition based on design propeller experiments.

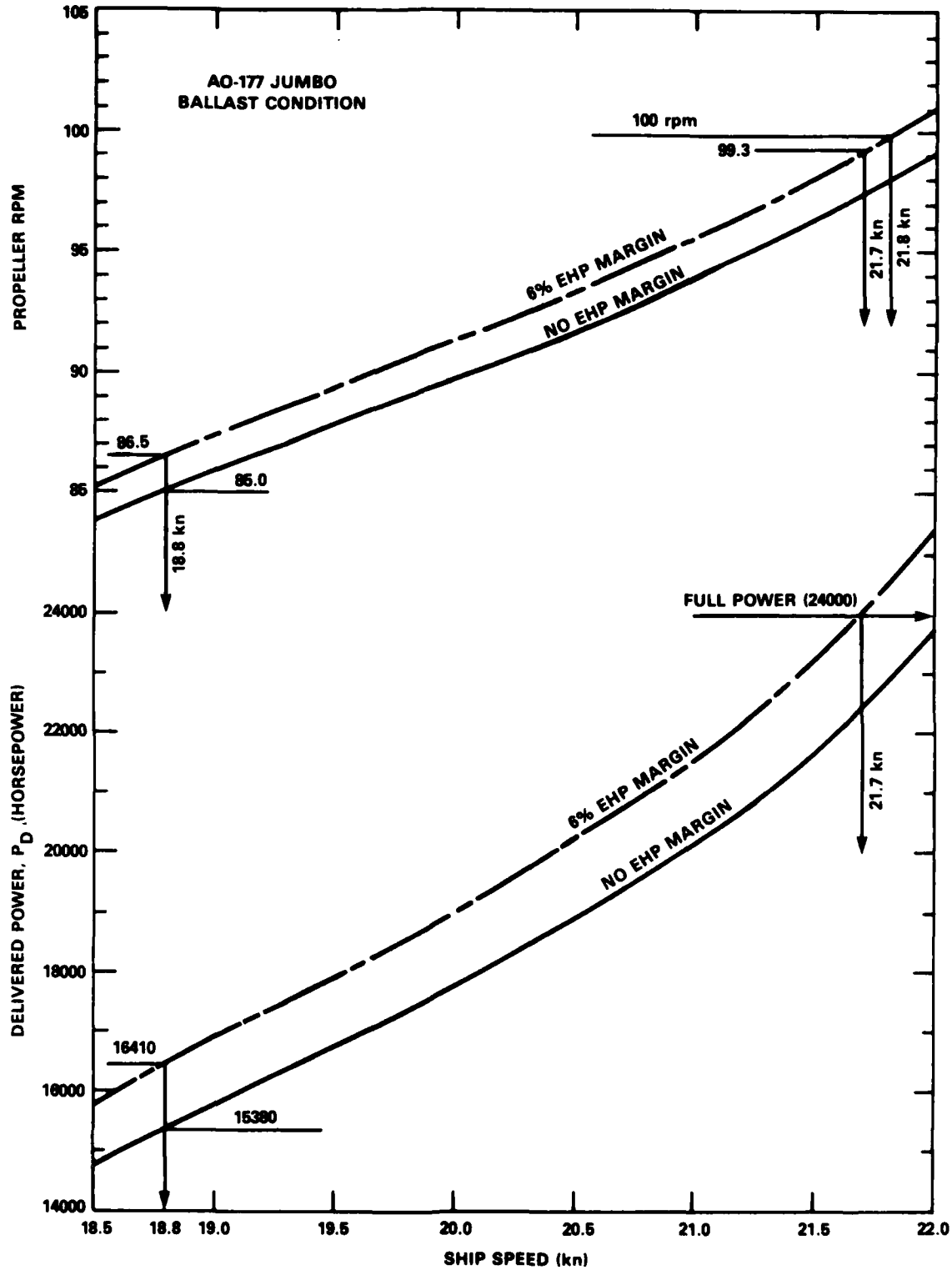

Fig. 25. Predicted full-scale power and rpm of AO-177 JUMBO at ballast condition based on design propeller experiments.

This page was intentionally left blank.

Table 2. (Continued)

A0177 (JUMBO) WAKE SURVEY DONE AT HYDRONAUTICS
PROPELLER DIAMETER = 21.00 FEET JV = 0.994

HARMONIC ANALYSES OF TANGENTIAL VELOCITY COMPONENT RATIOS (VT/V)

HARMONIC =	1	2	3	4	5	6	7	8
RADIUS = 0.410								
AMPLITUDE =	0.0733	0.0077	0.0302	0.0071	0.0118	0.0034	0.0061	0.0018
PHASE ANGLE =	184.2	310.9	357.3	138.6	354.6	154.6	349.0	126.6
RADIUS = 0.550								
AMPLITUDE =	0.1206	0.0058	0.0179	0.0032	0.0104	0.0064	0.0064	0.0048
PHASE ANGLE =	181.4	154.2	8.8	35.3	341.4	135.3	327.2	131.0
RADIUS = 0.650								
AMPLITUDE =	0.1339	0.0173	0.0070	0.0050	0.0081	0.0045	0.0038	0.0053
PHASE ANGLE =	182.2	186.0	3.8	23.2	356.0	137.3	333.6	147.5
RADIUS = 1.040								
AMPLITUDE =	0.1441	0.0559	0.0270	0.0128	0.0149	0.0090	0.0101	0.0055
PHASE ANGLE =	176.5	172.7	175.8	176.0	165.2	170.1	165.7	173.0
RADIUS = 1.140								
AMPLITUDE =	0.1380	0.0555	0.0233	0.0093	0.0078	0.0012	0.0009	0.0067
PHASE ANGLE =	175.6	171.3	174.8	177.6	166.6	186.9	273.3	338.6
RADIUS = 0.200								
AMPLITUDE =	0.0642	0.0502	0.0498	0.0325	0.0204	0.0154	0.0130	0.0090
PHASE ANGLE =	341.8	277.0	331.5	151.2	49.0	293.6	81.4	285.4
RADIUS = 0.300								
AMPLITUDE =	0.0167	0.0254	0.0395	0.0184	0.0139	0.0051	0.0065	0.0029
PHASE ANGLE =	222.7	287.8	344.3	149.1	23.6	278.1	45.1	283.4
RADIUS = 0.400								
AMPLITUDE =	0.0687	0.0089	0.0310	0.0079	0.0118	0.0030	0.0059	0.0015
PHASE ANGLE =	184.8	307.8	356.2	140.6	356.7	160.2	352.5	128.5
RADIUS = 0.500								
AMPLITUDE =	0.1075	0.0016	0.0226	0.0025	0.0111	0.0060	0.0067	0.0041
PHASE ANGLE =	181.7	115.0	5.7	79.7	342.5	137.5	330.8	126.6
RADIUS = 0.600								
AMPLITUDE =	0.1278	0.0113	0.0123	0.0044	0.0093	0.0053	0.0051	0.0050
PHASE ANGLE =	182.0	179.9	6.8	26.1	348.6	135.6	330.4	140.2
RADIUS = 0.700								
AMPLITUDE =	0.1382	0.0258	0.0018	0.0019	0.0014	0.0079	0.0029	0.0094
PHASE ANGLE =	181.1	180.7	155.9	101.7	52.2	155.3	172.2	158.4
RADIUS = 0.800								
AMPLITUDE =	0.1441	0.0397	0.0153	0.0081	0.0104	0.0126	0.0118	0.0142
PHASE ANGLE =	179.3	176.6	175.3	167.7	160.8	164.2	164.3	164.0
RADIUS = 0.900								
AMPLITUDE =	0.1466	0.0495	0.0238	0.0123	0.0160	0.0137	0.0151	0.0141
PHASE ANGLE =	178.0	174.7	176.1	173.2	163.8	167.3	163.9	166.4
RADIUS = 1.000								
AMPLITUDE =	0.1455	0.0550	0.0271	0.0133	0.0163	0.0110	0.0126	0.0089
PHASE ANGLE =	176.9	173.2	176.0	175.4	164.9	169.2	164.7	169.5

Table 3. Powering Predictions at Full-Load Condition Based on Model Propulsion Test Using Stock Propeller (Model 4677)

SHIP LENGTH	668.6 FEET
T (MEAN)	33.76 FEET
TRIM BY BOW	1.50 FEET
SHIP DISPLACEMENT	37575 LONG TONS
CORRELATION ALLOWANCE 0.0005	(ITTC FRICTION USED)
WITH STILL AIR DRAG AND NO POWER MARGIN	

SHIP SPEED (KNOTS)	EHP(P_E)	1-t	1-w_T	RELATIVE ROTATIVE EFFICIENCY
10	1815	0.846	0.774	1.042
11	2399	0.845	0.774	1.044
12	3094	0.844	0.773	1.044
13	3911	0.843	0.774	1.043
14	4858	0.843	0.773	1.045
15	5963	0.842	0.773	1.044
16	7269	0.841	0.773	1.044
17	8820	0.844	0.774	1.043
18	10595	0.847	0.774	1.042
19	12609	0.847	0.774	1.043
20	14930	0.849	0.774	1.044
21	17835	0.853	0.776	1.040
22	21962	0.859	0.779	1.038

Note: 1. The data in this Table were provided by NAVSEA Code 56X7, Memorandum 9200 Ser 56X7/154, dated 7 May 1986.
2. The data were prepared by David G. Sanders of D&P, Inc. for NAVSEA based on reanalyzed model test data from Tracor Hydronautics, Inc.

Table 1. Circumferential Average of Wake Velocity, Mean and Variation of Angle of Advance of AO-177 JUMBO

AO177 (JUMBO) WAKE SURVEY DONE AT HYDRONAUTICS
PROPELLER DIAMETER = 21.00 FEET JV = 0.994

RADIUS =	0.410	0.550	0.650	1.040	1.140	0.200	0.300	0.400	0.500	0.600	0.700	0.800	0.900	1.000
VXBAR =	0.563	0.674	0.720	0.802	0.790	0.295	0.438	0.553	0.640	0.698	0.742	0.776	0.796	0.803
VTBAR =	0.002	-0.008	-0.002	-0.009	-0.008	0.057	0.025	0.003	-0.007	-0.005	-0.004	-0.007	-0.009	-0.009
VRBAR =	0.001	0.001	0.001	0.001	0.001	0.001	0.001	0.001	0.001	0.001	0.001	0.001	0.001	0.001
1-WVX =	0.475	0.544	0.593	0.707	0.722	0.000	0.381	0.447	0.513	0.567	0.612	0.649	0.680	0.704
1-WX =	0.467	0.542	0.593	0.708	0.724	0.000	0.364	0.437	0.507	0.566	0.612	0.650	0.681	0.705
BBAR =	23.45	21.29	19.35	13.75	12.39	23.19	24.22	23.56	22.15	20.27	18.59	17.11	15.69	14.30
BPOS =	9.22	6.92	5.43	2.12	1.94	17.76	11.37	9.40	7.70	6.12	4.66	3.49	2.72	2.24
THETA =	120.00	115.00	110.00	105.00	97.50	237.50	122.50	120.00	117.50	110.00	110.00	110.00	107.50	107.50
BNEG =	-10.91	-10.22	-9.21	-6.41	-7.59	-14.01	-11.93	-10.98	-10.54	-9.66	-8.50	-7.56	-6.93	-6.52
THETA =	7.50	0.00	2.50	0.00	7.50	305.00	10.00	7.50	0.00	2.50	0.00	0.00	0.00	0.00

VXBAR IS CIRCUMFERENTIAL MEAN AXIAL VELOCITY.
VTBAR IS CIRCUMFERENTIAL MEAN TANGENTIAL VELOCITY.
VRBAR IS CIRCUMFERENTIAL MEAN RADIAL VELOCITY.
1-WVX IS VOLUMETRIC MEAN WAKE VELOCITY WITHOUT TANGENTIAL CORRECTION.
1-WX IS VOLUMETRIC MEAN WAKE VELOCITY WITH TANGENTIAL CORRECTION.
BBAR IS MEAN ANGLE OF ADVANCE.
BPOS IS VARIATION BETWEEN THE MAXIMUM AND MEAN ADVANCE ANGLES (DELTA BETA PLUS).
BNEG IS VARIATION BETWEEN THE MINIMUM AND MEAN ADVANCE ANGLES (DELTA BETA MINUS).
THETA IS ANGLE IN DEGREES AT WHICH CORRESPONDING BPOS OR BNEG OCCURS.

Table 2. Harmonic Contents of Axial and Tangential Velocity Components

AD177 (JUMBO) WAKE SURVEY DONE AT HYDRONAUTICS
PROPELLER DIAMETER = 21.00 FEET JV = 0.994

HARMONIC ANALYSES OF AXIAL VELOCITY COMPONENT RATIOS (VX/V)

HARMONIC =	1	2	3	4	5	6	7	8
RADIUS = 0.410								
AMPLITUDE =	0.1654	0.1575	0.0697	0.0284	0.0213	0.0114	0.0053	0.0048
PHASE ANGLE =	270.8	269.8	88.3	254.3	93.7	263.3	81.9	242.4
RADIUS = 0.550								
AMPLITUDE =	0.1665	0.1871	0.0422	0.0385	0.0407	0.0281	0.0186	0.0126
PHASE ANGLE =	270.5	267.4	78.4	259.0	83.1	252.3	66.5	233.8
RADIUS = 0.650								
AMPLITUDE =	0.1605	0.1865	0.0169	0.0475	0.0423	0.0277	0.0267	0.0206
PHASE ANGLE =	272.8	267.1	54.5	256.1	79.0	247.3	70.3	237.9
RADIUS = 1.040								
AMPLITUDE =	0.1609	0.1100	0.0410	0.0212	0.0017	0.0087	0.0021	0.0082
PHASE ANGLE =	269.0	268.0	269.5	263.6	206.6	245.4	228.8	244.8
RADIUS = 1.140								
AMPLITUDE =	0.1846	0.1217	0.0671	0.0341	0.0222	0.0172	0.0135	0.0079
PHASE ANGLE =	268.1	266.9	266.1	261.3	249.9	241.2	242.0	245.6
RADIUS = 0.200								
AMPLITUDE =	0.1445	0.0534	0.0910	0.0259	0.0481	0.0524	0.0234	0.0078
PHASE ANGLE =	280.1	298.3	100.8	213.9	252.3	69.3	215.9	324.1
RADIUS = 0.300								
AMPLITUDE =	0.1569	0.1101	0.0836	0.0240	0.0112	0.0166	0.0093	0.0037
PHASE ANGLE =	274.0	275.7	94.4	237.4	226.7	62.2	209.0	305.4
RADIUS = 0.400								
AMPLITUDE =	0.1649	0.1541	0.0712	0.0279	0.0192	0.0095	0.0044	0.0044
PHASE ANGLE =	270.9	270.2	88.8	253.4	95.6	266.2	89.1	245.4
RADIUS = 0.500								
AMPLITUDE =	0.1674	0.1806	0.0533	0.0345	0.0360	0.0244	0.0141	0.0094
PHASE ANGLE =	270.1	268.0	82.7	258.9	85.4	254.6	66.5	233.1
RADIUS = 0.600								
AMPLITUDE =	0.1631	0.1878	0.0285	0.0438	0.0421	0.0281	0.0235	0.0172
PHASE ANGLE =	271.8	267.2	70.8	257.2	80.8	249.6	68.9	236.5
RADIUS = 0.700								
AMPLITUDE =	0.1523	0.1658	0.0142	0.0372	0.0402	0.0206	0.0245	0.0180
PHASE ANGLE =	272.5	267.5	50.1	256.8	78.3	248.6	69.7	238.5
RADIUS = 0.800								
AMPLITUDE =	0.1433	0.1341	0.0073	0.0228	0.0328	0.0106	0.0187	0.0137
PHASE ANGLE =	271.7	268.2	11.4	259.4	77.6	252.5	68.9	240.1
RADIUS = 0.900								
AMPLITUDE =	0.1439	0.1151	0.0136	0.0165	0.0215	0.0060	0.0113	0.0106
PHASE ANGLE =	270.7	268.5	289.2	263.2	77.8	255.4	69.1	242.1
RADIUS = 1.000								
AMPLITUDE =	0.1541	0.1089	0.0320	0.0182	0.0062	0.0068	0.0022	0.0087
PHASE ANGLE =	269.5	268.3	272.1	264.2	85.3	248.6	80.4	244.2

Table 4. Estimated Powering Performance at Ballast Condition

SHIP DISPLACEMENT 22146 LONG TONS
T (MEAN) 21.07 FEET
TRIM BY STERN 5.90 FEET
CORRELATION ALLOWANCE 0.0005 (ITTC FRICTION USED)
WITH STILL AIR DRAG AND NO POWER MARGIN

SHIP SPEED (KNOTS)	EHP(P_E)	1-t	1-w_T	RELATIVE ROTATIVE EFFICIENCY
10	2183	0.874	0.741	1.029
11	2920	0.875	0.741	1.031
12	3781	0.876	0.740	1.031
13	4775	0.877	0.741	1.030
14	5889	0.878	0.740	1.030
15	7160	0.878	0.740	1.029
16	8567	0.877	0.740	1.028
17	10131	0.880	0.741	1.026
18	11792	0.881	0.741	1.023
19	13437	0.878	0.741	1.021
20	15045	0.876	0.741	1.020
21	16713	0.875	0.743	1.014
22	18661	0.873	0.746	1.011

Note: 1. The data in this Table were provided by NAVSEA Code 56X7, Memorandum 9200 Ser 56X7/154, dated 7 May 1986.
2. The effective power in this Table were estimated by D.G. Sanders of D&P, Inc. for NAVSEA.

Table 5. Model Nominal and Effective Wake

r/R	Nominal Wake (V_x/V_m)	Effective Wake (V_x/V_m)
0.2	0.295	0.325
0.25	0.370	0.408
0.3	0.436	0.480
0.4	0.550	0.606
0.5	0.640	0.705
0.6	0.700	0.771
0.7	0.742	0.818
0.8	0.776	0.854
0.9	0.796	0.877
0.95	0.801	0.882
1.0	0.803	0.885
VOLUME MEAN $(1-w_v)$	0.703	0.774
$(1-w_T)/(1-w_v)$	1.101	

Note: 1. The model nominal wake was measured with five-hole pitot tubes in the towing tank at the model speed corresponding to the full-scale speed of 19 knots.

2. The effective wake distribution was approximated by scaling up the nominal wake by multiplying a constant value of $(1-w_T)/(1-w_v)$; see Equation (1) in the text.

Table 6. Effect of Radial Circulation Distribution on Propeller Performance at Full Power

TYPE OF CIRCULATION	SHIP SPEED (KNOTS) AT P_S = 24000 SHP RPM = 100	PROPULSIVE EFFICIENCY
G_o (LERBS OPTIMUM)	20.73	0.706
G_1 (TIP UNLOADING I)	20.58	0.688
G_2 (TIP UNLOADING II)	20.62	0.693
G_3 (TIP LOADING)	20.77	0.713

Note: The degree of tip unloading is defined as the ratio of unloaded circulation value to Lerbs optimum circulation value at 0.95 radius.

G_1 - Tip Unloading I : (G_1/G_o) at 0.95 radius = 0.79
G_2 - Tip Unloading II: (G_2/G_o) at 0.95 radius = 0.85
G_3 - Tip Loading : (G_3/G_o) at 0.95 radius = 1.08

Table 7. Computer Output from Lifting-Line Code EPPD

INPUT DATA : AO-177 JUMBO PROP (NON-OPT CIRC "G2", MODEL WAKE, FINAL THICKNESS)

NBL	= 5	PDEPTH	= 22.000 FT
NSHAFT	= 1	DESIGN	=24000.0
NR	= 11	TOL	= 0.00050
NPHI	= 11	ETAT	= 1.0000
NPROB	= 1	1-WT	= 0.7750
IOPT	= 0	EAR	= 0.8191
ICIRC	= 1	RHO	= 1.9905 SLUG/FT**3
IWAKE	= 1	RHOB	= 483.84 LBM/FT**3
IDRAG	= 1	NU*E5	= 1.2817 FT**2/SEC
ITHICK	= 1	VMEAN	= 0.7035 (NOMINAL)
ICONVG	= 1	VMEAN	= 0.7750 (EFFECTIVE)
IPRINT	= 0	DIAM	= 21.000 FT
		WEIGHT	=57298.4 LBS
IPBD10	= 0		
NCOEF	= 0		

INPUT DATA AT INPUT RADII

X	PHI	G	G COEF	1-W(X)	C/D	T/C	CDRAG
0.200000	0.000000	0.000000	0.034324	0.295000	0.215000	0.226700	0.008500
0.250000	28.955020	0.017000	0.000412	0.370000	0.239000	0.190600	0.008500
0.300000	41.409620	0.023500	-0.000223	0.436000	0.265000	0.157800	0.008500
0.400000	60.000000	0.030000	0.000649	0.550000	0.313000	0.108900	0.008500
0.500000	75.522480	0.033000	-0.000855	0.640000	0.352000	0.081400	0.008500
0.600000	90.000000	0.034000	0.000315	0.700000	0.379000	0.066800	0.008500
0.700000	104.477500	0.033200	-0.000369	0.742000	0.390000	0.057900	0.008500
0.800000	120.000000	0.030300	0.000082	0.776000	0.377000	0.052000	0.008500
0.900000	138.590400	0.023000	-0.000062	0.796000	0.316000	0.048300	0.008500
0.950000	151.045000	0.015253	0.000000	0.801000	0.237000	0.047100	0.008500
1.000000	180.000000	0.000000	0.000000	0.803000	0.000000	0.046000	0.008500

INPUT DATA INTERPOLATED AT 11 EQUAL ANGULAR POSITIONS

X	PHI	G	G COEF	1-W(X)	C/D	T/C	CDRAG
0.200000	0.000000	0.000000	0.034324	0.324975	0.215000	0.226700	0.008500
0.219577	18.000000	0.010461	0.000412	0.358737	0.223952	0.212336	0.008500
0.276393	36.000000	0.020861	-0.000223	0.446980	0.252693	0.172712	0.008500
0.364886	54.000000	0.028294	0.000649	0.564559	0.297034	0.123417	0.008500
0.476393	72.000000	0.032493	-0.000855	0.684565	0.343754	0.086376	0.008500
0.600000	90.000000	0.034000	0.000315	0.771126	0.379000	0.066800	0.008500
0.723607	108.000000	0.032741	-0.000369	0.827133	0.389523	0.056280	0.008500
0.835114	126.000000	0.028487	0.000082	0.864458	0.363779	0.050473	0.008500
0.923607	144.000000	0.019839	-0.000062	0.879898	0.285298	0.047699	0.008500
0.980423	162.000000	0.008047	0.000000	0.884117	0.149220	0.046441	0.008500
1.000000	180.000000	0.000000	0.000000	0.884592	0.000000	0.046000	0.008500

PROPULSION DATA :

VS (KNOTS)	EHP	THRUST DED	RPM
18.000	10595.00	0.1530	100.000
19.000	12609.00	0.1530	100.000
20.000	14930.00	0.1510	100.000
21.000	17835.00	0.1470	100.000
22.000	21962.00	0.1410	100.000

Table 7. (Continued)

AO-177 JUMBO PROP (NON-OPT CIRC "G2", MODEL WAKE, FINAL THICKNESS)

DIAM = 21.00 FT VS(VS/ND) = 0.9944 CT(DESIRED) = 0.7393 VS = 20.6201 KNOTS

OUTPUT AT INPUT RADII

N	X	PHI	G COEF	G	TANB	TANBI	PI.X.TANBI	UA/V	UT/V	VR/V	1-W(X)	CDRAG
1	0.2000	0.0	0.034385	0.000000	0.514295	0.735850	0.462348	0.075376	-0.087818	0.675491	0.324975	0.008500
2	0.2500	29.0	0.000413	0.017054	0.516062	0.937897	0.736622	0.158956	-0.189318	0.825769	0.407613	0.008500
3	0.3000	41.4	-0.000224	0.023503	0.506713	0.933356	0.879667	0.200906	-0.214953	1.000609	0.480275	0.008500
4	0.4000	60.0	0.000650	0.030075	0.479738	0.790803	0.993752	0.238353	-0.197898	1.359876	0.606276	0.008500
5	0.5000	75.5	-0.000856	0.033055	0.446021	0.686867	1.078929	0.260513	-0.173745	1.705376	0.704583	0.008500
6	0.6000	90.0	0.000315	0.034061	0.406787	0.597045	1.125403	0.270090	-0.151700	2.031131	0.771126	0.008500
7	0.7000	104.5	-0.000370	0.033258	0.369775	0.523703	1.151682	0.271590	-0.131513	2.348082	0.817791	0.008500
8	0.8000	120.0	0.000082	0.030384	0.338020	0.468280	1.176915	0.274753	-0.115934	2.662964	0.854356	0.008500
9	0.9000	138.6	-0.000062	0.022964	0.308439	0.417215	1.179647	0.269957	-0.096547	2.976277	0.877039	0.008500
10	0.9500	151.0	0.000000	0.015328	0.293971	0.367305	1.096225	0.197520	-0.057023	3.137021	0.882337	0.008500
11	1.0000	180.0	0.000000	0.000000	0.279986	0.259361	0.814806	-0.056405	0.033768	3.298836	0.884592	0.008500

N	X	PHI	LOAD(PSI)	SIGMA	CL	FM/C	T/C	T/D	C/D	RE NO.	ALI(DEG)	F(X)
1	0.2000	0.0	0.000000	6.099924	0.000000	0.000000	0.226700	0.048740	0.215000	0.828E+07	0.000000	0.000000
2	0.2500	29.0	3.098813	4.051680	0.542859	0.036860	0.190600	0.045561	0.239038	0.113E+08	0.836002	0.233099
3	0.3000	41.4	4.669960	2.725825	0.557176	0.037832	0.157800	0.041798	0.264877	0.151E+08	0.858052	0.234391
4	0.4000	60.0	6.871525	1.443206	0.443877	0.030139	0.108900	0.034092	0.313062	0.243E+08	0.683571	0.238540
5	0.5000	75.5	8.423818	0.899277	0.346001	0.023430	0.081400	0.028651	0.351981	0.342E+08	0.532841	0.229992
6	0.6000	90.0	9.601128	0.620567	0.278006	0.018877	0.066800	0.025317	0.379000	0.439E+08	0.428130	0.224229
7	0.7000	104.5	10.534100	0.454176	0.228233	0.015497	0.057900	0.022577	0.389927	0.522E+08	0.351479	0.219776
8	0.8000	120.0	11.278360	0.345246	0.189987	0.012900	0.052000	0.019622	0.377342	0.573E+08	0.292580	0.211900
9	0.9000	138.6	11.397610	0.270077	0.153700	0.010436	0.048300	0.015234	0.315412	0.535E+08	0.236699	0.202441
10	0.9500	151.0	10.654580	0.240284	0.129333	0.008782	0.047100	0.011180	0.237377	0.425E+08	0.199173	0.237222
11	1.0000	180.0	0.000000	0.214750	0.000000	0.000000	0.046000	0.000000	0.000000	0.876E+00	0.000000	0.000000

THRUST = 308689.2 LBS CT = 0.7393 KT = 0.2871
TORQUE = 1260151.0 LBS-FT CP = 0.9081 KQ = 0.0558 ETA = 0.6309

VS = 20.620 KNOTS EHP = 16627.4 1-T = 0.8512
RPM = 100.00 SHP = 23993.2 1-WT = 0.7750
JS = 0.9944 ETAD = 0.6930 ETAH = 1.0984

NITER = 9
K1 = 11.54392
K2 = 1.00178

---------- BURRILL'S CAVITATION PARAMETERS ----------
(NOTE-WHEN SIGMA(0.7R) IS GREATER THAN 2.0, EAR(BURRILL) IS NOT RELIABLE)

BURRILL'S PARAMETERS		MAXIMUM ALLOWED CAVITATION EXTENT (PERCENT BLADE AREA)	TAUC AT SIGMA7=0.5319	MINIMUM REQUIRED EAR(BURRILL)
QT	= 45.7800			
TANBI(0.7R)	= 0.5259	2.5	0.1702	0.9903
SIGMA(0.7R)	= 0.5319	5.0	0.1990	0.8470
TAUC	= 0.2058	10.0	0.2590	0.6508
EAR(DESIGN)	= 0.8191	20.0	0.3516	0.4794
EAR(KELLER)	= 0.7066	30.0	0.3828	0.4403

---------- TIP VORTEX CAVITATION INCEPTION ----------

K-FACTOR	SPEED (KNOTS)	SIGMA
3.00	8.624	39.46
3.50	8.088	44.86
4.00	7.650	50.14
4.50	7.284	55.32

Table 8. Effect of Skew on Blade-Frequency Thrust and Torque

	NO SKEW	36 DEG SKEW	40 DEG SKEW
$(\tilde{K}_T)_5$ (PUF-2)	0.01666	0.01159	0.00714
$\overline{K}_T$ (PUF-2)	0.297	0.303	0.312
$\overline{K}_T$ (EPPD)	0.287	0.287	0.287
$\frac{(\tilde{K}_T)_5}{\overline{K}_T(\text{PUF-2})}$	5.61 %	3.83 %	2.29 %
$\frac{(\tilde{K}_T)_5}{\overline{K}_T\ (\text{EPPD})}$	5.80 %	4.04 %	2.49 %
$(\tilde{K}_Q)_5$ (PUF-2)	0.0030	0.00188	0.00101
$\overline{K}_Q$ (PUF-2)	0.0577	0.0586	0.0589
$\overline{K}_Q$ (EPPD)	0.0558	0.0558	0.0558
$\frac{(\tilde{K}_Q)_5}{\overline{K}_Q(\text{PUF-2})}$	5.20 %	3.21 %	1.71 %
$\frac{(\tilde{K}_Q)_5}{\overline{K}_Q\ (\text{EPPD})}$	5.38 %	3.37 %	1.81 %

Note: 1. In PUF-2, V=20.62 Knots, RPM=100, and the nominal wake ($1-w_V$=0.7034) were used as input.
2. Jessup's (t/c) was used.

Table 9. Pitch Distribution (P/D) from Lifting-Surface Computation Using Computer Code PBD-10

r/R	LL	$(LS)_1$	$(LS)_2$	$(LS)_3$	$(LS)_4$	$(LS)_5$	$(LS)_6$	FAIRED	FINAL
0.2	.4624	.6367	.6440	.6374	.5183	.5885	.5836	.5828	.7224
0.25	.7366	.9101	.9098	.9055	.8438	.8451	.8503	.8452	.8775
0.3	.8797	1.0331	1.0251	1.0238	.9974	.9871	.9923	.9902	.9994
0.4	.9937	1.1504	1.1340	1.1355	1.1295	1.1281	1.1270	1.1400	1.1405
0.5	1.0789	1.2188	1.1978	1.1988	1.2018	1.2005	1.2004	1.2080	1.2080
0.6	1.1254	1.2387	1.2198	1.2215	1.2293	1.2290	1.2289	1.2291	1.2342
0.7	1.1517	1.2242	1.2030	1.2035	1.2138	1.2156	1.2151	1.2280	1.2282
0.8	1.1769	1.1737	1.1611	1.1606	1.1901	1.1881	1.1882	1.1799	1.1804
0.9	1.1796	1.1008	1.0624	1.0573	1.0559	1.0574	1.0577	1.0376	1.0433
0.95	1.0962	.9303	.8189	.8031	.8134	.8191	.8200	.8696	.9051
1.0	.8148	.5062	.2597	.2239	.3348	.3609	.3634	.4428	.7048
K_T	.2871	.304	.300	.299	.299	.299	.300		
K_Q	.0558	.0579	.0563	.0563	.0569	.0570	.0570		
GRID NO.		8 x 9 : Key Blade 4 x 9 : Others			16 x 35 : Key Blade 4 x 9 : Others				

Note:
1. LL means lifting-line computations using the code, EPPD. LS means lifting-surface computations using the code, PBD-10, and the subscript represents the iteration number.
2. For computations with finer grid arrangement, i.e., iterations 4, 5 and 6, wake alignment process was skipped.
3. For lifting-line computations, a constant blade section drag coefficient of 0.0085 was used. The K_T and K_Q for lifting-surface computations are values corresponding to a constant section drag coefficient of 0.0085.

Table 10. Camber Distribution (f_M/c) from Lifting-Surface Computation Using Computer Code PBD-10

r/R	LL	$(LS)_1$	$(LS)_2$	$(LS)_3$	$(LS)_4$	$(LS)_5$	$(LS)_6$	FAIRED (FINAL)
0.2	--	.0230	.0497	.0554	.0364	.0224	.0223	.0604
0.25	.0369	.0458	.0636	.0668	.0680	.0667	.0684	.0589
0.3	.0378	.0541	.0651	.0664	.0679	.0678	.0687	.0564
0.4	.0301	.0455	.0485	.0483	.0480	.0480	.0480	.0468
0.5	.0235	.0330	.0341	.0342	.0348	.0350	.0351	.0353
0.6	.0189	.0300	.0301	.0300	.0290	.0289	.0289	.0289
0.7	.0155	.0246	.0254	.0254	.0255	.0255	.0255	.0263
0.8	.0129	.0263	.0273	.0271	.0265	.0265	.0265	.0258
0.9	.0104	.0251	.0292	.0295	.0270	.0271	.0271	.0267
0.95	.0088	.0107	.0233	.0257	.0253	.0252	.0251	.0276
1.0	.0000	-.0199	.0093	.0158	.0283	.0296	.0294	.0286
GRID ARRANGEMENT		8 x 9 : Key Blade 4 x 9 : Others			16 x 35 : Key Blade 4 x 9 : Others			

Note: LL - lifting-line computations using the code, EPPD.
LS - lifting-surface computations using the code, PBD-10 where the subscript indicates the iteration number.

Table 11. Geometric Characteristics of Design Propeller of AO-177 JUMBO

Diameter (D) = 21.0 feet

Number of Blades (Z) = 5

Expanded Area Ratio (A_E/A_O) = 0.819

Camber Distribution: NACA a=0.8 Meanline

Thickness Distribution: NACA 66 (Modified)

Design Advance Coefficient, J_A = 0.771

Design Thrust Coefficient, K_T = 0.287

Design Thrust-Loading Coefficient, C_T = 0.739

r/R	P/D	c/D	t/c	t/D	f_M/c	θ_S	i_T/D
0.2	0.7224	0.2150	0.2267	0.0487	0.0604	0.0	.0000
0.25	0.8775	0.2405	0.1906	0.0458	0.0589	0.0	.0000
0.3	0.9994	0.2648	0.1578	0.0418	0.0564	0.0	.0000
0.4	1.1405	0.3100	0.1089	0.0338	0.0468	0.0	.0000
0.5	1.2080	0.3505	0.0814	0.0285	0.0353	1.2	.0040
0.6	1.2342	0.3790	0.0668	0.0253	0.0289	4.5	.0154
0.7	1.2282	0.3900	0.0579	0.0226	0.0263	10.0	.0341
0.8	1.1804	0.3775	0.0520	0.0196	0.0258	17.7	.0580
0.9	1.0433	0.3150	0.0483	0.0152	0.0267	28.5	.0826
0.95	0.9051	0.2380	0.0471	0.0112	0.0276	35.4	.0890
1.0	0.7048	0.0000	0.0460	0.0000	0.0286	40.0	.0783

Table 12. Predicted Ship Speed and RPM of AO-177 JUMBO at Full Load and Ballast Condition

	FULL LOAD CONDITION	BALLAST CONDITION
FULL POWER (24,000 SHP)	No EHP Margin V = 20.81 knots RPM = 99.50	No EHP Margin V = 21.64 knots RPM = 98.74
	6% EHP Margin V = 20.43 knots RPM = 99.12	6% EHP Margin V = 21.02 knots RPM = 98.11
80% FULL POWER (19,200 SHP)	No EHP Margin V = 19.54 knots RPM = 92.64	No EHP Margin V = 19.56 knots RPM = 91.23
	6% EHP Margin V = 19.13 knots RPM = 92.18	6% EHP Margin V = 18.93 knots RPM = 90.60

Table 13. Offsets of AO-177 JUMBO Design Propeller

Table 13a. No Trailing-Edge Modification

SECTION OFFSETS
(IN INCHES)

AO-177 JUMBO, SKEW-IND RAKE ONLY, T E MODIFICATION

ORDINATES (NO TRAILING-EDGE MODIFICATIONS) AT NONDIMENSIONAL RADIUS R/RO

FRACTION OF CHORD		2000	2500	3000	3500	4000	5000	6000	7000	8000	9000	9500	9600	9700	9800	9900	1 0000
0.00000U		0.0000	0.0000	0 0000	0.0000	0.0000	0.0000	0 0000	0.0000	0.0000	0.0000	0.0000	0.0000	0.0000	0.0000	0.0000	0.0000
	L	0 0000	0.0000	0 0000	0 0000	0 0000	0 0000	0 0000	0 0000	0 0000	0 0000	0 0000	0 0000	0 0000	0 0000	0 0000	0 0000
.00313U		.7382	7080	6594	6039	5499	4657	4131	3717	3288	2608	1948	1756	1531	1255	0887	0 0000
	L	- 5560	- 5092	- 4498	- 3929	- 3463	- 2921	- 2594	- 2278	- 1921	- 1428	- 1026	- 0918	- 0794	- 0645	- 0452	0 0000
.00500U		.9545	.9185	.8586	.7887	.7196	.6096	.5407	.4872	.4322	.3440	.2574	.2322	.2026	.1661	.1174	0 0000
	L	- 6786	- 6175	- 5412	- 4691	- 4113	- 3466	- 3079	- 2693	- 2252	- 1653	- 1178	- 1052	- 0908	- 0737	- 0518	0 0000
.00625U		1 0785	1 0394	.9733	.8955	.8178	.6928	.6144	.5541	.4921	.3924	.2939	.2652	.2314	.1898	.1341	0 0000
	L	- 7447	- 6753	- 5894	- 5088	- 4448	- 3747	- 3329	- 2904	- 2418	- 1762	- 1250	- 1115	- 0962	- 0780	- 0544	0 0000
.00938U		1 3471	1 3021	1 2232	1 1284	1 0323	.8747	.7758	.7005	.6236	.4988	.3741	.3377	.2948	.2419	.1710	0 0000
	L	- 8788	- 7913	- 6846	- 5859	- 5091	- 4285	- 3808	- 3306	- 2724	- 1955	- 1372	- 1222	- 1051	- 0850	- 0592	0 0000
.01000U		1 3958	1 3499	1 2687	1 1709	1 0715	.9080	.8052	.7272	.6477	.5183	.3889	.3511	.3064	.2514	.1778	0 0000
	L	- 9018	- 8110	- 7006	- 5987	- 5196	- 4373	- 3886	- 3370	- 2772	- 1983	- 1390	- 1238	- 1083	- 0880	- 0599	0 0000
.01250U		1 5785	1 5292	1 4399	1 3310	1 2192	1 0333	.9163	.8282	.7385	.5920	.4446	.4015	.3504	.2876	.2034	0 0000
	L	- 9849	- 8817	- 7573	- 6434	- 5560	- 4677	- 4157	- 3593	- 2933	- 2078	- 1443	- 1282	- 1101	- 0888	- 0617	0 0000
.02500U		2 3199	2 2599	2 1405	1 9883	1 8270	1 5490	1 3735	1 2442	1 1142	.8979	.6763	.6110	.5337	.4383	.3102	0 0000
	L	-1 2819	-1 1277	- 9467	- 7859	- 6674	- 5600	- 4980	- 4243	- 3357	- 2256	- 1512	- 1332	- 1134	- 0908	- 0624	0 0000
.05000U		3 4241	3 3537	3 1947	2 9817	2 7480	2 3307	2 0665	1 8759	1 6866	1 3659	1 0316	.9328	.8150	.6697	.4742	0 0000
	L	-1 6496	-1 4181	-1 1540	- 9261	- 7656	- 6400	- 5698	- 4743	- 3557	- 2166	- 1340	- 1157	- 0964	- 0753	- 0506	0 0000
.07500U		4 2982	4 2224	4 0346	3 7750	3 4848	2 9562	2 6209	2 3819	2 1459	1 7424	1 3179	1 1917	1 0418	.8562	.6065	0 0000
	L	-1 9050	-1 6119	-1 2823	-1 0028	- 8111	- 6760	- 6024	- 4916	- 3511	- 1924	- 1073	- 0900	- 0728	- 0547	- 0351	0 0000
.10000U		5 0373	4 9581	4 7472	4 4491	4 1113	3 4880	3 0923	2 8124	2 5372	2 0635	1 5622	1 4129	1 2353	1 0155	.7195	0 0000
	L	-2 1043	-1 7587	-1 3741	-1 0516	- 8345	- 6936	- 6185	- 4958	- 3375	- 1640	- 0786	- 0627	- 0476	- 0332	- 0192	0 0000
.15000U		6 2457	6 1629	5 9160	5 5561	5 1410	4 3624	3 8673	3 5206	3 1815	2 5930	1 9653	1 7778	1 5548	1 2784	.9060	0 0000
	L	-2 4040	-1 9723	-1 4978	-1 1060	- 8491	- 7022	- 6271	- 4862	- 3003	- 1049	- 0220	- 0093	- 0009	.0083	.0112	0 0000
.20000U		7 1960	7 1119	6 8382	6 4308	5 9553	5 0539	4 4802	4 0809	3 6918	3 0128	2 2851	2 0675	1 8083	1 4871	1 0540	0 0000
	L	-2 6191	-2 1193	-1 5745	-1 1289	- 8419	- 6931	- 6198	- 4658	- 2591	- 0486	.0301	.0395	.0451	.0459	.0387	0 0000
.25000U		7 9455	7 8617	7 5681	7 1240	6 6011	5 6024	4 9663	4 5256	4 0972	3 3468	2 5397	2 2981	2 0102	1 6533	1 1719	0 0000
	L	-2 7717	-2 2180	-1 6179	-1 1307	- 8209	- 6729	- 6024	- 4390	- 2188	.0041	.0774	.0837	.0849	.0796	.0633	0 0000
.30000U		8 5226	8 4404	8 1327	7 6612	7 1022	6 0280	5 3436	4 8709	4 4125	3 6071	2 7383	2 4780	2 1877	1 7830	1 2640	0 0000
	L	-2 8707	-2 2752	-1 6327	-1 1141	- 7879	- 6431	- 5765	- 4088	- 1736	.0534	.1206	.1239	.1210	.1100	.0854	0 0000
.35000U		8 9467	8 8671	8 5506	8 0598	7 4747	6 3444	5 6240	5 1279	4 6477	3 8016	2 8869	2 6126	2 2857	1 8802	1 3329	0 0000
	L	-2 9240	-2 2975	-1 6241	-1 0833	- 7461	- 6062	- 5441	- 3709	- 1307	.0990	.1596	.1599	.1532	.1371	.1050	0 0000
.40000U		9 2295	9 1535	8 8326	8 3302	7 7280	6 5597	5 8147	5 3031	4 8085	3 9352	2 9892	2 7054	2 3670	1 9471	1 3805	0 0000
	L	-2 9364	-2 2888	-1 5951	-1 0403	- 6973	- 5638	- 5068	- 3325	- 0887	.1406	.1940	.1917	.1814	.1607	.1220	0 0000
.45000U		9 3743	9 3027	8 9822	8 4754	7 8652	6 6764	5 9181	5 3986	4 8970	4 0096	3 0465	2 7573	2 4126	1 9847	1 4072	0 0000
	L	-2 9074	-2 2485	-1 5448	- 9843	- 6403	- 5149	- 4636	- 2907	- 0468	.1788	.2247	.2197	.2062	.1813	.1368	0 0000
.50000U		9 3687	9 3033	8 9888	8 4862	7 8778	6 6874	5 9278	5 4087	4 9083	4 0210	3 0560	2 7661	2 4204	1 9913	1 4119	0 0000
	L	-2 8237	-2 1639	-1 4617	- 9047	- 5658	- 4516	- 4075	- 2392	.0004	.2179	.2547	.2468	.2300	.2009	.1507	0 0000
.55000U		9 2227	9 1645	8 8608	8 3700	7 7727	6 5984	5 8489	5 3380	4 8464	3 9725	3 0201	2 7338	2 3923	1 9683	1 3957	0 0000
	L	-2 6970	-2 0461	-1 3558	- 8107	- 4821	- 3809	- 3447	- 1837	.0479	.2540	.2808	.2703	.2503	.2175	.1623	0 0000
.60000U		8 9319	8 8819	8 5938	8 1226	7 5456	6 4059	5 6782	5 1837	4 7088	3 8623	2 9374	2 6591	2 3271	1 9148	1 3580	0 0000
	L	-2 6270	-1 8954	-1 2279	- 7033	- 3901	- 3036	- 2760	- 1248	.0948	.2859	.3024	.2894	.2666	.2304	.1712	0 0000
.65000U		8 4902	8 4492	8 1815	7 7376	7 1907	6 1050	5 4113	4 9417	4 4919	3 6874	2 8056	2 5400	2 2231	1 8295	1 2977	0 0000
	L	-2 3161	-1 7143	-1 0809	- 5856	- 2930	- 2225	- 2037	- 0651	.1387	.3113	.3175	.3023	.2771	.2385	.1764	0 0000
.70000U		7 8896	7 8576	7 6147	7 2062	6 6995	5 6881	5 0418	4 6060	4 1901	3 4432	2 6211	2 3733	2 0775	1 7100	1 2112	0 0000
	L	-2 0701	-1 5096	- 9219	- 4649	- 1979	- 1435	- 1333	- 0095	.1745	.3259	.3227	.3057	.2791	.2392	.1762	0 0000
.75000U		7 1164	7 0926	6 8782	6 5128	6 0569	5 1428	4 5584	4 1662	3 7937	3 1213	2 3775	2 1531	1 8851	1 5520	1 1015	0 0000
	L	-1 8011	-1 2945	- 7653	- 3557	- 1187	- 0786	- 0752	.0320	.1927	.3212	.3112	.2938	.2673	.2283	.1675	0 0000
.80000U		6 1330	6 1129	5 9285	5 6138	5 2211	4 4332	3 9293	3 5926	3 2746	2 6976	2 0561	1 8623	1 6309	1 3432	9539	0 0000
	L	-1 5470	-1 1103	- 6542	- 3014	- 0975	- 0637	- 0612	.0297	.1650	.2726	.2637	.2489	.2262	.1929	.1411	0 0000
.85000U		4 6991	4 6744	4 7191	4 4623	4 1465	3 5204	3 1204	2 8531	2 6023	2 1460	1 6364	1 4824	1 2986	1 0701	.7606	0 0000
	L	-1 3492	-1 0022	- 6365	- 3502	- 1806	- 1382	- 1262	- 0493	.0601	.1531	.1593	.1518	.1389	.1189	.0869	0 0000
.90000U		3 4860	3 4550	3 3317	3 1405	2 9125	2 4721	2 1914	2 0038	1 8303	1 5127	1 1545	1 0462	.9172	.7567	.5389	0 0000
	L	-1 1389	- 8947	- 6324	- 4216	- 2903	- 2359	- 2117	- 1499	- 0699	.0074	.0328	.0343	.0333	.0295	.0215	0 0000
.95000U		1 9871	1 9342	1 8502	1 7326	1 6002	1 3575	1 2035	1 1020	1 0130	.8447	.6472	.5872	.5160	.4272	.3061	0 0000
	L	- 8463	- 7117	- 5613	- 4343	- 3481	- 2898	- 2583	- 2168	- 1724	- 1189	- 0803	- 0713	- 0622	- 0518	- 0385	0 0000
.97500U		1 1872	1 1568	1 0960	1 0183	.9359	.7935	.7036	.6464	.6016	.5101	.3936	.3580	.3158	.2629	.1900	0 0000
	L	- 6515	- 5724	- 4799	- 3978	- 3374	- 2831	- 2517	- 2233	- 1998	- 1631	- 1226	- 1114	- 0988	- 0834	- 0622	0 0000
1.00000U		.4094	.3850	.3509	.3153	.2835	.2397	.2127	.2000	.2000	.1850	.1480	.1360	.1220	.1040	.0780	0 0000
	L	- 4094	- 3850	- 3509	- 3153	- 2835	- 2397	- 2127	- 2000	- 2000	- 1850	- 1480	- 1360	- 1220	- 1040	- 0780	0 0000

U = OFFSET OF UPPER SURFACE (SUCTION SIDE, SUCTION FACE, BACK) OF BLADE SECTION
MEASURED FROM REFERENCE LINE (NOSE-TAIL LINE)
L = OFFSET OF LOWER SURFACE (PRESSURE SIDE, PRESSURE FACE, FACE) OF BLADE SECTION
MEASURED FROM REFERENCE LINE (NOSE-TAIL LINE)

Table 13b. With Trailing-Edge Modification

SECTION OFFSETS
(IN INCHES)

AD-177 JUMBO, SKEW AND RAKE ONLY, T.E. MODIFICATION

ORDINATES (WITH TRAILING-EDGE MODIFICATIONS) AT NON-DIMENSIONAL RADIUS R/RO

FRACTION OF CHORD		.2000	.2500	.3000	.3500	.4000	.5000	.6000	.7000	.8000	.9000	.9500	.9800	.9700	.9800	.9900	1.0000
.45000U		9.3745	9.3029	8.9823	8.4755	7.8653	6.6765	5.9182	5.3987	4.8970	4.0096	3.0465	2.7574	2.4126	1.9848	1.4072	0.0000
	L	-2.9076	-2.2486	-1.5450	-.9844	-.6404	-.5150	-.4637	-.2908	-.0469	.1787	.2247	.2197	.2062	.1813	.1368	0.0000
.50000U		9.3687	9.3033	8.9888	8.4862	7.8778	6.6874	5.9278	5.4087	4.9083	4.0210	3.0560	2.7661	2.4204	1.9913	1.4119	0.0000
	L	-2.8237	-2.1639	-1.4617	-.9047	-.5658	-.4516	-.4075	-.2392	.0004	.2179	.2547	.2468	.2300	.2009	.1507	0.0000
.90000U		3.4860	3.4550	3.3317	3.1405	2.9125	2.4721	2.1914	2.0038	1.8303	1.5127	1.1545	1.0462	.9172	.7587	.5389	0.0000
	L	-1.1389	-.8947	-.6324	-.4216	-.2903	-.2359	-.2117	-.1499	-.0899	.0074	.0328	.0343	.0333	.0295	.0215	0.0000
.95000U		1.9671	1.9342	1.8502	1.7326	1.5515	1.3575	1.2035	1.1020	1.0130	.8447	.6472	.5872	.5160	.4272	.3081	0.0000
	L	-.8463	-.7117	-.5613	-.4343	-.3481	-.2898	-.2583	-.2168	-.1724	-.1189	-.0803	-.0713	-.0622	-.0518	-.0385	0.0000
.95500U		1.8116	1.7791	1.6994	1.5896	1.3885	1.2448	1.1034	1.0107	.9304	.7775	.5962	.5411	.4757	.3942	.2827	0.0000
	L	-.8105	-.6870	-.5480	-.4299	-.3487	-.2907	-.2590	-.2199	-.1795	-.1291	-.0898	-.0802	-.0703	-.0588	-.0437	0.0000
.96000U		1.6558	1.6237	1.5486	1.4454	1.2179	1.1312	1.0033	.9195	.8480	.7104	.5453	.4951	.4355	.3612	.2594	0.0000
	L	-.7731	-.6607	-.5334	-.4241	-.3479	-.2906	-.2588	-.2222	-.1859	-.1386	-.0988	-.0887	-.0781	-.0655	-.0487	0.0000
.96500U		1.4998	1.4681	1.3976	1.2952	1.0408	1.0107	.9032	.8283	.7656	.6434	.4945	.4492	.3954	.3283	.2362	0.0000
	L	-.7342	-.6330	-.5172	-.4169	-.3459	-.2893	-.2575	-.2236	-.1914	-.1475	-.1073	-.0968	-.0854	-.0718	-.0534	0.0000
.97000U		1.3435	1.3124	1.2467	1.1352	.8588	.8745	.8033	.7372	.6834	.5766	.4440	.4035	.3555	.2955	.2131	0.0000
	L	-.6937	-.6036	-.4994	-.4082	-.3424	-.2869	-.2552	-.2240	-.1961	-.1557	-.1153	-.1043	-.0924	-.0778	-.0579	0.0000
.97500U		1.1872	1.1568	1.0960	.9645	.6740	.7190	.7032	.6464	.6016	.5101	.3936	.3580	.3158	.2629	.1900	0.0000
	L	-.6515	-.5724	-.4799	-.3978	-.3374	-.2831	-.2517	-.2233	-.1998	-.1631	-.1226	-.1114	-.0988	-.0834	-.0622	0.0000
.98000U		1.0308	1.0013	.9456	.7845	.4887	.5451	.5865	.5557	.5200	.4438	.3435	.3126	.2762	.2304	.1670	0.0000
	L	-.6074	-.5194	-.4586	-.3856	-.3307	-.2779	-.2470	-.2215	-.2024	-.1697	-.1294	-.1178	-.1048	-.0886	-.0661	0.0000
.98500U		.8747	.8462	.7956	.5992	.3035	.3589	.4293	.4412	.4228	.3590	.2778	.2531	.2235	.1868	.1352	0.0000
	L	-.5614	-.5044	-.4353	-.3716	-.3222	-.2712	-.2409	-.2184	-.2039	-.1753	-.1354	-.1236	-.1102	-.0934	-.0697	0.0000
.99000U		.7169	.6915	.6463	.4131	.1182	.1698	.2337	.2651	.2606	.2159	.1669	.1524	.1348	.1133	.0820	0.0000
	L	-.5132	-.4672	-.4098	-.3554	-.3117	-.2627	-.2334	-.2140	-.2042	-.1798	-.1406	-.1286	-.1149	-.0976	-.0729	0.0000
.99100U		.6878	.6607	.6165	.3759	.0812	.1320	.1922	.2234	.2202	.1807	.1398	.1278	.1131	.0954	.0892	0.0000
	L	-.5033	-.4595	-.4044	-.3519	-.3094	-.2608	-.2318	-.2129	-.2041	-.1806	-.1415	-.1295	-.1158	-.0983	-.0735	0.0000
.99200U		.6567	.6298	.5868	.3387	.0441	.0941	.1507	.1804	.1781	.1442	.1118	.1024	.0908	.0770	.0580	0.0000
	L	-.4933	-.4517	-.3989	-.3482	-.3089	-.2588	-.2299	-.2118	-.2039	-.1813	-.1424	-.1304	-.1166	-.0991	-.0741	0.0000
.99300U		.6255	.5991	.5571	.3015	.0071	.0563	.1092	.1368	.1350	.1071	.0833	.0765	.0681	.0583	.0427	0.0000
	L	-.4831	-.4437	-.3933	-.3445	-.3044	-.2568	-.2280	-.2106	-.2037	-.1820	-.1433	-.1313	-.1174	-.0998	-.0747	0.0000
.99400U		.5926	.5683	.5275	.2643	.0300	.0185	.0877	.0931	.0916	.0698	.0547	.0506	.0454	.0395	.0294	0.0000
	L	-.4710	-.4357	-.3876	-.3407	-.3017	-.2546	-.2281	-.2093	-.2033	-.1826	-.1441	-.1321	-.1182	-.1005	-.0752	0.0000
.99600U		.5544	.5355	.4978	.2271	-.0670	-.0193	.0261	.0495	.0482	.0325	.0261	.0247	.0227	.0208	.0161	0.0000
	L	-.4535	-.4254	-.3818	-.3368	-.2990	-.2524	-.2241	-.2079	-.2030	-.1831	-.1449	-.1328	-.1189	-.1012	-.0757	0.0000
.99800U		.5072	.4955	.4656	.1899	-.1041	-.0572	-.0154	.0058	.0048	-.0047	-.0025	-.0012	.0000	.0021	.0028	0.0000
	L	-.4268	-.4078	-.3731	-.3327	-.2961	-.2501	-.2220	-.2065	-.2025	-.1836	-.1456	-.1335	-.1196	-.1018	-.0762	0.0000
.99700U		.4463	.4421	.4224	.1527	-.1411	-.0950	-.0569	-.0378	-.0386	-.0420	-.0310	-.0271	-.0227	-.0166	-.0106	0.0000
	L	-.3863	-.3767	-.3634	-.3286	-.2932	-.2476	-.2198	-.2050	-.2020	-.1841	-.1463	-.1342	-.1203	-.1024	-.0767	0.0000
.99800U		.3654	.3672	.3576	.1154	-.1782	-.1328	-.0984	-.0814	-.0820	-.0792	-.0596	-.0530	-.0454	-.0353	-.0239	0.0000
	L	-.3295	-.3238	-.3118	-.3243	-.2901	-.2451	-.2175	-.2034	-.2014	-.1845	-.1469	-.1349	-.1209	-.1030	-.0772	0.0000
.99900U		.2518	.2565	.2544	.0782	-.2152	-.1706	-.1399	-.1251	-.1254	-.1165	-.0882	-.0789	-.0681	-.0540	-.0372	0.0000
	L	-.2320	-.2349	-.2318	-.3199	-.2868	-.2424	-.2152	-.2018	-.2008	-.1848	-.1475	-.1355	-.1215	-.1035	-.0776	0.0000
.99925U		.2148	.2194	.2185	.0672	-.2245	-.1801	-.1503	-.1360	-.1362	-.1258	-.0953	-.0853	-.0737	-.0587	-.0405	0.0000
	L	-.2000	-.2032	-.2014	-.3170	-.2860	-.2418	-.2146	-.2013	-.2006	-.1848	-.1476	-.1356	-.1216	-.1036	-.0777	0.0000
.99950U		.1716	.1756	.1755	.0425	-.2337	-.1895	-.1607	-.1469	-.1471	-.1351	-.1025	-.0918	-.0794	-.0614	-.0418	0.0000
	L	-.1617	-.1649	-.1641	-.3005	-.2852	-.2411	-.2139	-.2009	-.2004	-.1849	-.1477	-.1357	-.1217	-.1038	-.0778	0.0000
.99975U		.1172	.1202	.1204	-.0125	-.2430	-.1990	-.1711	-.1578	-.1579	-.1444	-.1096	-.0983	-.0852	-.0686	-.0482	0.0000
	L	-.1122	-.1148	-.1147	-.2536	-.2843	-.2404	-.2133	-.2004	-.2002	-.1849	-.1479	-.1358	-.1217	-.1034	-.0769	0.0000
1.00000U		0.0000	0.0000	0.0000	-.1372	-.2679	-.2241	-.1971	-.1844	-.1844	-.1694	-.1324	-.1204	-.1064	-.0884	-.0642	0.0000
	L	0.0000	0.0000	0.0000	-.1372	-.2679	-.2241	-.1971	-.1844	-.1844	-.1694	-.1324	-.1204	-.1064	-.0884	-.0642	0.0000

U = OFFSET OF UPPER SURFACE (SUCTION SIDE, SUCTION FACE, BACK) OF BLADE SECTION
MEASURED FROM REFERENCE LINE (NOSE-TAIL LINE)
L = OFFSET OF LOWER SURFACE (PRESSURE SIDE, PRESSURE FACE, FACE) OF BLADE SECTION
MEASURED FROM REFERENCE LINE (NOSE-TAIL LINE)

Table 14. Comparison of Full-Scale Powering Predictions Based on Model Powering Experiments Using Stock and Design Propellers

		FULL LOAD CONDITION		BALLAST CONDITION	
		PREDICTION	EXPERIMENT	PREDICTION	EXPERIMENT
FULL POWER (24000 SHP)		No EHP Margin		No EHP Margin	
	V	20.81	21.0	21.64	22.0
	RPM	99.50	99.5	98.74	99.4
		6% EHP Margin		6% EHP Margin	
	V	20.43	20.6	21.02	21.7
	RPM	99.12	99.3	98.11	99.3
SUSTAINED POWER (19200 SHP)		No EHP Margin		No EHP Margin	
	V	19.54	19.8	19.56	20.6
	RPM	92.64	92.4	91.23	92.1
		6% EHP Margin		6% EHP Margin	
	V	19.13	19.4	18.93	20.1
	RPM	92.18	92.2	90.60	91.6

Note: 1. Data under PREDICTION columns were taken from Figures 20 and 21. These predictions were made by using the estimated open-water performance and stock propeller powering characteristics.

2. Data under EXPERIMENT columns were provided by Code 1521, DTNSRDC via Memorandum dated 9 October 1986. These data were obtained based on the experimental open-water and powering tests using the design propeller. The data are preliminary in nature and the final data might be slightly different.

Table 15. Comparison of EHP and Propeller/Hull Interaction Coefficients Between Stock and Design Propellers

SHIP SPEED (KNOTS)	EHP(P_E)		1-t		$1-w_T$		RELATIVE ROTATIVE EFFICIENCY	
	T.H.	DTNSRDC	STOCK	DESIGN	STOCK	DESIGN	STOCK	DESIGN
10	1815	1800	.846	.855	.774	.790	1.042	1.010
11	2399	2370	.845	.855	.774	.785	1.044	1.010
12	3094	3060	.844	.855	.773	.780	1.044	1.010
13	3911	3870	.843	.855	.774	.775	1.043	1.005
14	4858	4800	.843	.855	.773	.770	1.045	1.005
15	5963	5890	.842	.865	.773	.770	1.044	1.000
16	7269	7140	.841	.870	.773	.775	1.044	.995
17	8820	8580	.844	.870	.774	.775	1.043	.995
18	10595	10280	.847	.875	.774	.775	1.042	.995
19	12609	12210	.847	.870	.774	.775	1.043	.995
20	14930	14360	.849	.870	.774	.780	1.044	1.000
21	17835	17000	.853	.855	.776	.780	1.040	1.000
22	21962	20740	.859	.835	.779	.785	1.038	1.015

Note:
1. The data in this Table are for a full-scale condition with still air drag and no power margin.
2. The stock propeller powering data were taken from Table 3 provided by Tracor Hydronautics, Inc. (T.H.).
3. The design propeller powering data were provided by Code 1521, DTNSRDC via Memorandum data 9 October 1986.

APPENDIX A - PROPELLER DESIGN REQUIREMENTS FOR AO-177 JUMBO

1. PRINCIPAL SHIP CHARACTERISTICS

- o Length Overall = 668.6 feet (108 ft Parallel Midbody Added to the Original Ship)
- o Beam = 88.0 feet
- o Number of Shafts = 1
- o Shaft Inclination Angle = 0 degree
- o Shaft Centerline above Ship Baseline = 11.75 feet
- o Propulsion Machinery Plant: Steam Turbine
- o Full Load Condition:
  - Displacement = 37,575 Long Tons
  - Draft = 33.76 feet
  - Trim = 0 feet (goal)
  - Block Coefficient = 0.661
  - Prismatic Coefficient = 0.676
  - Submergence of Depth of Propeller Shaft Centerline = 22.0 feet
- o Ballast Arrival Condition:
  - Displacement = 22,146 Long Tons
  - Draft = 21.07 feet
  - Trim = 5.90 feet down by Stern
  - Submergence of Depth of Propeller Shaft Centerline = 15.2 feet

2. PROPELLER GEOMETRY CONSTRAINTS

- o Fixed Pitch Propeller
- o Number of Blades : 5
- o Direction of Rotation : Right-Hand
- o Propeller Diameter = 21.0 feet
- o Maximum Propeller Weight = 73,000 pounds (actual)
- o Maximum Blade Weight = 56,400 pounds (LL106 calculation)
- o Maximum Forward Blade Location: Not less than 2.0 inches aft of forward end of hub (for handling purposes)
- o Maximum Aft Blade Location: Comparable to AO-177 dimension
- o Blade Skew: Use the amount practical in order to minimize vibration excitation forces imparted to the hull and propulsion machinery. Not to exceed 45 deg.
- o Blade Rake: Use as necessary to maintain proper fore/aft clearances.

3. DESIGN POINT

- o SHP = 24,000 HP (Full Power)
- o RPM = 100
- o Full-Load Condition
- o Wake Survey Data: See NAVSEA 55W3/DTNSRDC Code 1521
- o EHP vs Ship Speed Data (With Still Air Drag, No Power Margin, C_A = 0.0005: See Table 3)
- o Propeller-Hull Interaction Coefficients: See Table 3
- o Blade Drag Coefficients: Model Scale

4. PERFORMANCE REQUIREMENTS

- o Sustained Speed Requirement at Full Load: 18.8 Knots at 19,200 SHP (80% of Full Power) for EHP with 6% margin
- o Machinery Operating Limits - RPM at design condition (24,000 SHP), 97.5 - 102.5
- o Cavitation:
  - No significant thrust breakdown or erosion.
  - 10% speed margin on the inception of back bubble cavitation.
  - Impact of cavitation on ship performance to be minimized.
- o Acoustic: No specific requirements.
- o Unsteady Shaft Forces: No greater than 3 times AO-177 levels (determined from vibration analysis)
- o Ballast Arrival Condition:
  - Satisfactory cavitation performance at ballast arrival condition, i.e., no significant thrust breakdown, blade erosion or hull vibration.
  - 18.8 knots (or not to exceed 100 rpm)
  - Wake survey data: Assume same as full-load
  - EHP vs Ship Speed Data: With still air drag, no power margin, C_A = 0.0005 - See Table 4.
  - Propeller-Hull Interaction Coefficients: See Table 4.

5. PROPELLER MATERIAL (FULL SCALE)

- o Ni-Al-Bronz, ABS Grade 4
- o Density = 0.275 pounds/inches^3

6. STRENGTH REQUIREMENTS

- o Static Stress: Not to exceed 12,500 psi using beam theory.
- o Fatigue Strength: Alternating stress, 12,500 psi for 10^8 cycles in sea water.

7. HUB DIMENSIONS

- o Diameter = 20 % of Propeller Diameter
- o Hub Forward Diameter = 59 9/16 in.
- o Hub Aft Diameter = 45 in.
- o Hub Length = 55 1/8 in.
- o Hub Forward End to Blade Reference Line = 28.9 in.

APPENDIX B - STRESS ANALYSIS OF AO-177 JUMBO PROPELLER BY USING FINITE ELEMENT METHOD

A structural analysis has been performed for AO-177 JUMBO propeller by the Advanced Concepts Group, Code 1720.1, DTNSRDC*. The analysis was made utilizing the ABAQUS finite element code developed by Hibbit, Karlsson and Sorensen, Inc.

A blade of the AO-177 Jumbo propeller was modelled using 120 three dimensional bricks with twenty-nodes as shown in Figure B-1. The analysis was made for full power ahead condition at 99.5 rpm. Loading for the analysis was based on the pressure distribution calculated by the modified PSF-2 code by Kim and Kobayashi [32].

Figures B-2 and B-3 show the contours plots of Von Mises stress on both pressure and suction sides of the blade surface. The maximum stress of about 6,700 psi occurs near 0.95 chord length at 0.45 radius of the pressure side. The finite element analysis predicted the maximum displacement of 0.33 inches on the blade (see Figure B-4). These results indicate that the AO-177 Jumbo propeller is structurally adequate.

*The structural analysis results presented in this Appendix were provided by Code 172.1, DTNSRDC, via Memorandum dated 31 July 1987.

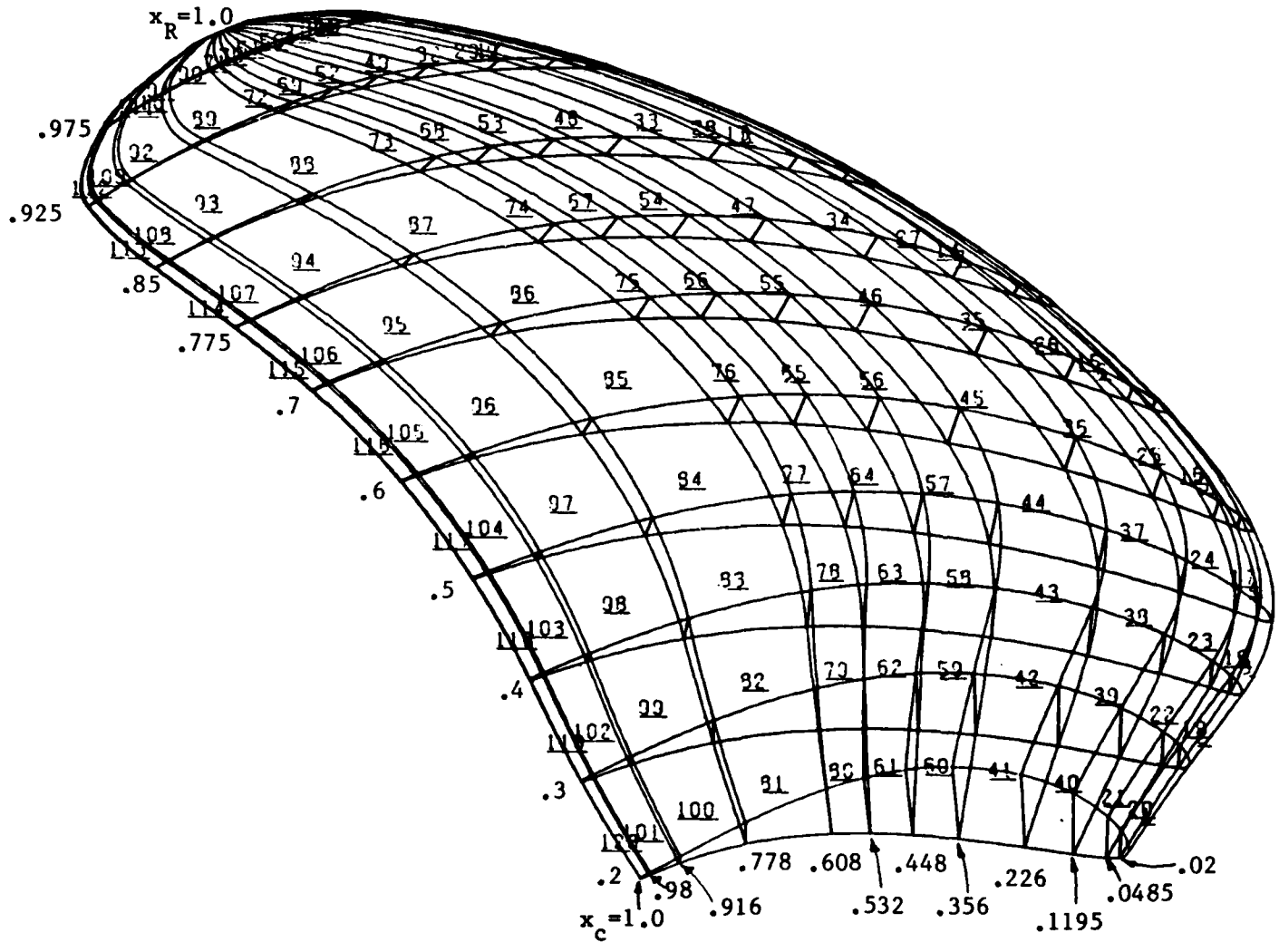

Figure B-1. Finite Element Model of AO-177 JUMBO Propeller

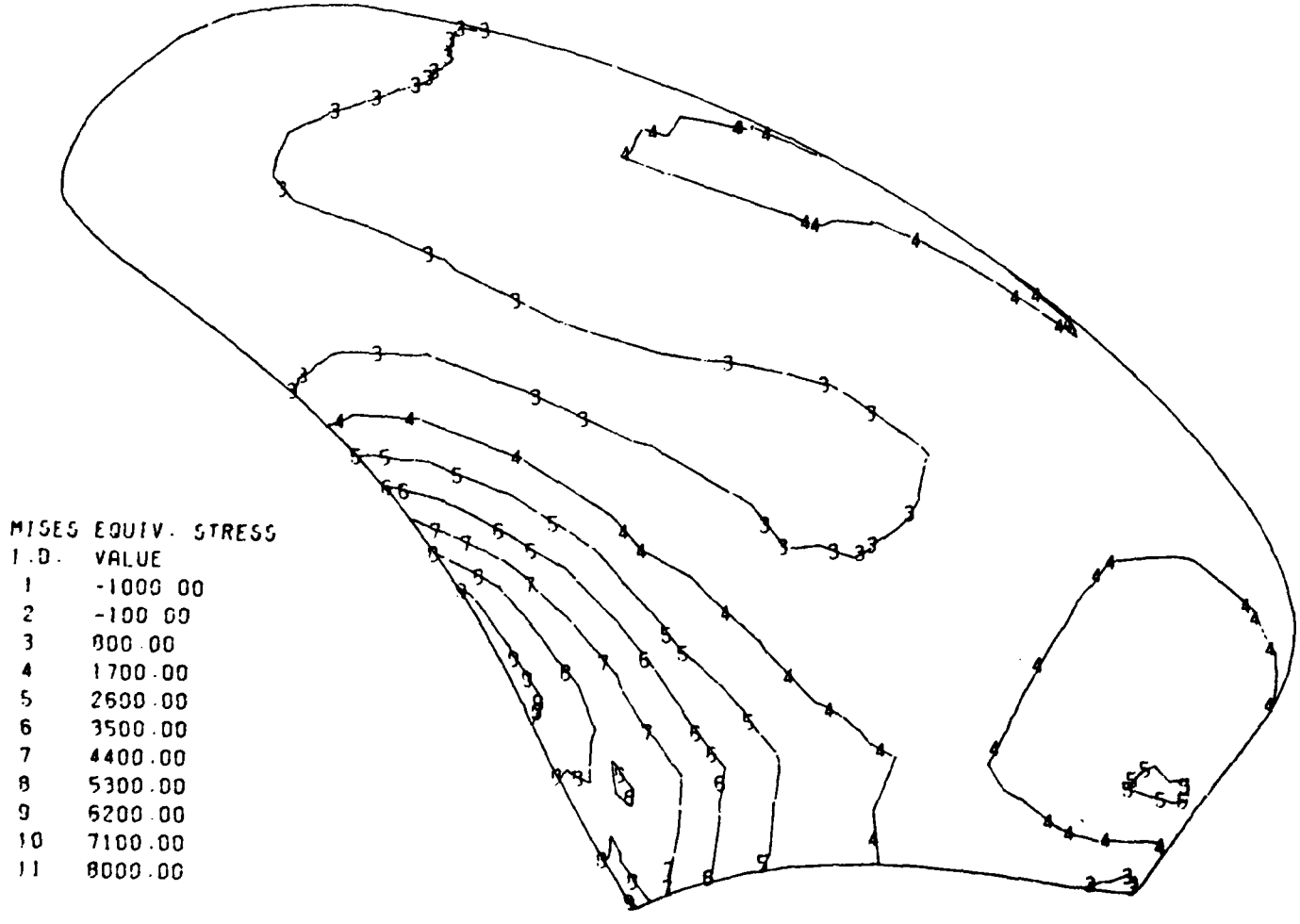

Figure B-2. Von Mises Stress Contours on Pressure Side at Full Load, Full Power Ahead Condition

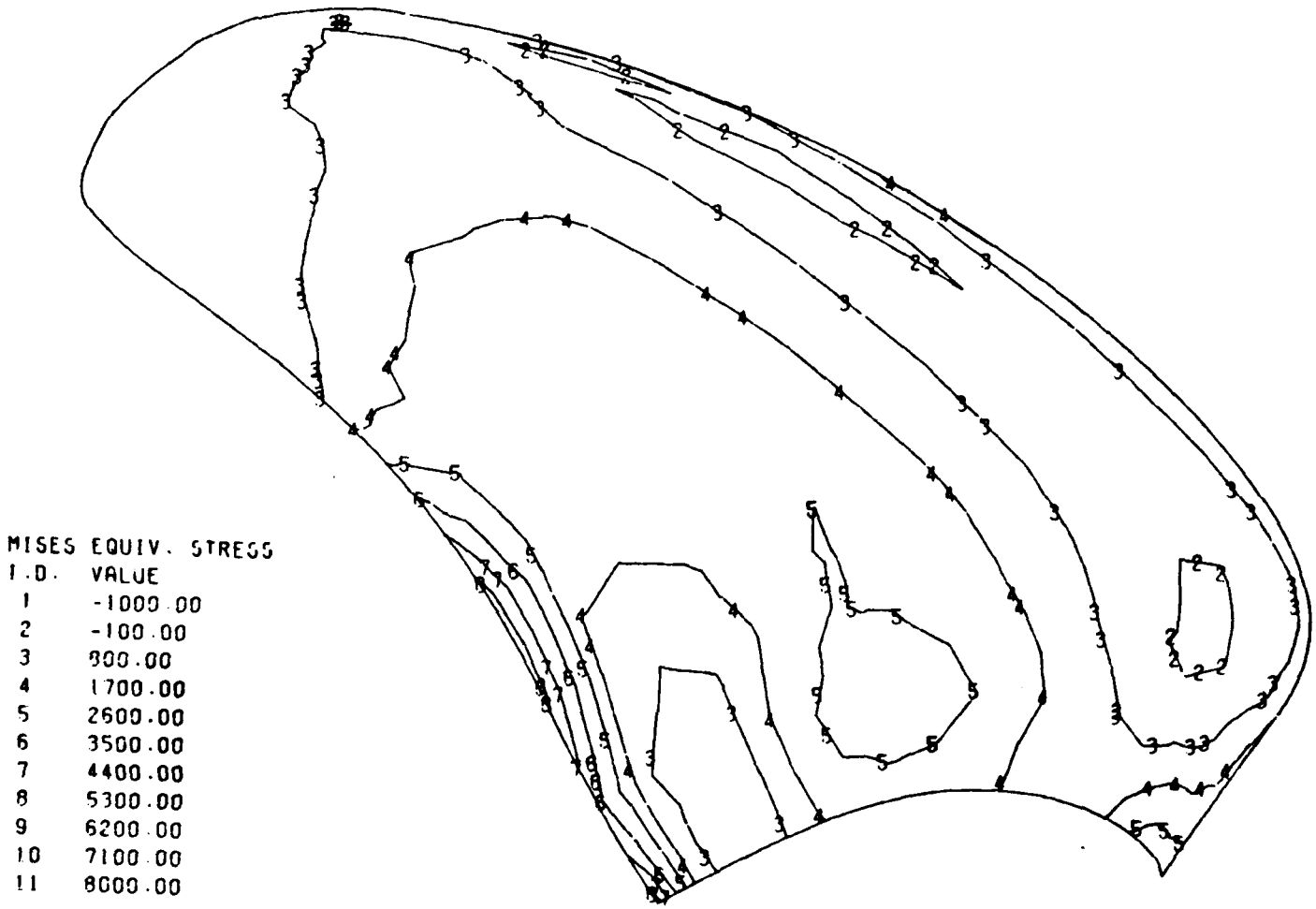

Figure B-3. Von Mises Stress Contours on Suction Side at Full Load, Full Power Ahead Condition

Mag. Factor = 45.9

Solid Lines: Displaced Mesh

Dashed Lines: Original Mesh

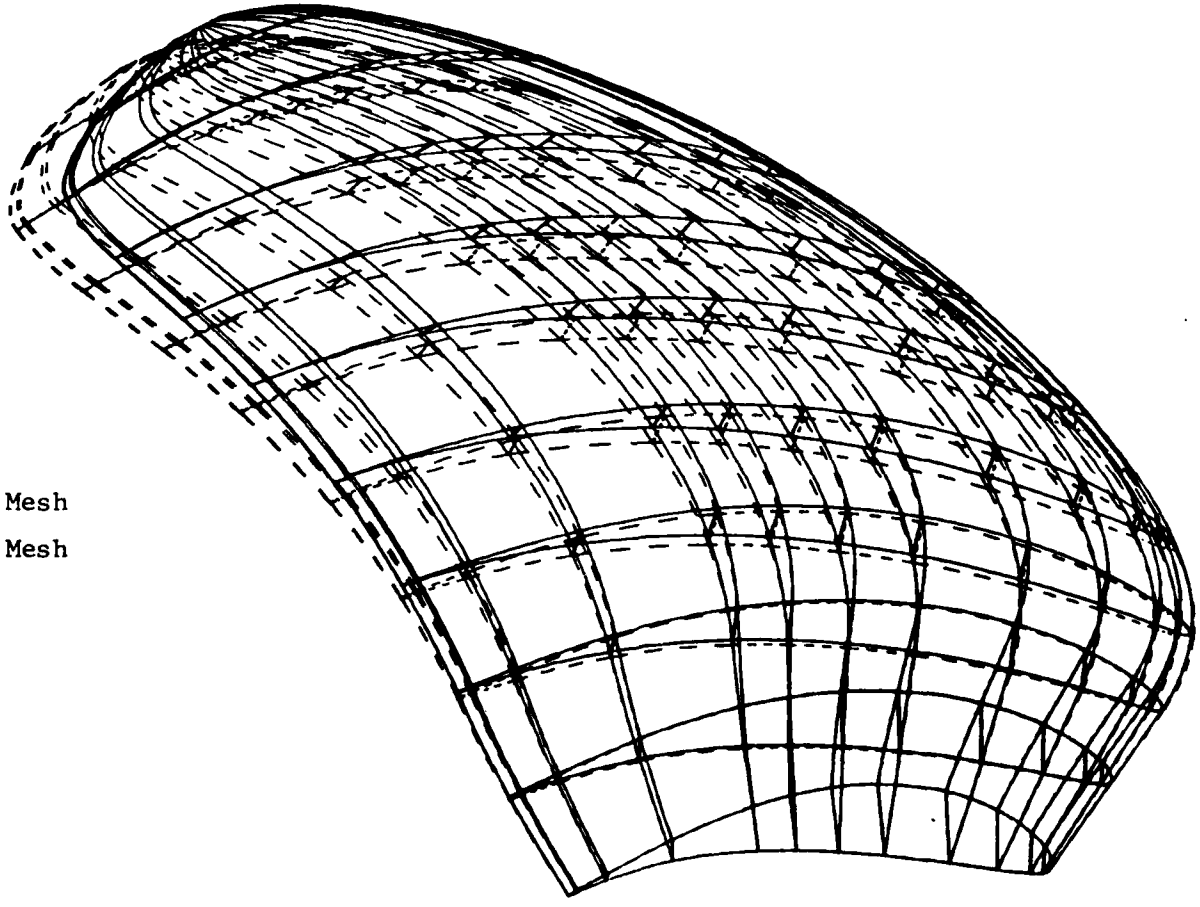

Figure B-4. Blade Displacement at Full Load, Full Power Ahead Condition

REFERENCES

1. Wilson, M.B., D.N. McCallum, R.J. Boswell, D.D. Bernhard and A.B. Chase, "Causes and Corrections for Propeller-Excited Airborne Noise on a Naval Auxiliary Oiler," Transactions, SNAME (1982).

2. Hampton, G.A., "Analysis of Wake Survey for Tunnel-Fin and Accelerating Fin Configurations for the Naval Auxiliary Oiler (AO-177) Represented by Model 5326-1," DTNSRDC Report SPD-0544-18 (Apr. 1981).

3. Bjärne, E., "U.S. Navy Oiler, AO-177 Class - Model Tests in SSPA Cavitation Tunnel No. 2 - Ship Model with Alternative Fins and Duct," SSPA Report No. 2564-3, Göteborg, Sweden (Dec 1980).

4. Hagen, A., "AO-177 (Jumboized) Longitudinal Shafting Study," Preliminary Report, DTNSRDC Code 1962 (Apr. 1986).

5. Bjärne, E., "U.S. Navy Oiler, AO-177 Class - Model Tests in SSPA Cavitation Tunnel No. 2 with Alternative Propeller Models," SSPA Report No. 2564-2, Göteborg, Sweden (Dec. 1980).

6. Valentine, D.T. and A. Chase, "Highly Skewed Propeller Design for a Naval Auxiliary Oiler (AO-177)," DTNSRDC Report SPD-544-12 (Sep. 1976).

7. Boswell, R.J., "Design, Cavitation Performance and Open-Water Performance of a Series of Research Skewed Propellers," DTNSRDC Report 3339 (Mar. 1971).

8. Cumming, R.A., W.B. Morgan and R.J. Boswell, "Highly Skewed Propellers," Transactions, SNAME, Vol. 80 (1972).

9. Jessup, S.D., "Preliminary Redesign of the AO-177 Propeller," DTNSRDC Report SPD-0544-22 (Nov. 1982).

10. Lerbs, H.W., "Moderately Loaded Propellers with a Finite Number of Blades and Arbitrary Distribution of Circulation," Transactions SNAME, Vol. 60 (1952).

11. Greeley, D.S. and J.E. Kerwin, "Numerical Methods for Propeller Design and Analysis in Steady Flow," Transactions SNAME, Vol. 90 (1982).

12. Glover, E.J. and G. Patience, "Aspects of the Design and Application of Off-Loaded Tip Propellers," Proceedings, Symposium on Propeller Induced Ship Vibration, The Royal Institution of Naval Architects (1979).

13. Lindgren, H. and E. Bjärne, "Studies of Propeller Cavitation Erosion," Conference on Cavitation, Edinburg, Institute of Mechanical Engineers (Sep. 1974).

14. Björheden, O., "Vibration Performance of Highly Skewed CP Propellers," Proceedings, Symposium on Propeller Induced Ship Vibration, The Royal Institution of Naval Architects, London, Paper No. 8 (1979).

15. Brockett, T.E., "Minimum Pressure Envelopes for Modified NACA-66 Sections with NACA a=0.8 Camber and Buships Type I and Type II Sections," DTNSRDC Report 1789 (Feb. 1966).

16. Koh, I.-Y., R.P. Cross and C.G. Queen, "Ship Model Correlation of Powering Performance on USS Cimarron, AO-177," DTNSRDC Report SPD-1044-01 (Aug. 1983).

17. Grant, J. and C. Wilson, "Design Practices for Powering Predictions," DTNSRDC Report SPD-693-01 (1976).

18. Huang, T.T., H.T. Wang, N. Santelli and N. Groves, "Propeller/-Stern/Boundary-Layer Interaction on Axisymmetric Bodies: Theory and Experiment," DTNSRDC Report 76-0113 (1976).

19. Kim, K.-H., "An Extended Lifting-Line Computer Program for Preliminary Design of Propellers," DTNSRDC Report SHD-1239-01 (1987).

20. Caster, E.B., J.A. Diskin and T.A. LaFone, "A Lifting Line Computer Program for Preliminary Design of Propellers," DTNSRDC Report No. SPD-595-01 (Nov. 1975).

21. Brockett, T.E., "A Lifting-Line Computer Program Based on Circulation for Preliminary Hydrodynamic Design of Propellers," Canadian Department of National Defense, DREA, Tech. Memo. 79/E (1979).

22. Abbott, I.H. and A.E. Von Doenhoff, Theory of Wing Sections Including a Summary of Airfoil Data, Dover Publication Inc., New York (1958).

23. Hoerner, S.F., Fluid-Dynamic Drag, Published by the Author, Midland Park, New Jersey (1965).

24. Brockett, T.E. and R. Korpus, "Parametric Evaluation of the Lifting-Line Model for Conventional and Preswirl Propulsors," Proceedings of the International Symposium on Propeller and Cavitation, Wuxi, China (1986).

25. Kerwin, J.E., W.B. Coney and C.-Y. Hsin, "Optimum Circulation Distributions for Single and Multi-Component Propulsors," Presented to the 21st American Towing Tank Conference, Washington D.C. (Aug. 1986).

26. Holden, K. and T. Kvinge, "On the Application of Skew Propeller Designs to Increased Propulsion Efficiency," Proceedings, 5th Lips Propeller Symposium, Drunen (1983).

27. Burrill, L.C. and A. Emerson, "Propeller Cavitation: Further Tests on 16-Inch Propeller Models in the Kings College Cavitation Tunnel," Transactions of the North East Coast Institution of Engineers and Ship Builders, Vol. 78, pp 295-320 (1963-64).

28. Keller, J. Auf'm, " Enige aspectedm bij het ontwerpen van Scheepsschroeven," Schip en Werk, No. 24 (1966).

29. Kerwin, J.E., "A Vortex Lattice Method for Propeller Blade Design: MIT-PBD-10 User's Manual," M.I.T. Department of Ocean Engineering Report No. 84-2 (1984).

30. Kerwin J.E. and C.S. Lee, "Prediction of Steady and Unsteady Marine Propeller Performance by Numerical Lifting Surface Theory," Transactions SNAME, Vol. 86 (1978).

31. Lerbs, H.W. and H.P. Rader, "Uber der Auftriebsgradienten von Profilen im Propeller Verband," Schiffstechnik, Vol. 9, No. 48 (1962).

32. Kim, K.-H. and S. Kobayashi, "Pressure Distribution on Propeller Blade Surface Using Numerical Lifting-Surface Theory," Proceedings SNAME Propellers '84 Symposium (1984).

INITIAL DISTRIBUTION

Copies	
15	NAVSEA
	1 SEA 504 (Grant)
	3 SEA 55W3 (Comstock, McCallum, Engle)
	1 SEA 56X11 (Maria)
	1 SEA 56X13 (Calvin)
	3 SEA 56X7 (Crockett, Platzer, Majumdar)
	1 SEA 5011 (Howell)
	2 SEA 55D (North)
	1 SEA 55N2 (Paladino)
	1 SEA 56D (Melsom)
	1 SEA 99612 (Library)
2	PMS 383 (Nunnery, Perin)
1	MSC M4E2 (Jacobson)
1	SSNO 100 (Jenkins)
1	USCG G-MSC (Reid)
1	ABS AAM/fd (Stromer)
1	NAVSHIPYD PHILA/Lib
1	NAVSHIPYD NORVA/Lib
1	NAVSHIPYD PUGET/Lib
1	NAVSHIPYD PEARL/Lib
1	USNA/Lib
1	NAVPGSCL/Lib
1	NOSC/Lib
1	NCSC/712
1	NUSC/Lib
2	MARAD
	1 Div of Ship R&D
	1 Lib

Copies	
1	MIT (J.E. Kerwin)
2	U. of Michigan (NAME Dept)
	1 Lib
	1 T. Brockett
1	Penn State U/ARL Lib
1	SNAME/Lib
2	Tracor, Hydronautics
	1 R. Kowalyshin
	1 S. Kobayashi
1	Bird Johnson (J. Norton)
1	HRA Assoc. (B. Cox)
1	Atlantic Research (D. Greeley)
1	D & P, Inc. (J. Slager)

CENTER DISTRIBUTION

Copies	Code	Name
1	012.3	D.D. Moran
1	15	W.B. Morgan
1	1504	V.J. Monacella
1	1506	S. Hawkins
1	1508	R. Boswell
1	152	W.C. Lin
2	1521	W. Day K. Forgach
2	1522	M. Wilson K. Remmers
1	154	R. Folb
1	1540	R. Cummings

CENTER DISTRIBUTION

Copies	Code	Name
1	1542	Huang
25	1544	G. Dobay S. Jessup K.-H. Kim (20) F. Peterson A. Reed C. Yang
2	172.1	T. Tinley W. Martin
1	1905.1	W. Blake

END

DATE

FILMED

MARCH

1988

DTIC